*Estudios Geol., 57: 175-273 (2001)*

# GEOLOGY AND VOLCANOLOGY OF LA PALMA AND EL HIERRO, WESTERN CANARIES

J. C. Carracedo[1], E. R. Badiola[2], H. Guillou[3], J. de la Nuez[4] and F. J. Pérez Torrado[5]

Dedicamos este trabajo a la memoria de José María Fúster Casas. El profesor Fúster dirigió en la década de los 60 del pasado siglo el primer estudio geológico moderno y detallado de las Islas Canarias, a las que dedicó, hasta su fallecimiento, la mayor parte de su investigación. Los autores de este artículo, que fuimos inicialmente sus alumnos y posteriormente sus colaboradores y amigos, intentamos seguir sus pasos y su ejemplo.


## SUMMARY

The western Canaries, relatively little studied until a few years ago from the geological point of view, have however provided decisive data for understanding many of the most important geological problems of the Archipelago, which would probably have been dilucidated earlier, had the study begun with the most recent islands, as occurs in similar chains of oceanic volcanic islands in other parts of the world.

To summarize the main geological features and evolutionary characteristics of both islands we emphasize the following stages of development:

During the Pliocene, a submarine volcanic edifice or seamount formed in the island of La Palma, made up of pillow lavas, pillow breccias and hyaloclastites, intruded by trachytic domes, plugs of gabbros, and a highly dense dyke swarm. The intense magmatic and dyke intrusion uplifted the seamount up to 1,500 m, tilting it 45-50° to the SW. This intrusive phase was followed by a period of quiescence and erosion of the emerged submarine edifice. The definitive consolidation and progression of the construction of the island continued from at least 1.77 ma in angular and erosive discordance over the submarine basement. The subaerial volcanic reactivation, in which explosive volcanism predominated during the initial stages, producing abundant volcanoclastic and phreatomagmatic materials at the base of the subaerial edifice, persisted in a highly continuous manner until at least 0.41 ma. This initial subaerial stage shaped the northern volcanic shield, formed by the accumulation of several superimposed volcanoes, approximately concentric in relation to one another and the submarine basement.

The initial stage of the northern volcanic shield lasted between 1.77 and 1.20 ma, during which period the Garafía volcano was built to a height of 2,500-3,000 m, with steeply sloping flanks, formed predominantly by alkaline basalts with abundant pahoehoe lavas. The rapid growth and progressive instability of the Garafía volcano culminated some 1.20 ma ago in a gravitational landslide of the south flank of the volcanic edifice. The eruptive activity that followed the collapse built the Taburiente volcano, that rests upon a clear angular discordance caused by the landslide. The landslide depression was filled completely some 0.89 ma ago, as shown by the age of the first lavas to overflow the collapse embayment. The filling-in of the depression by the Taburiente volcano lavas finally formed a sequence of horizontal lavas, predominantly alkaline basalts, that ponded against the headwall of the landslide scarp forming a plateau in the centre of the volcanic shield.



[1] Estación Volcanológica de Canarias, IPNA-CSIC, Tenerife, Spain «jcarracedo@ipna.csic.es».
[2] Museo Nacional de Ciencias Naturales, CSIC, Madrid, Spain.
[3] Laboratoire des Sciences du Climat et de l'Environnement, CEA-CNRS, Gif-sur-Yvette, France.
[4] University of La Laguna, Tenerife, Spain.
[5] University of Las Palmas de Gran Canaria, Spain.

Coinciding approximately with the Matuyama-Brunhes boundary (0.78 ma) an important reorganisation of the Taburiente volcano took place, the dispersed emission centres of which progressively concentrated in three increasingly defined rifts (NW, NE and N-S) and subsequently in a central edifice situated at the geometrical centre of the volcanic shield. The abundant emissions of this final stage covered the earlier formations with sequences of lava flows up to 1,000 m thick in places, with the exception of a part of the alignments of cones of the rifts. The basaltic lavas evolved towards more differentiated phonolitic and trachytic terms at the terminal phases of construction of the volcano. One of these rifts, the southern or Cumbre Nueva rift, developed more than the others, possibly because the volcanism already began to migrate southwards, forming a N-S trending dorsal ridge over 2,500 m high. The progressive instability of the Cumbre Nueva rift, due to overgrowth, triggered the gravitational landslide of the western flank, in a process that took place about 560 ka ago, involving the detachment of some 180-200 $km^3$ and the formation of a wide depression (the Valle de Aridane) and the beginning of the formation, by incision and retrogressive erosion, of the Caldera de Taburiente.

The activity subsequent to the collapse in the northern shield was preferentially concentrated in the interior of the new collapse basin, quickly building the Bejenado stratovolcano. This activity was coetaneous with that of other residual centres dispersed over the flanks of the shield. The initially basanite lavas of Bejenado volcano evolved to mafic tephrites in differentiated lateral and terminal vents. The activity of the volcanic shield ceased definitively some 0.4 ma ago. After a transition period with a certain degree of activity associated with Bejenado late peripheral vents, volcanism was definitively located until the present in the new Cumbre Vieja volcano, at the south of the island. The oldest Cumbre Vieja lavas have been dated in 123 ka, although the first eruptions of the volcano may be considerably older. During this last stage of volcanism in La Palma a N-S trending rift has been formed, with predominantly basanitic, tephritic and tephri-phonolitic lavas, and intrusions of domes of tephri-phonolites and phonolites, frequently associated with eruptive vents. Numerous submarine eruptive vents, several of which are apparently very recent, have recently been observed and sampled at the prolongation of the Cumbre Vieja rift southwards in the ocean.

The foreseeable geological evolution of this rift is similar to that of its Cumbre Nueva predecessor, towards a progressive development and increasing instability, although changes may take place that may modify it towards more stable configurations, fundamentally the submarine progression of the southern tip of the rift, that could redistribute the volume of emitted materials, reduce the aspect ratio of the volcano and, consequently, its instability. The en echelon faults generated during the 1949 eruption have been interpreted as a possible detachment of the western flank of the volcano, although a more favourable hypothesis would be that such faults are surficial and contribute to accommodating the volcano by reducing its instability. A noteworthy aspect is the important role played by the mobility of the general feeding system of the volcanism in shaping the form and structure of the island. If the volcanism had not continually migrated southward since the final stages of construction of the northern shield, the island of La Palma would probably have taken on a similar configuration to that of the islands of El Hierro or Tenerife, in the shape of a triangular pyramid, with triple-armed rifts and landslide lobes between the rifts. The southward migration of volcanism in La Palma left the northern shield extinct, the rifts incomplete and finally configured an island lengthened in a N-S direction. Another point of interest is that the islands of La Palma and El Hierro are the first of the Canaries to form simultaneously, with possibly alternating eruptive activity, at least in the most recent period. This separation in a «dual line» of islands and the greater depth of its oceanic basement account for the long time they have required to emerge since the formation of the prior island of La Gomera.

The island of El Hierro is geologically somewhat younger than La Palma and, because it formed over a stationary source of magma, it presents, in comparison, a perfect, concentric development, with superimposed volcanoes and a regular three-armed rift geometry. The activity of the subaerial volcanism began in El Hierro with the development of Tiñor volcano on the NE flank of the island (approximately from 1.12 to 0.88 ma), with the emission of massive typical basalts. The volcano developed quickly, with different stages of growth, the eruption of Ventejís volcano being the terminal explosive stage, and probably the precursor of the collapse of the NW flank of the edifice some 882 ka ago. The emissions of the new volcano —El Golfo, approximately 545 to 176.000 ka— totally filled the depression of the lateral collapse of Tiñor volcano, the lava flows of which then spilled over the flanks of the earlier volcano. The beginning of the construction of the El Golfo volcano seems to have taken place after a relatively long

period of activity, probably coinciding with the maximum development of the Cumbre Nueva rift on La Palma. The initial subaerial activity at El Golfo was characterised by basaltic lavas that evolved to trachybasalts and trachytes, and finally towards more differentiated eruptive episodes indicative of the terminal state of the volcanic activity of the El Golfo volcano. The excessive growth of this volcano triggered the failure of its north flank, generating the spectacular scarp and present El Golfo depression. Subsequent volcanism, from emission vents arranged in a three-armed rift system (rift volcanism, with ages ranging from 145 ka to 2,500 years, with probably prehistoric eruptions), implies the much more moderate continuation of the earlier predominantly basanitic-tephritic volcanic activity. This period may correspond to that of maximum development of the Cumbre Vieja rift, in the island of La Palma.

**RESUMEN**

Las Canarias occidentales, relativamente poco estudiadas hasta hace unos años desde el punto de vista geológico, han aportado sin embargo datos decisivos para la comprensión de muchos de los problemas geológicos más importantes del archipiélago, que posiblemente se hubieran dilucidado más prontamente si su estudio se hubiese comenzado, como en la mayoría de las cadenas de islas volcánicas oceánicas, por su extremo más reciente.

Como resumen de sus principales rasgos geológicos evolutivos de ambas islas destacamos las siguientes etapas de desarrollo:

Durante el Plioceno se levanta en el extremo occidental del Archipiélago, en la isla de La Palma, un edificio o monte submarino constituido por pillow lavas, pillow brechas e hialoclastitas de composición basáltica, intruido por domos traquíticos, plutones de gabros y una densísima red de diques. Por el efecto de la intensa intrusión magmática y filoniana el edificio submarino sufrió un levantamiento hasta cotas de 1.500 m y basculamiento de 45-50° al SO, seguido de un período de quiescencia y erosión del edificio submarino emergido. La consolidación definitiva y progresión de la construcción de la isla se hace en discordancia angular y erosiva sobre el basamento submarino a partir de al menos unos 1,77 millones de años. La reactivación volcánica subaérea, con predominio de volcanismo explosivo en las fases iniciales con producción de abundantes materiales volcanoclásticos y freatomagmáticos en la base del edificio subaéreo, persistió de forma muy continua hasta al menos 0,41 millones de años. Esta fase subaérea inicial configura el Escudo Volcánico Norte, formado por la superposición de varios edificios volcánicos superpuestos y aproximadamente concéntricos entre sí y con el basamento submarino.

El Escudo Volcánico Norte tiene una primera etapa, desde 1,77 a 1,20 ma, en la que se construye el edificio volcánico Garafía, formado por lavas predominantemente basálticas alcalinas poco diferenciadas y abundancia de lavas «pahoe-hoe», que alcanza una altura de 2.500-3.000 m, con flancos de acusadas pendientes. El rápido crecimiento y progresiva inestabilidad del edificio Garafía culminó hace unos 1,20 millones de años en un deslizamiento gravitatorio del flanco meridional del edificio. La actividad eruptiva que siguió al colapso comienza rellenando la depresión de deslizamiento, levantando un nuevo edificio volcánico —el edificio volcánico Taburiente—, que se apoya sobre una clara discordancia angular producto del deslizamiento. La depresión se rellenó completamente hace unos 0,89 ma, edad de las primeras lavas en desbordarla. El relleno de la depresión por las lavas del Taburiente acaba conformando un apilamiento de coladas horizontales —predominantemente basaltos alcalinos— que se remansan contra la cabecera del escarpe de deslizamiento formando una meseta colgada en el centro del escudo volcánico. Coincidiendo aproximadamente con el límite Matuyama/Brunhes (0,78 ma) se produce una importante reorganización del edificio volcánico Taburiente, cuyos centros de emisión se concentran progresivamente en tres rifts (NO, NE y N-S) cada vez más definidos, y posteriormente en un aparato central situado en el centro geométrico del escudo volcánico. Las abundantes emisiones de esta etapa final recubren las formaciones anteriores, excepto parte de las alineaciones de conos de los rifts. Las lavas se diferencian hacia términos fonolíticos y traquíticos.

El rift meridional (Cumbre Nueva) se desarrolla más que los otros, posiblemente por el comienzo de la migración hacia el sur del volcanismo, formando una dorsal con más de 2.500 m de altura y con el eje mayor en dirección N-S. La progresiva inestabilidad del rift de Cumbre Nueva, por un crecimiento excesivo, provoca el deslizamiento gravitatorio del flanco occidental, proceso que ocurrió hace unos 560 ka y supuso el desgarro de unos 180-200 $km^3$ y la formación de una amplia depresión (el Valle de Aridane) y el inicio de la formación —por encajamiento y erosión remontante— de la Caldera de Tabu-

riente. La actividad posterior al colapso en el escudo norte se concentra preferentemente en el interior de la cuenca de deslizamiento, construyendo rápidamente el estratovolcán Bejenado. Esta actividad es coetánea con la de otros centros residuales y dispersos en los flancos del escudo. Las lavas inicialmente basaníticas del edificio Bejenado evolucionaron hacia tefritas máficas en centros laterales y terminales diferenciados. La actividad del escudo volcánico terminó definitivamente hace unos 0,4 millones de años. Tras un periodo de transición en que hay cierta actividad asociada a centros periféricos del Bejenado, el volcanismo se localiza de forma definitiva y hasta el presente en un nuevo edificio —Cumbre Vieja—, que prolonga la isla hacia el sur. Las lavas más antiguas han sido datadas en 123 Ka, aunque las primeras erupciones del edificio volcánico Cumbre Vieja deben ser bastante más antiguas. En esta última fase del volcanismo de La Palma se ha configurado un rift progresivamente estructurado en la dirección N-S, con lavas predominantemente basaníticas, tefritas y tefri-fonolitas, e intrusiones en forma de domos y coladas de tefri-fonolitas y fonolitas, asociados a episodios eruptivos que se continúan hasta la actualidad. Recientemente se han observado y muestreado numerosos centros eruptivos submarinos que prolongan el rift de Cumbre Vieja hacia el sur en el océano, algunos de éstos aparentemente muy recientes.

La previsible evolución geológica de este rift es similar a la de su antecesor de Cumbre Nueva, hacia un progresivo desarrollo y creciente inestabilidad, aunque pueden originarse cambios que la modifiquen hacia configuraciones más estables, fundamentalmente la progresión submarina del extremo sur del rift, que podría redistribuir el volumen de productos emitidos, rebajar la relación de aspecto del edificio volcánico y, en consecuencia, su inestabilidad. Las fallas escalonadas generadas en la erupción de 1949 han sido interpretadas como un posible desgarre del flanco occidental del edificio volcánico, aunque una hipótesis más favorable sería la de que tales fallas son superficiales y contribuyen a acomodar el edificio volcánico reduciendo su inestabilidad. Un aspecto a destacar es el importante papel que ha jugado la movilidad del sistema general de alimentación del volcanismo en la forma y estructura de la isla. De no haberse producido una emigración continua del volcanismo desde las fases finales de construcción del escudo norte, la isla de La Palma posiblemente hubiera adquirido una configuración similar a la de las islas de El Hierro o Tenerife, con forma de pirámide triangular, dorsales triples y lóbulos de deslizamiento entre las dorsales. La emigración del volcanismo hacia el sur en La Palma dejó el escudo norte extinguido, los rifts inacabados y configuró finalmente una isla alargada en dirección N-S. Otro interesante aspecto es que las islas de La Palma y El Hierro son las primeras de las Canarias que se están formando de forma simultánea, con una posible alternancia de la actividad eruptiva entre ambas islas, al menos en el período más reciente. Esta «doble» alineación de islas y la mayor profundidad de su asentamiento explican el largo tiempo que han necesitado para emerger desde la emersión de La Gomera, la anterior isla en formarse.

La Isla de El Hierro es geológicamente algo más joven que La Palma y, por haberse formado sobre una fuente magmática estacionaria, ofrece en comparación un perfecto desarrollo concéntrico, con edificios superpuestos y un sistema regular de dorsales triples. La actividad del volcanismo subaéreo se inicia en El Hierro con el desarrollo del edificio Tiñor en la zona NE de la isla desde aproximadamente 1,12 a 0,88 Ma, con emisión de típicos basaltos masivos poco diferenciados. El edificio se desarrolla rápidamente con diferentes estadios de crecimiento, siendo la erupción del centro eruptivo del Ventejís del estadio explosivo terminal, probablemente precursor del colapso del flanco NO del edificio volcánico hace unos 0,88 Ma. Las emisiones del nuevo edificio volcánico —El Golfo, aproximadamente 545 a 176 Ka— rellenan totalmente la depresión originada por el colapso lateral del edificio Tiñor, con coladas que acaban vertiendo por los flancos del edificio anterior. El comienzo de la construcción del edificio volcánico de El Golfo parece haberse producido tras un periodo relativamente largo de inactividad, probablemente coincidente con el máximo desarrollo del rift de Cumbre Nueva en la isla de La Palma. La actividad subaérea inicial de El Golfo se caracteriza por la emisión de lavas basálticas, que evolucionan hacia traquibasaltos y traquitas hacia la parte alta del edificio, y finalmente hacia episodios eruptivos más diferenciados e indicativos del estadio terminal de la actividad volcánica del edificio El Golfo. El excesivo crecimiento de este edificio volcánico provocó el deslizamiento de su flanco norte, generando el espectacular escarpe y depresión actual de El Golfo, proceso que tuvo lugar entre 21 y 133 Ka. El volcanismo posterior, a partir de centros agrupados formando un rift triple (volcanismo de Rift, con edades comprendidas entre los 145 Ka y 2.500 años, con probables erupciones prehistóricas), supone la continuación, mucho más moderada, de la actividad volcánica, predominantemente de basanitas y tefritas. Este periodo de menor actividad eruptiva relativa podría corresponderse con el máximo desarrollo del rift de Cumbre Vieja, en la isla de La Palma.

# LA PALMA AND EL HIERRO IN THE GEOLOGICAL CONTEXT OF THE CANARIAN ARCHIPELAGO

## Regional geological framework

La Palma and El Hierro, located at the western edge of the 450-km-long Canarian archipelago, are the last islands to form and the most active in the Quaternary.

The Canaries rest on old (Jurassic) oceanic lithosphere, La Palma and El Hierro lying along the magnetic anomaly M25 (about 156 ma, according to Klitgord and Schouten, 1986). Each island forms an independent edifice, except Fuerteventura and Lanzarote (Fig. 1 B and C). These edifices developed on increasingly deep ocean floor, reaching a maximum of -4 km in La Palma and El Hierro (Fig. 1 A). Their relative topographic heights and submarine/subaerial volume ratios reflect their stage of development. The island of Tenerife is clearly at its peak of volcanic growth, whereas La Palma and El Hierro are still in the juvenile stage of development, while La Gomera and the eastern islands of Gran Canaria and Fuerteventura–Lanzarote are already deeply eroded (Fig. 1).

The magmatic processes that generated the Canaries are related to a hotspot either spreading westward beneath the lithosphere or fixed under a plate slowly progressing eastward (Carracedo, 1979, 1999; Hoernle and Schmincke, 1993; Carracedo et al., 1998). According to some authors, the Canarian hotspot would be a part of a superplume responsible for the volcanism extending from the Cape Verde islands to eastern Europe (Hoernle et al., 1995; Oyarzun et al., 1997).

Geldmacher et al. (2001) dated the Madeira and Selvagem Islands and modelled three parallel hotspot pathways in the eastern North Atlantic, the Madeira, Canaries and Sahara tracks. The Canarian hotspot track extended from the Lars Seamount, to the north, to the island of El Hierro, in about 70 ma. Any relationship of the Canaries with the Atlas tectonics seems, therefore, out of place, since these tracks are parallel and congruent with the rotation of the African plate defined by Morgan (1983). Only the Canaries are located in the prolongation of the Atlas system, which may merely represent a geographical coincidence.

Radiometric dating of the oldest subaerial volcanism (Guillou et al., 1996, 1998, and 2001) and new ages from La Gomera and Tenerife (work in progress) show that the islands have developed in agreement with the continuous westward progression expected from the hotspot activity. La Palma and El Hierro are the only islands of the archipelago at present in the juvenile shield stage and the remainder of the Canaries are already in the posterosional stage (Fig. 2).

An important change occurred after the formation of La Gomera, apparently splitting the E-W trending, single line, Canarian volcanic belt into a N-S trending dual line, perpendicular to the general trend of the archipelago (see Fig. 3). Large-scale distribution and age progression in most oceanic island chains are well explained by the steady movement of lithospheric plates over fixed mantle plumes, yielding chains of consecutive discrete volcanoes. In this model, a new island starts to form when the bulk of the previous one has already developed, the inter-island distance governed by lithospheric thickness and rigidity (Voght, 1974; ten Brink, 1991). In the Canaries, however, the western islands have developed contemporaneously (Fig. 3). This important change in style may also account for the time interval of about 7-8 ma between the emergence of La Gomera and the western Canaries. This is considerably longer than the time gap between the formation of the single-line islands, decreasing from about 5 ma between Fuerteventura and Gran Canaria, to <3 ma between Tenerife and La Gomera (Figs. 2 and 3).

Dual-line volcanoes, such as the Kea and Loa trends in the Hawaiian Islands, have been associated with changes in plate motion, resulting in the location of a volcanic load off the hotspot axis. In this model of Hieronymus and Bercovici (1999) compressive stresses related to the off-axis volcano block the formation of the next island and split the single line of volcanoes into a dual line of alternating positions of volcanoes. However, the association of the dual line in the Canarian chain with a change in direction of the African plate is not clear (Carracedo et al., 1998; Carracedo, 1999).

This feature may finally explain the distribution of recent (Quaternary) volcanism in the western Canaries. Extensive radiometric dating and magnetic stratigraphy indicate that main phases of eruptive activity alternate in both islands, at least in the last 500 ka, as discussed later (see section III.1 and Fig. 72). This feature may be related to changes in the regional stress fields associated with giant gravitational collapses of the unstable volcanoes at their peak of development. This may also account for the lack of historical eruptions (last 500 years) in El Hierro while most of the historical volcanism of the Canarian archipelago has been located in La Palma.

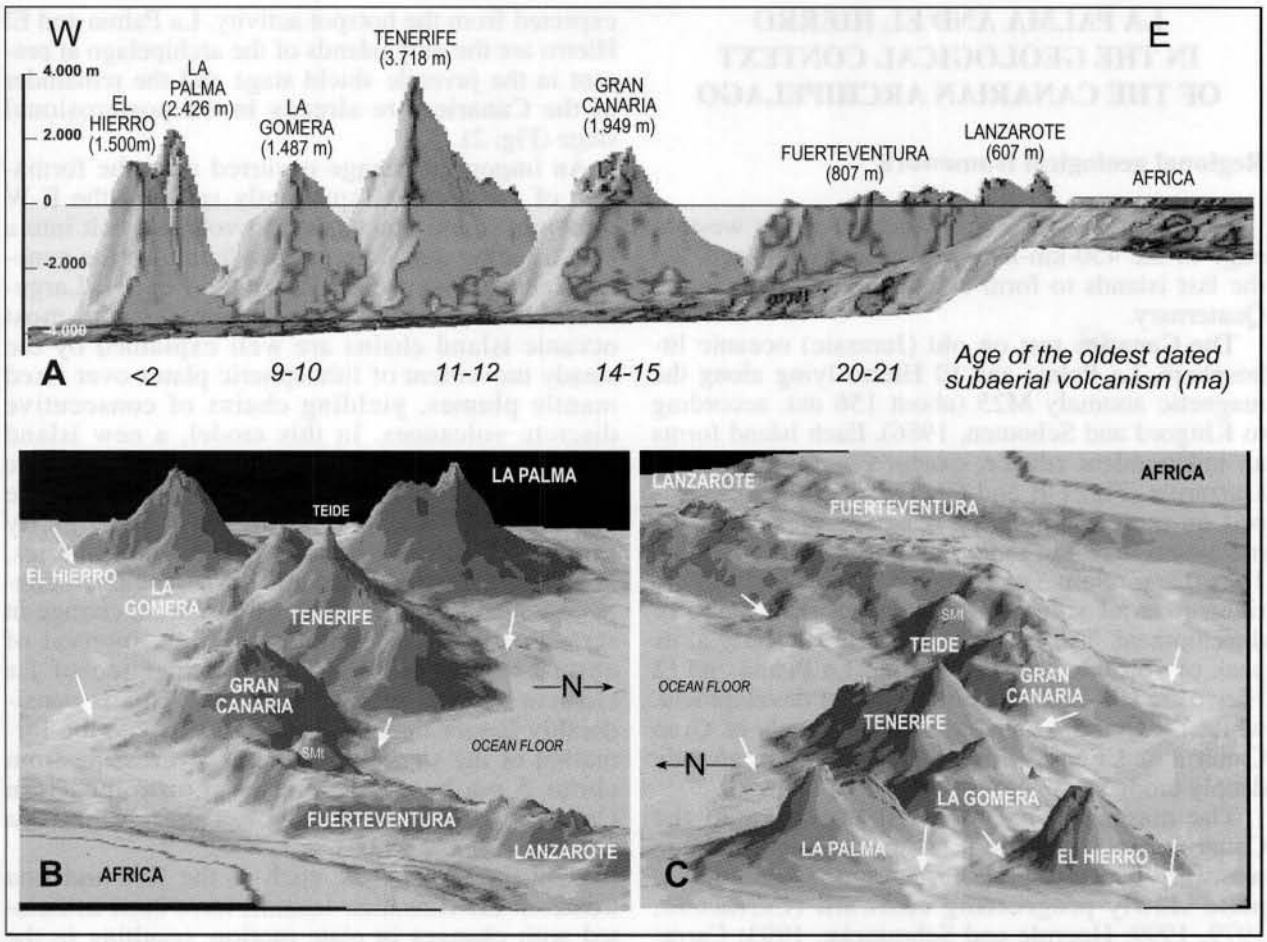


Fig. 1.—Computer-generated 3-D images of the Canary Islands (bathymetry from Hunter et al., 1983) A) Cross section showing age vs. height of the different islands. B) Views from the E and W of the archipelago. The progressive decrease in volume of the island towards the continent due to mass wasting is clearly observed, as well as the change from single to dual line after La Gomera.

## Development of concepts of the geological history of the western Canaries

Fúster and coworkers (1968 a-d) initiated the first modern and comprehensive geological study of the Canaries in the island of Lanzarote. This apparently irrelevant fact may have imposed important difficulties on understanding key geological features of the Canary Islands. The volcanostratigraphic units defined in the eastern, posterosional islands, proved unfeasible in the western Canaries. The definition of 'Old' and 'Recent' Series led to considerable confusion, since the 'Old' Series of La Palma or El Hierro were found to be considerably younger than the 'Recent' Series of Fuerteventura, Lanzarote or Gran Canaria. This circumstance may explain why the knowledge of the geology of the western Canaries was at best scant until a few years ago, lacking even a basic geological map. Concurrently, the insufficient geological knowledge of the juvenile islands hindered the earlier understanding of the role of rift zones, gravitational collapses, etc., as key features in the evolution of the Canaries and oceanic islands in general, as well as the definition of volcanostratigraphic units applicable to the entire archipelago. Furthermore, this approach accounted for the difficulties in defining a model for the genesis and evolution of the Canary Islands that would most probably have been avoided, had the study of the Canaries started, as in the Hawaiian Islands, in the youngest part of the volcanic belt. The persistence of concepts such as the connection of the Canarian magmatism to fractures associated with the Atlas tectonics, or the apparently contrasting structural features in the eastern and western Canaries, would probably have been identified much earlier as lacking geological support or reflecting the different stages of evolution of the islands (Carracedo et al., 1998; Carracedo, 1999).

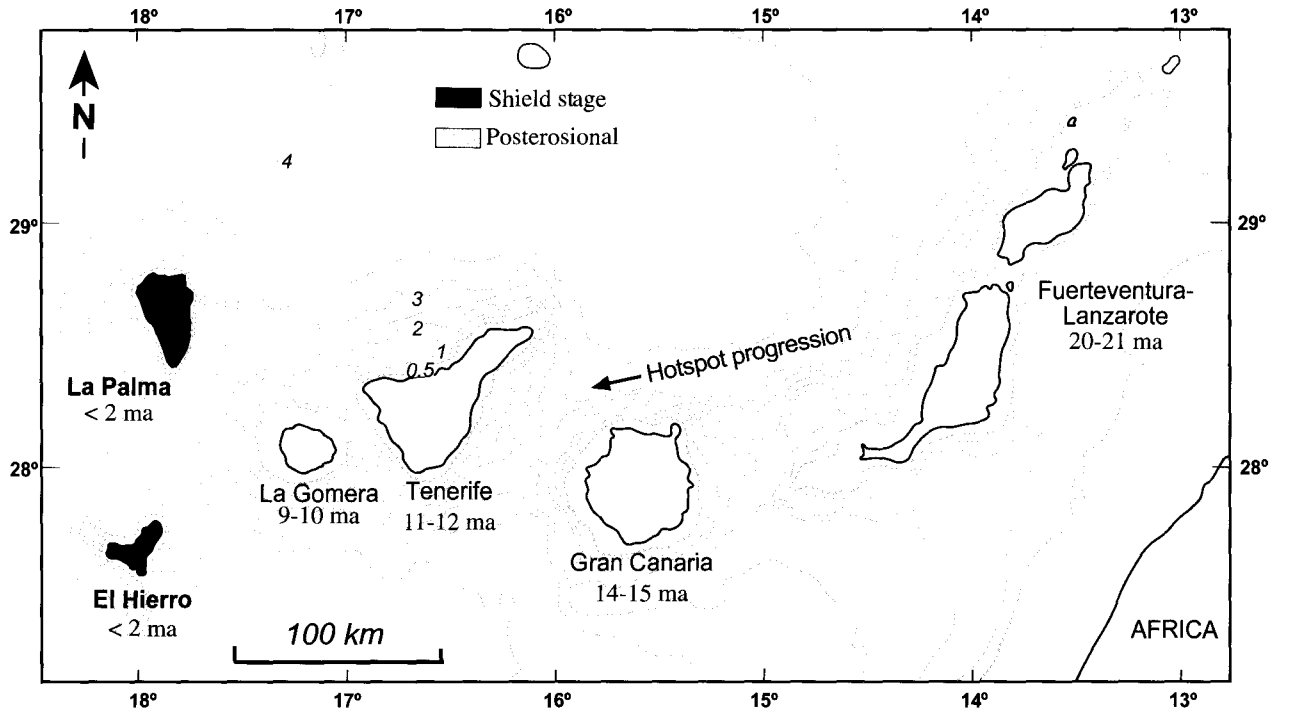


Fig. 2.—Revised oldest ages obtained for the emerged volcanism (work in progress). One of the main inconsistencies of the Canarian hotspot model disappears as the island of Tenerife and La Gomera fit in the general age progression scheme (new ages of Tenerife and La Gomera in work in progress). Note the extended period of time elapsed between the emergence of La Gomera and La Palma-El Hierro dual-line islands.

Several important concepts have been revised following the work carried out in the western Canaries. The structure and composition of the submarine part of the islands was poorly understood prior to the study carried out in La Palma by Staudigel (1981) and Staudigel and Schmincke (1984). In the islands of Fuerteventura, La Gomera and La Palma, the products of shield volcanism rest upon variably deformed and uplifted sequences of submarine sediments, volcanic rocks, dyke swarms and plutonic intrusions which form the cores of these islands. These formations, named 'Basal Complex' by Bravo in 1964, are consistently separated from the subaerial volcanism by a major unconformity. Early interpretations relating these formations to uplifted blocks of 'oceanic basement' in the pre-plate tectonic sense (Hausen, 1958; Fúster et al., 1968 a, b) proved to be inconsistent since the igneous rocks are younger than the oceanic sedimentary sequences (Robertson and Stillman, 1979 a, b). The studies by Staudigel (1981) and Staudigel and Schmincke (1984) demonstrated that the majority of the formations of the 'basal complexes' represent the seamount stage of the growth of these islands. Similar conclusions had been reached for the 'basal complex' of Fuerteventura (Stillman, 1987). Detailed geological mapping inside the Caldera de Taburiente (Carracedo et al., 2001 a, b) showed that several formations previously included in the 'basal complex' of La Palma could be assigned to younger subaerial stratigraphic units. When these units were excluded, the remaining formations conformed to the seamount described by Staudigel (1981) and Staudigel and Schmincke (1984), making the use of the term 'basal complex' unnecessary and confusing, except probably in the island of Fuerteventura, where this formation includes uplifted oceanic sediments.

Caldera-type depressions in the Canaries were incorrectly believed to be originated by erosive, collapse or explosive processes (Fúster et al., 1968 d; Araña, 1971). Some authors had tentatively related these depressions to slumps or gravitational collapses (Hausen, 1956, 1961; Bravo, 1962; Machado, 1963; Navarro and Coello, 1989; Holcomb and Searle, 1991). On-shore and off-shore studies in the western Canaries provided clear evidence that many of these features were initiated by gravitational flank failures of steep, unstable volcanoes, including the prototypical erosion Caldera de Taburiente (Machado, 1963; Ancochea et al., 1994; Carracedo, 1994; Masson, 1996; Urgeles et al.,

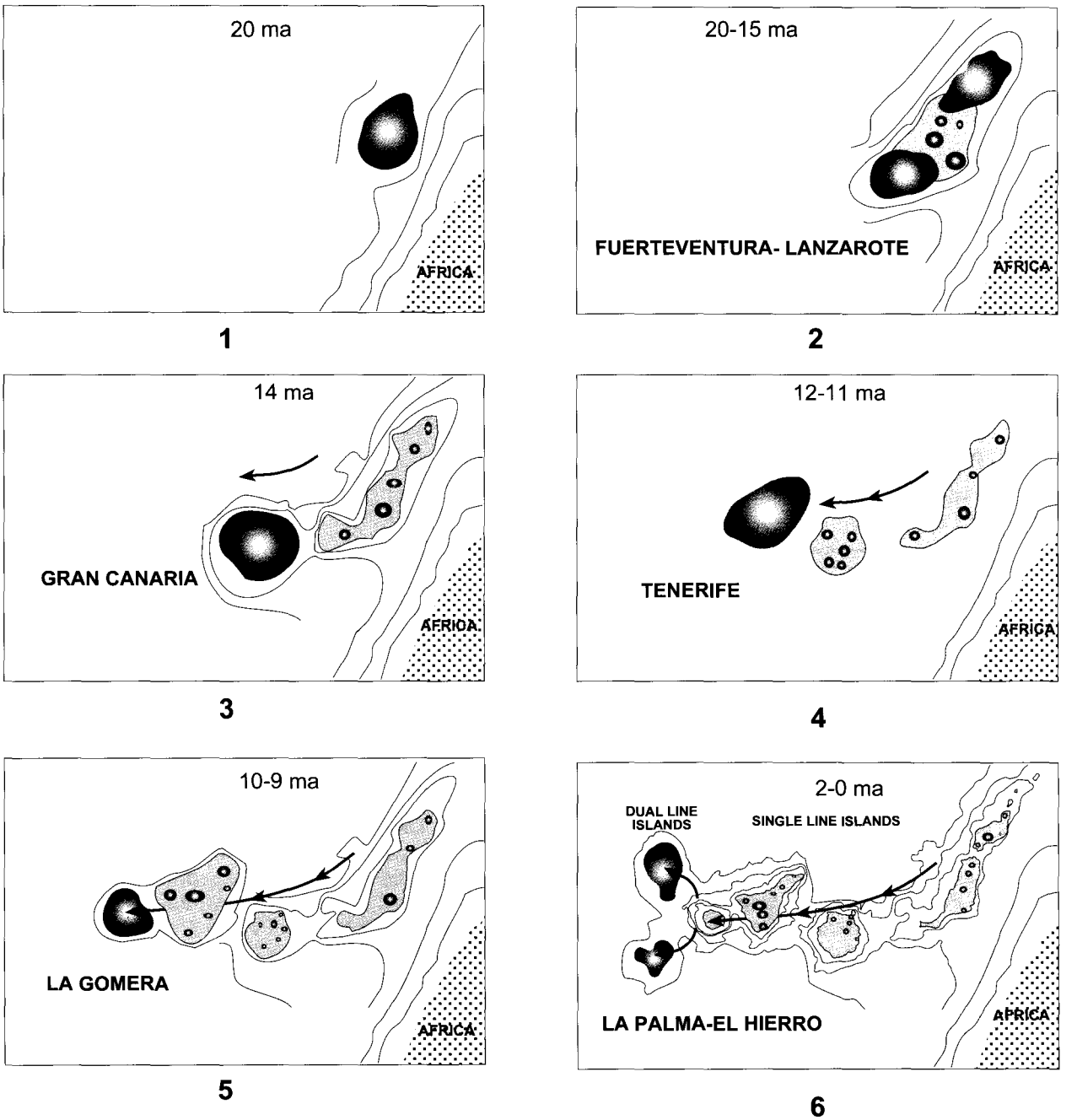


Fig. 3.—Sequential surfacing of the Canary Islands. New ages of Tenerife and La Gomera (work in progress).

1997, 1999; Carracedo et al., 1999 a, b; Masson et al., 2002).

The geological and geochronological study of the western Canaries evidenced the advantages of using the volcano-stratigraphic units defined in the Hawaiian Islands (MacDonald and Abbot, 1970; Walker 1990): the *shield stage* and the *posterosional or rejuvenated stage*. These units were applied to the Canaries (Carracedo et al., 1998; Carracedo, 1999) instead of volcanic series or cycles (Fúster et al., 1968 a-d; Schmincke, 1982). The studies carried out in the western Canaries and in the Madeira and Selvagem islands greatly contributed to show the Canaries not as a singular volcanic archipelago related to the Atlas tectonics, but as a part of the numerous hotspot island chains in the eastern North

Atlantic, strikingly similar to the Hawaiian group and, in general, to oceanic volcanic islands (Carracedo, 1979, 1999 a; Carracedo et al., 1998; Geldmacher et al., 2001). However, the Canaries preserve important peculiarities, such as the lack of significant subsidence (Schmincke et al., 1997; Carracedo et al., 1998; Carracedo, 1999 a) and other features summarized by Schmincke (1994).

## GEOLOGY AND VOLCANOLOGY OF THE ISLAND OF LA PALMA

### Geomorphological features

The island of La Palma is the fifth in extension (706 $km^2$) of the Canaries and the second in elevation (2.423 m asl), after Tenerife. The island is elongated in a N-S trend and is made up of two main polygenetic stratovolcanoes separated by a saddle (the Valle de Aridane depression): the conical northern shield and the elongated Cumbre Vieja volcano at the southern part of the island (Fig. 4). Both volcanoes reach considerable heights (2.430 and 1.990 m asl, respectively).

Rainfall is relatively high (up to 900 mm in the summit areas) because of the altitude and the island's location within the Atlantic. High erosion rates have originated deep, Oahu-type barrancos in the northern shield, whereas the younger Cumbre Vieja volcano is barely incised. Perched ice sheets seem to have formed on the summit of the northern shield, particularly during glaciations, accounting for the periglacial features observed. Rainfall is, however, much lower than in most tropical oceanic islands (Hawaii, Réunion, etc.). Consequently, the island is less vegetated and rock outcrops are abundant and fresh. The demand for water by farming prompted the perforation of several hundred kilometres of horizontal wells or *galerías* to mine groundwater, providing a unique mode of access to the deep structure of the island volcanoes.

Steep slopes are frequent in the island, being mainly structural in the flanks of the Cumbre Vieja volcano, and structural and erosive in the northern shield. The main depressions of the island, the Valle de Aridane and the Caldera de Taburiente, the latter formerly considered to be the prototypical erosion caldera after Lyell's report in 1864, were initiated by gravitational landslides (Machado, 1963; Ancochea et al., 1994; Carracedo, 1994; Carracedo et al., 1999 a, b).

High coastal cliffs are frequent in the northern shield, where rockfalls favour the rapid regression of the coastline. Conversely, the cliffs of the Cumbre Vieja volcano are lower and the verticality frequently smoothed by lava flows and coastal platforms that fossilize the cliffs and retard the progression of coastal erosion. Beaches are sparse and made up of basaltic blocks, pebbles and sand. Beachrocks have formed and are in progress in several beaches of the western coast of the Cumbre Vieja volcano (Calvet et al., in press).

Swath bathymetry coverage around La Palma (Masson et al., 2002) shows important features related to the constructional and destructive events of the submarine part of the island. The shaded relief images obtained by these authors (Fig. 5) clearly outline the debris avalanche deposits originated in gravitational slope failures (DAD in Fig. 5) and the submarine extension of the main rift zones (SSR in Fig. 5).

### Age of volcanism

About 118 radiometric ages (K/Ar, $^{40}Ar$-$^{39}Ar$ and $^{14}C$) of volcanics of La Palma have been published since the first ages obtained by Abdel Monem and co-workers in 1972. However, the increase in the number of ages can hinder rather than contribute to the precise reconstruction of the geochronology and volcanic history of the islands, because of the absence in some cases of stringent controls in the selection of rock samples and inter-laboratory cross-checking. Contrarily to geochemical analyses, dating methods lack precise controls of the accuracy and reliability of the results (ages). Argon loss or excess in rock samples can result in erroneous ages that nevertheless are usually published and generally accepted. As the number of ages increases the errors also increase and, if all the ages are equally considered, the stages of volcanic history of the islands tend to be artificially enlarged and confusing, as illustrated in Fig. 6.

The precision of these ages has been greatly improved by: 1) using both K/Ar and $^{40}Ar$-$^{39}Ar$ methods, 2) using replicate age determinations, 3) collecting samples in stratigraphic sequences, 4) separating out microcrystalline groundmass for K and Ar analysis, 5) using an unspiked K-Ar technique (Cassignol et al., 1978) to determine the isotopic composition of Ar and Ar content with a precision of 0.4% (± 2s), 6) cross-correlating the ages and their polarities with the magnetostratigraphy defined by field and laboratory measurements and with the established geomagnetic and astronomic polarity time scales (GPTS and APTS) (Carracedo, 1975; Carracedo and Soler, 1995; Guillou et al., 1996, 1998, 2001).

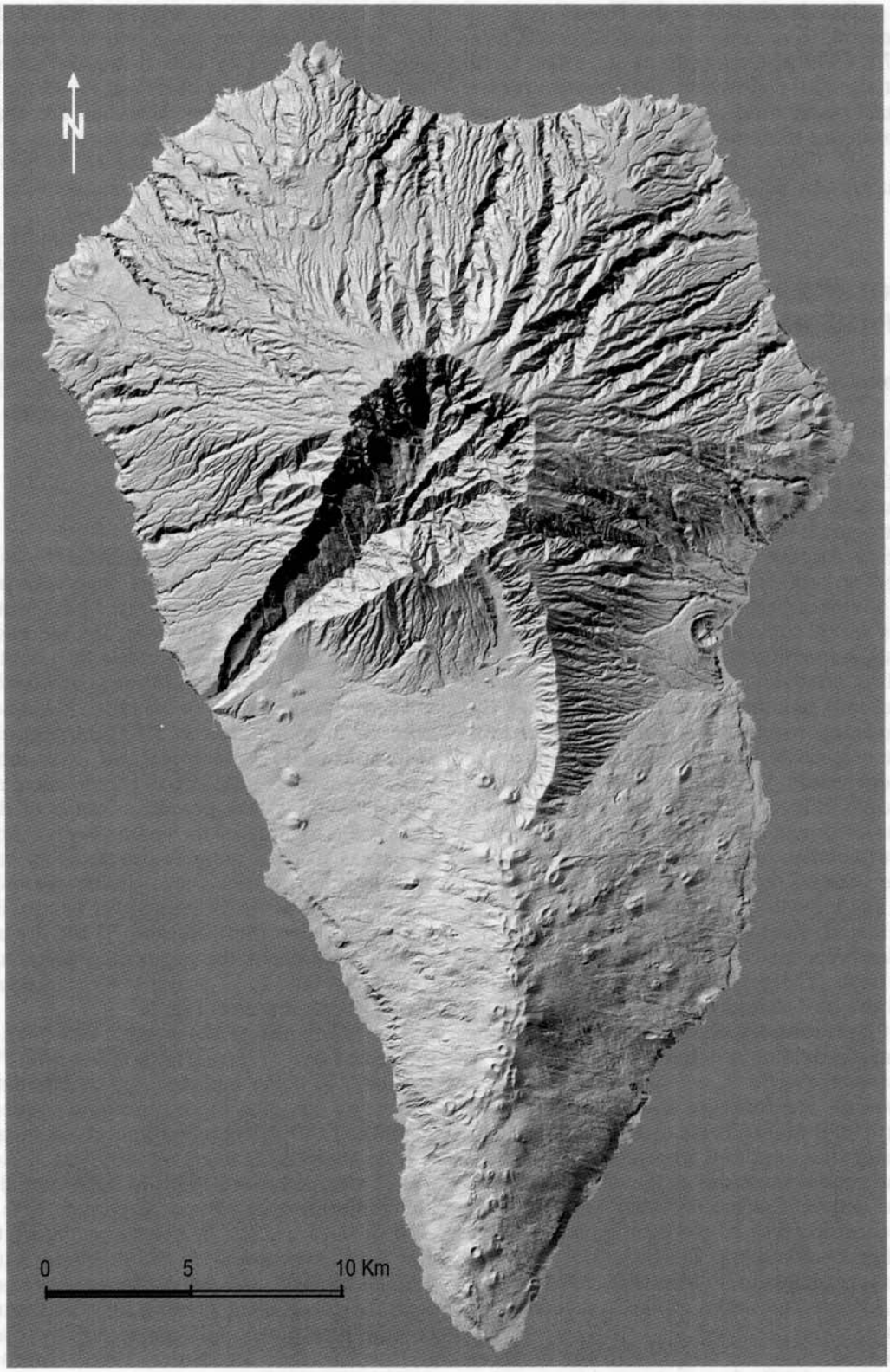


Fig. 4.—Shaded relief image of La Palma showing the main geomorphological features (image GRAFCAN).

The island of La Palma is probably a prime scenario to study the duration of each volcanic stage of an oceanic volcano and to check the consistency of the radiometric ages obtained. The rapid and continued growth of the island and the homogeneity of the volcanic formations make the combination of geological mapping, magnetostratigraphy and radiometric dating extremely useful to individualize each unit stratigraphically and temporally. This provides a framework for further control of the reliability of the ages and to cross-examine the results obtained by the different methods. Preliminary works in La Palma by Abdel Monem et al. (1972), Staudigel et al. (1986) and Ancochea et al. (1994) established an age interval from about 2 ma to present for the volcanic activity of La Palma (B, C and D in Fig. 6). Another 85 unspiked K/Ar and $^{40}Ar$-$^{39}Ar$ ages from La Palma (Fig. 7 and Table 1) have been published by Guillou and co-workers (1998, 2001) and Carracedo and co-workers (2001 a, b). Moreover, some of these flows recorded reversals of the earth's magnetic field and/or magnetic events (Abdel-Monem et al., 1972; Carracedo, 1979; Quidelleur and Valet, 1994; Guillou et al., 1998, 2001; Carracedo et al., 2001 a, b; Singer et al., 2002). Nevertheless, only recently has an extensive comparison been attempted between the radiometric ages and the geomagnetic and astronomical polarity time scales (GPTS and APTS) in order to test the geological significance of the published K-Ar ages for the western Canaries (Guillou et al., 2001; Carracedo et al., 2001 a, b).

Detailed geological and palaeomagnetic polarity mapping of the islands of Tenerife, La Palma and El Hierro allowed the sampling of rocks for dating after defining their relative stratigraphic position and geomagnetic polarity (Carracedo, 1979; Guillou et al., 1996, 2001; Carracedo et al., 2001 a, b). In La Palma, two dating techniques from different laboratories, the unspiked K-Ar (Guillou et al., 1996) and $^{40}Ar$-$^{39}Ar$ (Guillou et al., 2001) methods, were combined to ensure the overall geological significance of the ages. Samples of the same volcanic units were dated using both techniques for comparison purposes. The magnetic polarity of each unit was established on the field using a portable magnetometer (fluxgate) and confirmed by laboratory measurements. Radiometric ages were confronted to polarity ages and, when possible, dated samples were collected within well-established stratigraphic sections in lava sequences, and at the lower and upper limits of the main volcanic sequences and geomagnetic polarity units. The results of this restrictive multidisciplinary approach for dating the island of La Palma are shown in Figs. 7 and 8 and Table 1. These ages show that two separate volcanoes, corresponding to the northern shield and the Cumbre Vieja volcano, form the subaerial part of the island. The apparent gap separating the development of these volcanoes (see Figs. 6 and 8) may correspond either to a period of volcanic quiescence, or to incomplete sampling of the earlier, inaccessible sequences of the initial stages of Cumbre Vieja volcano.

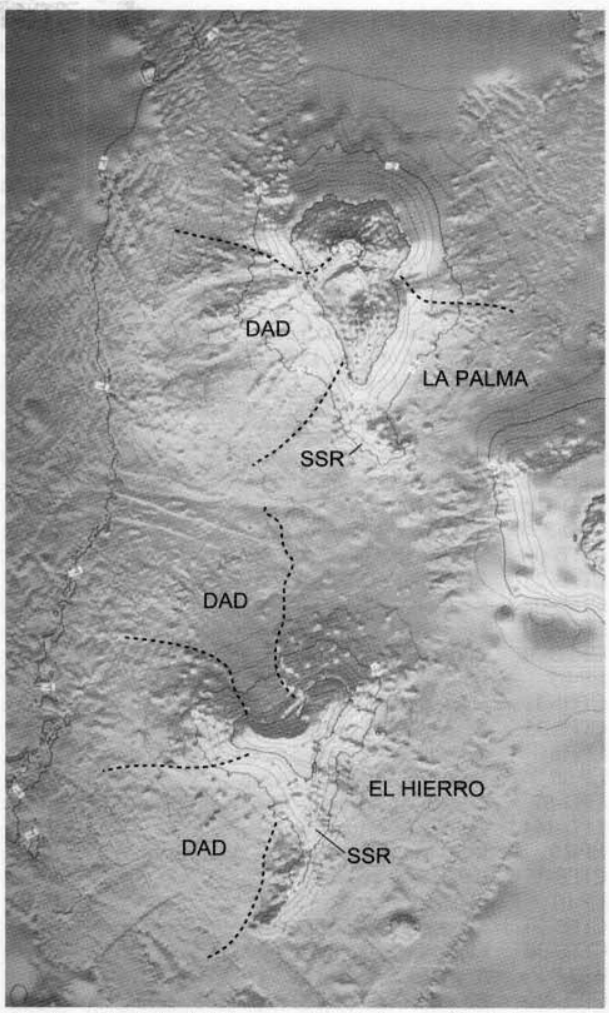


Fig. 5.—Shaded relief image of La Palma and El Hierro with indication of the main features of the submarine flanks: submarine rifts (SSR in the figure) and debris avalanche deposits from gravitational flank collapses (DAD). Images from Masson et al., 2002.

Several features of Fig. 6 are worthy of analysis. Since the ages reported by the different groups are taken from the same volcanic formations they should be consistent within some error margin. However, as indicated in Fig. 6, there is a clear disparity in the ages and duration of the Cumbre Vieja and Bejenado volcanoes. New (25) radiometric ages

Table 1.—**Location, type of rock, geomagnetic polarity and age of volcanics from La Palma (Ages from Guillou et al., 1998, 2001)**

| Sample | Locality | Type of rock | UTM | Pol | Method | Age mean value |
|---|---|---|---|---|---|---|
| CILP 62 | Galería Cuevitas, 2,600 m | Basalt | 2245/31906 | R | K/Ar | 1.72 ± 0.02 ma |
| LPD-159 | Galería Los Hombres, 1,500 m | Basalt | 2197/31882 | R | $^{40}Ar/^{39}Ar$ | 1.65 ± 0.08 ma |
| LPD-155 | Galería Los Hombres, 2,100 m | Basalt | 2197/31882 | R | $^{40}Ar/^{39}Ar$ | 1.61 ± 0.12 ma |
| LPD-119 | Bco. El Agua, 1,365 m | Basalt | 2235/31856 | R | $^{40}Ar/^{39}Ar$ | 1.52 ± 0.10 ma |
| CITB-21 | Bco. Las Grajas, 1,630 m | Basalt | 2165/31865 | R | K/Ar | 1.49 ± 0.22 ma |
| CITB -06 | Bco. Gallegos, 455 m | Basalt | 2236/31907 | R | K/Ar | 1.44 ± 0.02 ma |
| CITB -05 | Bco. El Agua, 485 m | Basalt | 2262/31879 | R | K/Ar | 1.44 ± 0.03 ma |
| LPD-118 | Bco. El Agua, 1,465 m | Basalt | 2235/31854 | R | $^{40}Ar/^{39}Ar$ | 1.38 ± 0.14 ma |
| CITB-22 | Bco. Franceses, 415 m | Basalt | 2222/31910 | R | K/Ar | 1.37 ± 0.02 ma |
| CILP-63 | Galería Cuevitas, 1,600 m | Basalt | 2245/31906 | N | K/Ar | 1.27 ± 0.01 ma |
| LPD-376 | Bco. Los Hombres, 115 m | Basalt | 2195/31923 | R | $^{40}Ar/^{39}Ar$ | 1.23 ± 0.09 ma |
| CITB-19 | Bco. Gallegos, 470 m | Basalt | 2238/31909 | R | K/Ar | 1.20 ± 0.02 ma |
| LPD-372 | Bco. Jieque, 1,400 m | Basalt | 2146/31809 | N | $^{40}Ar/^{39}Ar$ | 1.20 ± 0.05 ma |
| LPD-160 | Galería Los Hombres, 1,400 m | Basalt | 2197/31882 | N | $^{40}Ar/^{39}Ar$ | 1.12 ± 0.20 ma |
| LPD-100 | Tamagantera trail, 2,160 m | Basalt | 2204/31854 | LI | $^{40}Ar/^{39}Ar$ | 1.08 ± 0.04 ma |
| LPD-106 | Tamagantera trail, 1,920 m | Basalt | 2204/31859 | N | $^{40}Ar/^{39}Ar$ | 1.02 ± 0.08 ma |
| LPD-366 | La Cumbrecita, 1,400 m | Basalt | 2213/31781 | N | $^{40}Ar/^{39}Ar$ | 1.02 ± 0.04 ma |
| CITB-09 | Bco. de Los Hombres, 245 m | Basalt | 2201/31925 | N | K/Ar | 948 ± 14 ka |
| CITB-23 | Bco. Franceses, road east of barranco, 440 m | Basalt | 2219/31912 | R | K/Ar | 936 ± 14 ka |
| CITB-08 | Bco. de Los Hombres, 15 m | Basalt | 2207/31931 | R | K/Ar | 932 ± 14 ka |
| LPD-93 | Lomo del Caballo, 1,860 m | Basalt | 2220/31877 | R | $^{40}Ar/^{39}Ar$ | 890 ± 160 ka |
| CI TB-38 | Bco. Gallegos, road east of barranco, 515 m | Basalt | 2238/31908 | R | K/Ar | 886 ± 14 ka |
| LP-05 | Bco. Las Angustias, 45 m | Basalt | 2126/31735 | R | K/Ar | 853 ± 10 ka |
| CITB-31 | Hacienda del Cura, 1,080 m | Basalt | 2160/31793 | R | K/Ar | 836 ± 14 ka |
| CITB-35 | Barranco de Los Hombres, 60 m | Basalt | 2196/31927 | R | K/Ar | 833 ± 14 ka |
| LP-18 | Road to Los Llanos-Sta. Cruz, Km 18.5 | Basalt | 2232/31721 | R | K/Ar | 834 ± 12 ka |
| LP 06 | Bco. Las Angustias, 445 m | Basalt | 2127/31776 | R | K/Ar | 833 ± 11 ka |
| LPD-87 | Bco. El Agua, trail to Marcos-Cordero, 360 m | Basalt | 2248/31851 | N | $^{40}Ar/^{39}Ar$ | 770 ± 90 ka |
| LPD-164 | Galería Los Hombres, 675 m | Basalt | 2197/31882 | N | $^{40}Ar/^{39}Ar$ | 770 ± 40 ka |
| LP-19 | Road to Los Llanos-Sta. Cruz, Km 18.3 | Basalt | 2233/31722 | N | K/Ar | 770 ± 11 ka |
| CITB-15 | Bco. Seco, 270 m | Basalt | 2309/31805 | N | K/Ar | 737 ± 12 ka |
| LP-07 | El Time, 465 m | Basalt | 2127/31747 | N | K/Ar | 734 ± 8 ka |
| CITB-36 | Road to La Fajana Los Hombres, 280 m | Basalt | 2202/31992 | R | K/Ar | 731 ± 11 ka |
| CITB-30 | La Cumbrecita, dyke, 1,395 m | Basalt | 2213/31781 | LI | K/Ar | 726 ± 12 ka |
| BEJ-02 | Borehole S-01 315 m | Basalt | 2168/31738 | N | K/Ar | 710 ± 11 ka |
| CITB-20 | Bco. del Cedro, 1,850 m (sobre discordancia) | Basalt | 2179/31861 | N | K/Ar | 681 ± 10 ka |
| CITB-32 | Barranco Jieque, 1,460 m | Basalt | 2151/31812 | N | K/Ar | 660 ± 11 ka |
| LP-22 | Camino Ermita La Peña, 1,247 m | Basalt | 2233/31745 | N | K/Ar | 659 ± 11 ka |
| LP-21 | Camino Ermita La Peña, 1,310 m | Basalt | 2234/31745 | N | K/Ar | 647 ± 10 ka |
| LP-20 | Camino Ermita La Peña, 1,370 m | Basalt | 2236/31746 | N | K/Ar | 621 ± 9 ka |
| CITB-39 | Bco. Franceses, road east of barranco, 470 m | Basalt | 2219/31913 | N | K/Ar | 620 ± 9 ka |
| LPD-91 | Lava from Mña. de La Yedra | Basalt | 2197/31735 | N | $^{40}Ar/^{39}Ar$ | 590 ± 40 ka |
| CITB-27 | Road El Roque to the coast, 635 m | Basalt | 2085/31846 | N | K/Ar | 585 ± 10 ka |
| LPD-91B | Lava from Mña. de La Yedra | Tephrite | 2197/31735 | N | $^{40}Ar/^{39}Ar$ | 580 ± 30 ka |
| CITB-37 | Road to La Fajana de Los Hombres, 330 m | Basalt | 2202/31926 | N | K/Ar | 575 ± 9 ka |
| CITB-07 | Bco. Gallegos, 520 m | Basalt | 2238/31913 | N | K/Ar | 567 ± 8 ka |
| LP-04 | Ermita de La Peña trail, 1,400 m | Basalt | 2238/31744 | N | K/Ar | 566 ± 8 ka |
| CITB-03 | Punta Gorda harbour cliff, 125 m | Basalt | 2066/31847 | N | K/Ar | 563 ± 8 ka |
| CITB-28 | Bco. del Roque, 560 m | Basalt | 2089/31841 | N | K/Ar | 560 ± 9 ka |
| CITB-12 | Coast of Puntallana (Pta. Salinas), 90 m | Basalt | 2334/31822 | N | K/Ar | 560 ± 8 ka |
| CITB-17 | Coast of La Fajana de Barlovento, 0 m | Basalt | 2276/31938 | N | K/Ar | 549 ± 8 ka |
| BEJ-01B | Lava from Bejenado, borehole S-01, 73 m | Basalt | 2168/31738 | N | K/Ar | 549 ± 12 ka |
| BEJ-01 | Lava from Bejenado, borehole S-01, 73 m | Basalt | 2168/31738 | N | K/Ar | 537 ± 8 ka |
| CITB-11 | Bco. El Jurado, 500 m | Basalt | 2116/31789 | N | K/Ar | 533 ± 8 ka |
| CITB-01 | Lava Mña. Negra, Pta. Gutiérrez, 360 m | Basalt | 2085/31884 | N | K/Ar | 531 ± 9 ka |
| LPD-165 | Galería Los Hombres, 220 m | Basalt | 2197/31882 | N | $^{40}Ar/^{39}Ar$ | 530 ± 70 ka |
| MLP-358 | Morro Pinos Gachos (western rim of the Caldera) | Phonolite | 2166/31817 | N | K/Ar | 525 ± 8 ka |
| CITB-24 | Coast of Juan Adalid, 250 m | Basalt | 2168/31942 | N | K/Ar | 507 ± 8 ka |
| MLP-419 | Piedra Llana (NE. Caldera) | Phonolite | 2229/31828 | N | K/Ar | 499 ± 7 ka |
| LPD-137 | Top of Bejenado, 1,580 m | Basalt | 2206/31773 | N | $^{40}Ar/^{39}Ar$ | 490 ± 60 ka |

Table 1.—**Location, type of rock, geomagnetic polarity and age of volcanics from La Palma (Ages from Guillou et al., 1998, 2001)** *(continued)*

| Sample | Locality | Type of rock | UTM | Pol | Method | Age mean value |
|---|---|---|---|---|---|---|
| CITB-33 | Tamagantera, trail 2,210 m | Basalt | 2206/31853 | N | K/Ar | 440 ± 8 ka |
| LPD-42 | Cliff of Playa de La Veta, 250 m | Basalt | 2092/31843 | N | $^{40}Ar/^{39}Ar$ | 410 ± 80 ka |
| LP 10 | Cliff of Playa Nueva | Basalt | 2161/31683 | N | K/Ar | 123 ± 3 ka |
| LP 12 | Cliff of Puerto Naos | Basalt | 2158/31658 | N | K/Ar | 121 ± 2 ka |
| LP 183 | Cliff of Puerto Tazacorte | Basalt | 2124/31723 | N | K/Ar | 120 ± 3 ka |
| LP 11 | Cliff of Puerto Naos | Basalt | 2157/31661 | N | K/Ar | 95 ± 4 ka |
| LP 08 | Cliff of Playa Nueva | Basalt | 2164/31679 | N | K/Ar | 100 ± 4 ka |
| LP 13 | Cliff of Puerto Naos | Basalt | 2172/31636 | N | K/Ar | 90 ± 3 ka |
| LP 25 | Roque Teneguía | Phonolite | 2203/31537 | N | K/Ar | 56 ± 2 ka |
| CV 154 | La Fajana., Lava from V. Fuego (W) | Tephrite | 2209/31555 | N | K/Ar | 36 ± 1 ka |
| LP 14 | C-832 Km 39. Dome of Dña. María | Phonolite | 2187/31642 | N | K/Ar | 34 ± 1 ka |
| CV 151 | Cliff of Puerto Tigalate | Tephri-Phonolite | 2265/31590 | N | K/Ar | 27 ± 1 ka |
| LP 16 | Lava dome of Mendo | Traqui-Phonolite | 2195/31622 | N | K/Ar | 26 ± 1 ka |
| CV 150 | Tiguerorte. Bco. La Lava | Tephrite | 2274/31629 | N | K/Ar | 25 ± 2 ka |
| CV 163 | Las Salineras | Basanita | 2297/31635 | N | K/Ar | 21 ± 2 ka |
| CV 152 | Cliff of Puerto Tigalate (80 m) | Tephrite-Trachybas | 2262/31586 | N | K/Ar | 20 ± 2 ka |
| LP 01 | C-832 Km 39 Km 34 | Tephri-Phonolite | 2196/31596 | N | K/Ar | 18 ± 2 ka |
| LP 02 | C-832 Km 39 Km 35.5 | Tephri-Phonolite | 2194/31613 | N | K/Ar | 15 ± 2 ka |
| LP 09 | Cliff of Playa Nueva | Basalt | 2164/31678 | N | K/Ar | 8 ± 2 ka |
| CV 165 | Road to airport, Km 1.2 | Basalt | 2301/31718 | N | K/Ar | 8 ± 1 ka |
| LP95SD14 | Charcoal in phreatomag. ash, Bco. Llanos del Agua | Charcoal | 2212/31656 | N | C14 | 7.99 ± 0.08 ka |
| LP95SD11 | Barranco Los Llanos del Agua | Charcoal | 2206/31657 | N | C14 | 6.85 ± 0.06 ka |
| LP 03 | Birigoyo, northern flank | Tephrite | 2216/31678 | N | K/Ar | 6 ± 2 ka |
| CV 156 | C-832 Km 25.5. Lava from V. Fuego (E) | Tephri-Phonolite | 2234/31569 | N | K/Ar | 4 ± 2 ka |
| CV 155 | Las Indias. Lava from V. La Fajana | Tephrite | 2197/31561 | N | K/Ar | 3 ± 2 ka |
| LPC14-01 | La Fajana | Charcoal | 2234/31569 | N | C14 | 3.2 ± 0.01 ka |
| LP94SD7 | Crater of El Fraile cone | Charcoal | 2227/31655 | N | C14 | 2.31 ± 0.05 ka |
| LPC14-03 | Nambroque, SE flank. | Charcoal | 2246/31643 | N | C14 | 1.04 ± 0.09 ka |
| LPC14-04 | Lava from Mña. Goteras volcano | Human bones | 2298/31657 | N | C14 | 1.09 ± 0.05 ka |

obtained by Guillou et al. (1998, 2001 and this work) from these volcanoes, many of them in stratigraphic sections, show the lava outcrops of the Cumbre Vieja constrained to the last 123 ka. Contrarily, the ages of Abdel Monem et al. (1972) and Ancochea et al. (1994) for the same volcanic sequences are significantly older, many of them from intrusions that are dated as older than the lavas they intrude. As discussed below, the Bejenado volcano developed unconformably on the debris avalanche deposits of the Cumbre Nueva flank collapse at about 560 ka (Carracedo et al., 1999 a, b) and should, therefore, be younger than this age. However, most of the ages reported by Ancochea et al. (1994) predate the collapse and, accordingly, this volcano should be anterior and not the filling of the collapse embayment. Finally, the apparently important gap between the Taburiente and Garafía volcanoes (Lower and Upper Old Series of Ancochea et al., 1994) merely reflects incomplete sampling, as in the ages from Abdel Monem et al. (1972) and Staudigel et al. (1986).

These differences are relevant to the definition of the volcanic stratigraphy and history of La Palma, and stress the convenience of interlaboratory cross-checking.

## Main stratigraphic units and volcanoes

The two main stages of the development of oceanic volcanoes, the *submarine* and *subaerial* stages, outcrop in La Palma, after the former was uplifted to about 1 km asl.

The main volcanic stratigraphy units of La Palma were defined from the ages and the magnetic stratigraphy shown in Fig. 8. Two different overlapping volcanoes, the Garafía and Taburiente volcanoes, were defined in the northern shield, notwithstanding the fact that the eruptive activity has been substantially uninterrupted. This separation was feasible because of the presence a regional angular discordance, the result of the lateral collapse of the Garafía volcano at about 1.2 ma, as already pointed out by Ancochea et al. (1994). As discussed below in detail, a change in eruptive style allowed the definition of two phases –Lower and Upper– in the Taburiente volcano. Another general discordance related to a

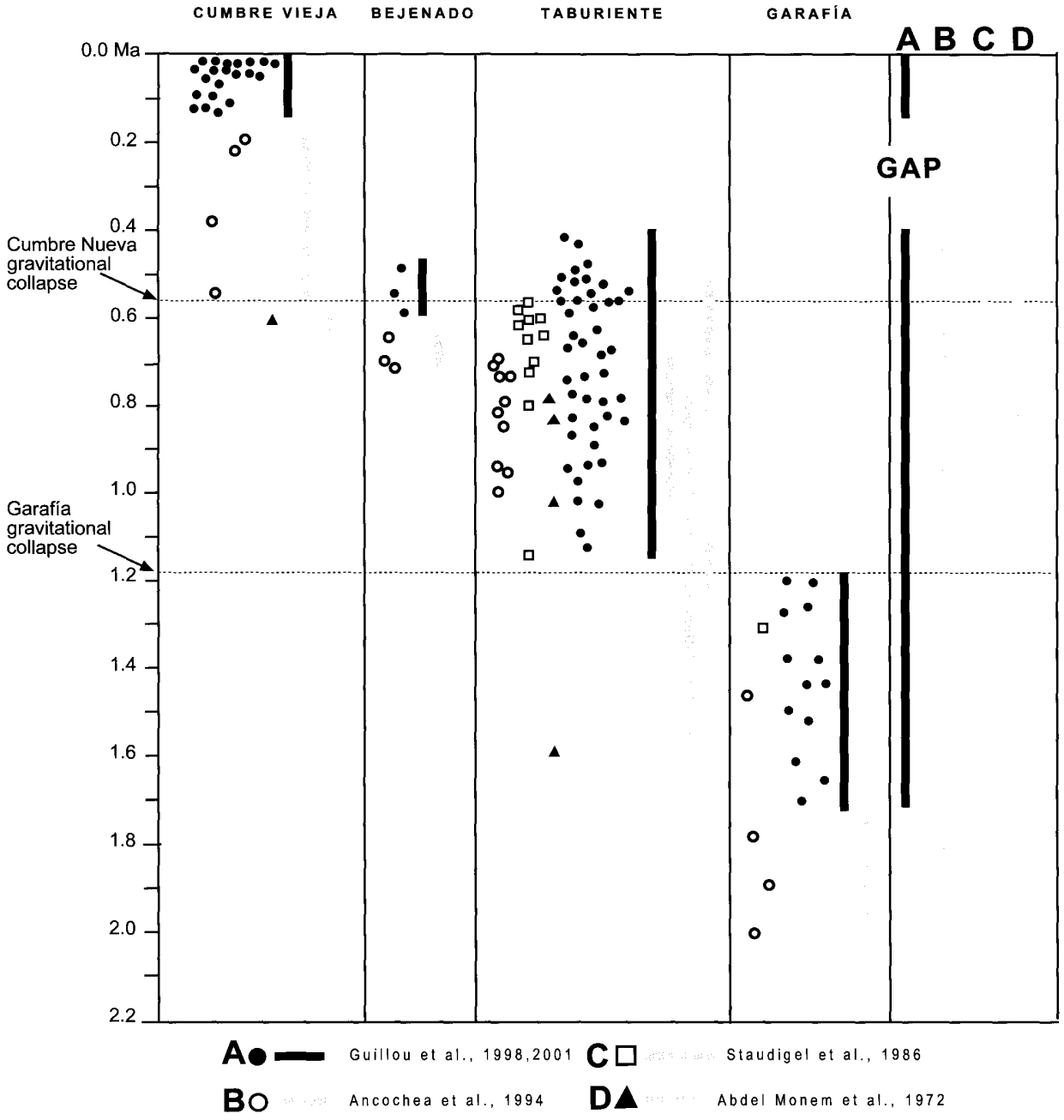


Fig. 6.—Comparison of the ages published from volcanics and intrusives of La Palma.

major gravitational collapse made the separation of the Bejenado volcano possible. All these volcanoes overlap to form the northern shield of La Palma, whereas the Cumbre Vieja forms a clearly independent feature (see Figs. 4, 6, 7 and 8).

Sections in different localities of the Taburiente and Garafía volcanoes, shown in Fig. 9, give a clear indication of the consistency of the ages obtained and their correlation with the established geomagnetic time scale. Similar agreement was attained with the palaeomagnetic and volcanostratigraphic units defined in water tunnels or *galerías* of the northern shield (Fig. 10). These stratigraphic units were, therefore, used in volcanostratigraphic corre-

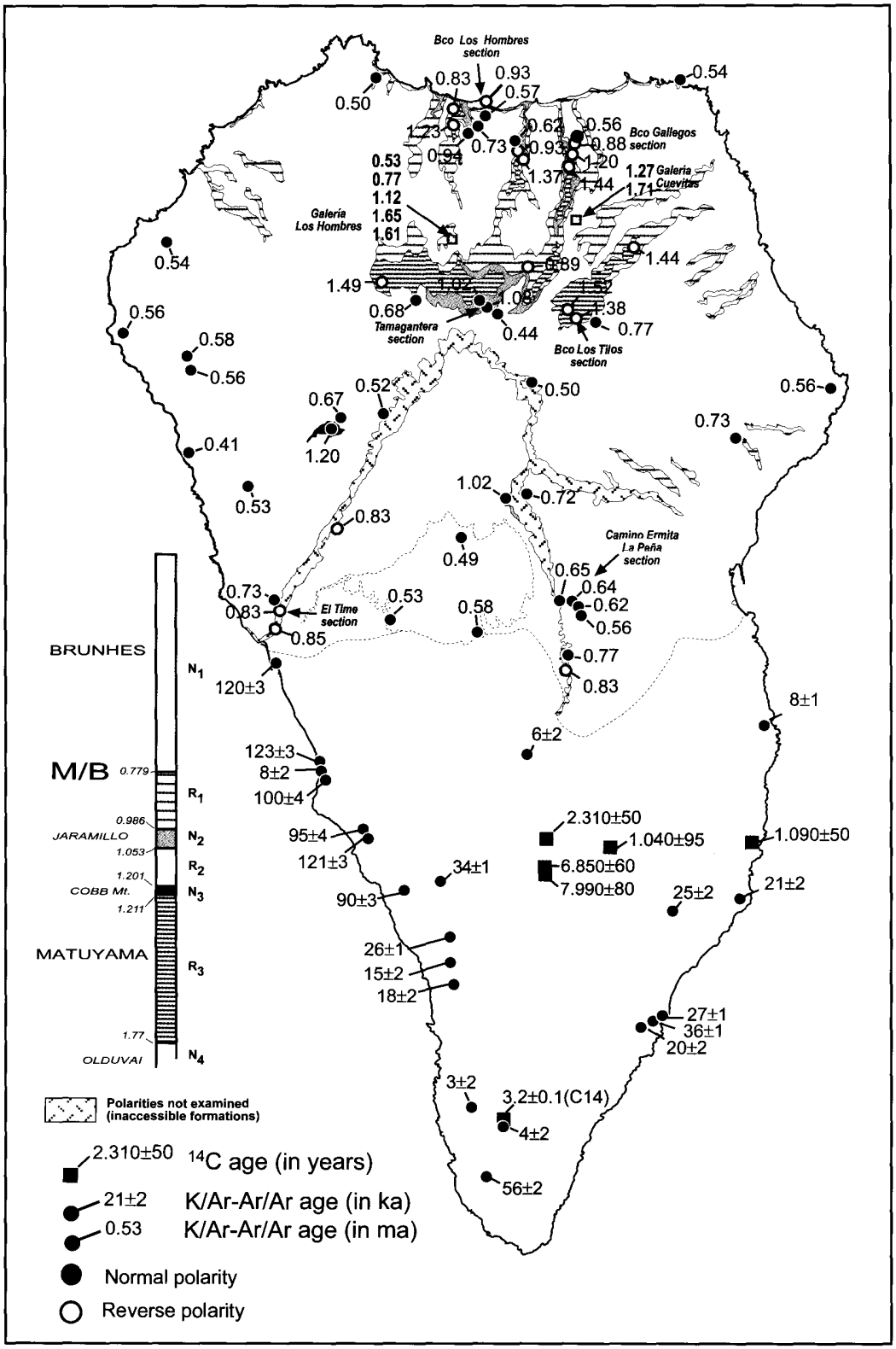


Fig. 7.—Ages and magnetozones of La Palma (ages from Guillou et al., 1998, 2001 and Carracedo et al., 2001 a, b).

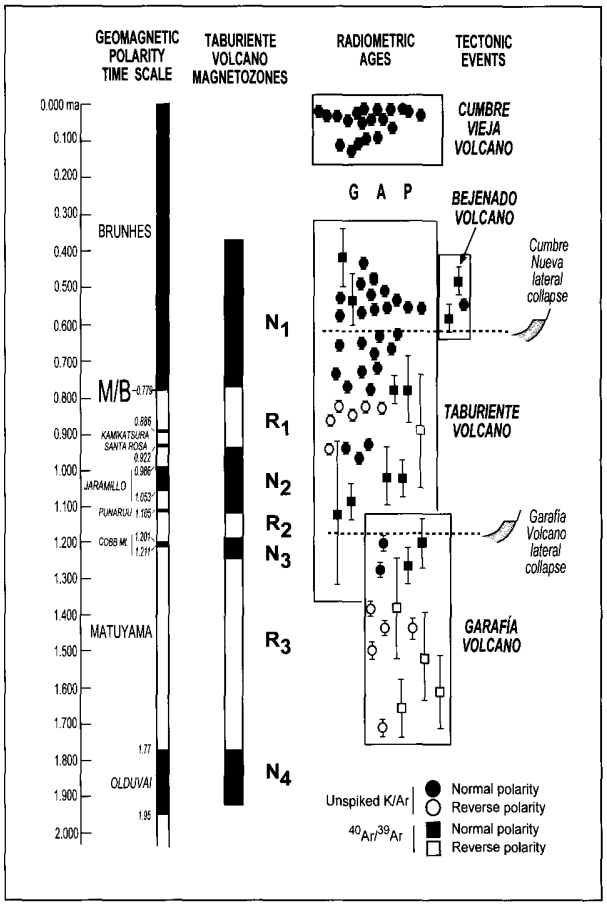


Fig. 8.—Definition of the main volcanostratigraphic units and constructive and destructive events of La Palma from the ages (Guillou et al., 1998, 2001 and Carracedo et al., 2001 a, b) and magnetostratigraphy. N: Normal polarity, R: Reverse polarity.

lation and geological mapping in the island of La Palma, as described below.

## Geological and volcanological description of the stratigraphic units and volcanoes

### *The Pliocene Seamount*

Staudigel (1981) and Staudigel and Schmincke (1984) interpreted the submarine and plutonic complex exposed in the walls and floor of the Caldera de Taburiente as an uplifted seamount. The Seamount Series of La Palma is a sequence of submarine volcanic and associated intrusive rocks outcropping to a maximum altitude of about 1 km above sea level, and separated from the overlying subaerial volcanic rocks of the Taburiente volcano by a distinct angular and erosive unconformity. Plutonic intrusions and a large number of dykes, which represent feeders to the subaerial volcanic sequence, cut Seamount Series rocks deep inside the Caldera.

As described in detail by Staudigel (1981) and Staudigel and Schmincke (1984), the Seamount Series outcropping in the bottom of the Barranco de Las Angustias represents a complete, 3.6-km-thick cross-section through a seamount. Similar formations are exposed in La Gomera (Bravo, 1964; Cendrero, 1971) and Fuerteventura (Fúster et al., 1968 b; Stillman and Robertson, 1977; Stillman, 1987). A comparable suite of rocks also occurs in Maio in the Cape Verde archipelago (Stillman et al., 1982). The original interpretation of these (Fúster et al., 1968 b), dating back to the pre-Plate Tectonic era, was that they represent uplifted blocks of a region-wide basement complex; a later modification was to interpret them as uplifted blocks of ophiolitic oceanic crust although palaeontological and radiometric work showed them to be much younger than the adjacent sections of the Atlantic ocean lithosphere. These «basal complexes» have most or all of the following features in their exposed sections:

— Uplifted and strongly deformed sequences of oceanic sediments, substantially older than other parts of the «basal complexes» as shown by palaeontological and radiometric evidence.

— Thick sequences of submarine volcanic rock (mainly pillow basalts, with shallow-water and littoral hyaloclastites present in the higher parts of the sections, indicating emergence).

— Intense basaltic dyke swarms, attaining, for example, over 80% of the outcrop in parts of Fuerteventura (Stillman, 1987).

— Substantial plutonic intrusive complexes, cutting and cut by different components of the dyke swarms.

— Moderately intense deformation of the dyke swarms and intrusive complexes, involving, variously, tilting (Staudigel and Schmincke, 1984), block faulting (Stillman, 1987), and radial thrusting (Stillman et al., 1982). This is generally related to emplacement of the plutonic intrusive complexes.

— Hydrothermal metamorphism, rising from zeolite to albite —epidote— hornfels facies, affecting all of the above components (Staudigel and Schmincke, 1984; Schiffman and Staudigel, 1994, 1995); localized high-grade thermal contact metamorphism and anatexis may be present around several of the plutonic complexes (Stillman, 1987).

— Late intrusive complexes (dykes, plugs, occasional ring complexes and other large plutons, which are inferred to be feeders to overlying rocks of the subaerial volcanic complexes).

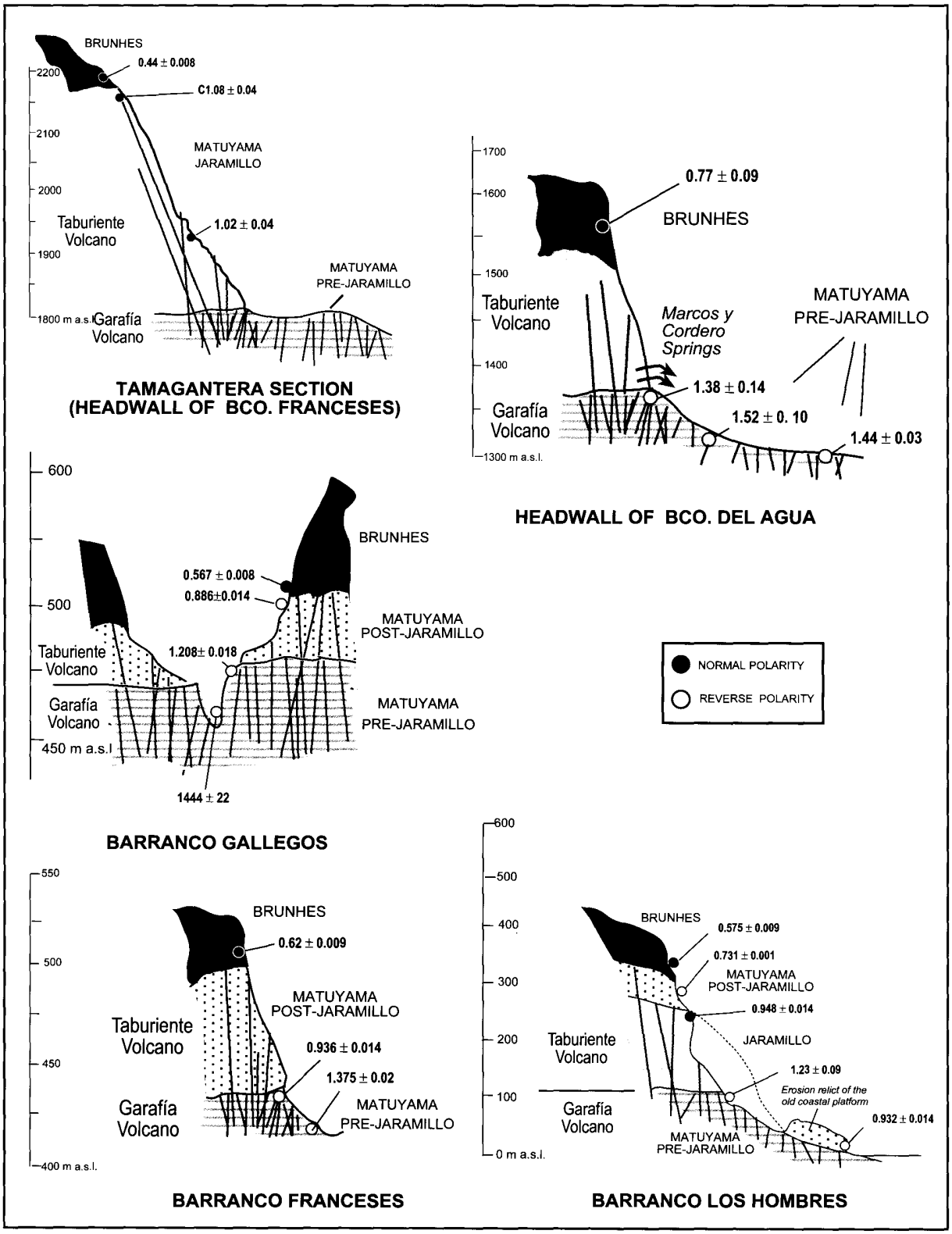


Fig. 9.—Representative cross sections in the northern shield showing the main volcanostratigraphic and magnetostratigraphic units.

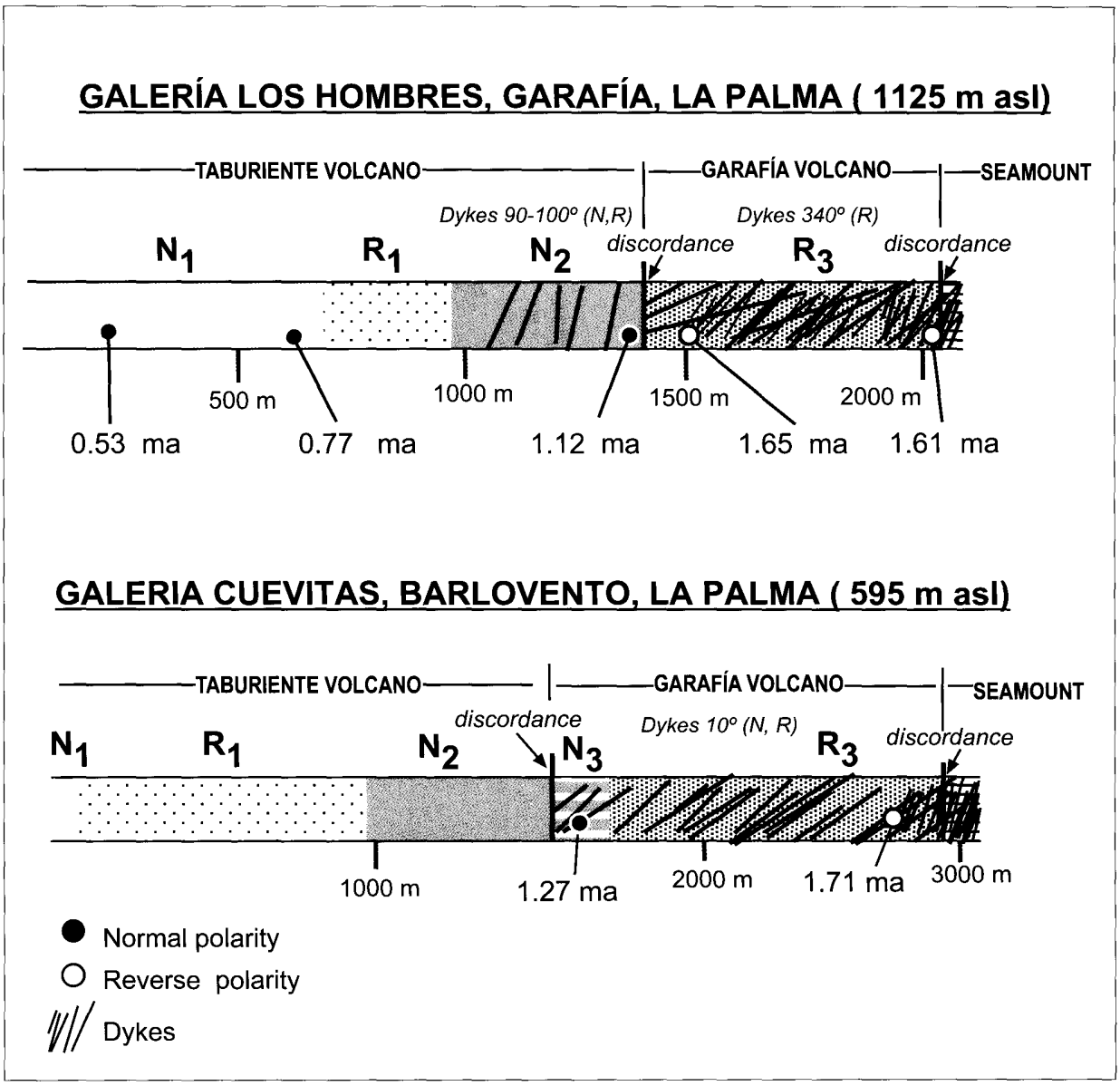


Fig. 10.—Disposition and extension of the main magnetozones defined in the northern shield in the Los Hombres and Cuevitas *galerías*. N: Normal polarity, R: Reverse polarity.

— Substantial terrestrial unconformities, with significant topography, which mark erosion down to the level of the dyke swarms and, in some cases, the plutonic complexes. In other places, however, transitional sequences with only moderate dyke swarm densities and, typically, littoral volcanic facies are present.

Radiometric data for the «basal complexes» are commonly in contradiction to field evidence, particularly in regard to their relationships to the overlying subaerial volcanic rocks. This most probably reflects the widespread use of dating techniques on unsuited, altered rocks. The Seamount Series of La Palma has been approximately dated as Pliocene (3-4 ma) using foraminifera (*Globorotalia crassaformis, Neogloboquadrina humerosa, Globoquadrina altispira* and *Globorotalia puncticulata)* found in hyaloclastites interbedded in the submarine lavas (Staudigel, 1981, 1997).

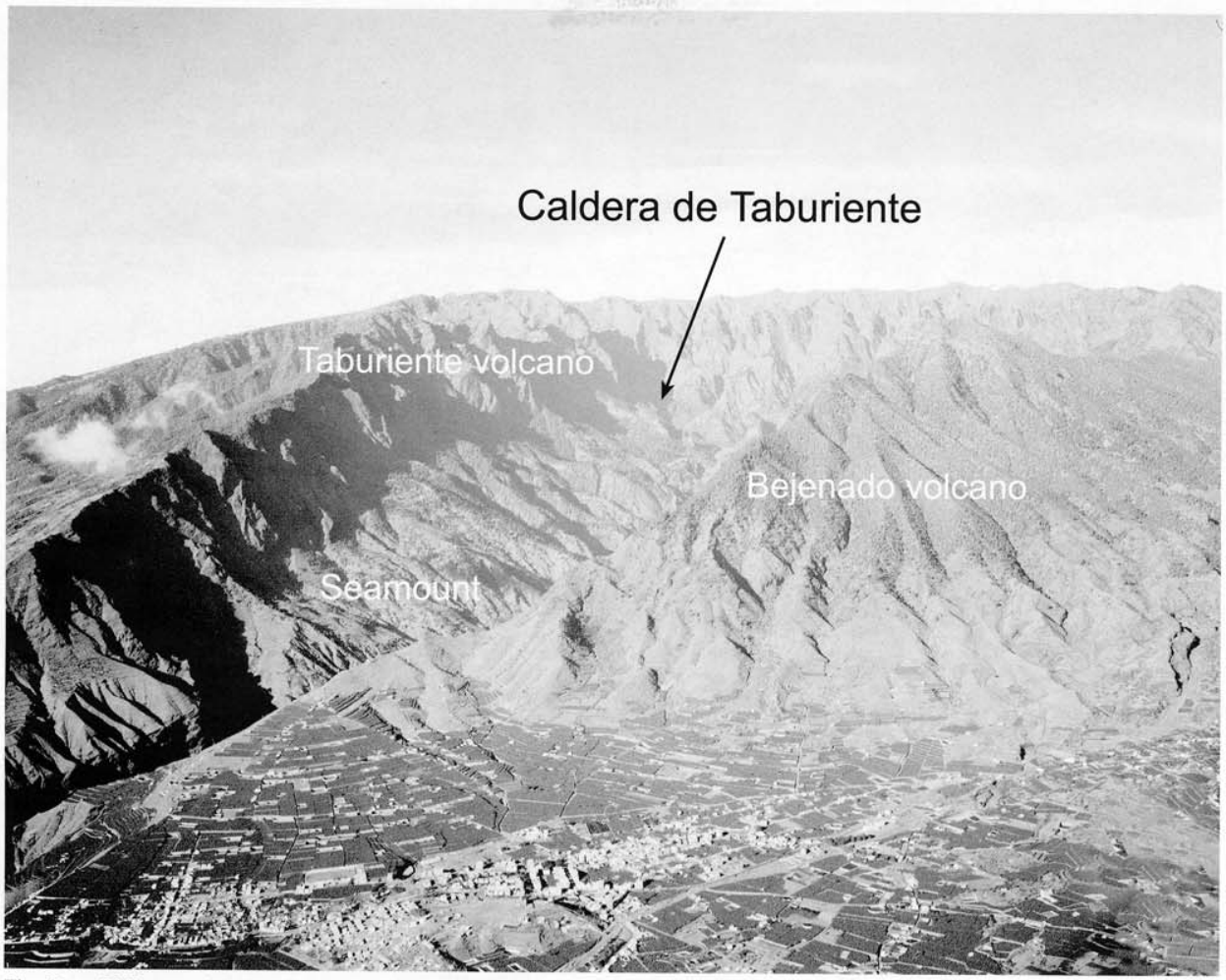


Fig. 11.—Oblique aerial view of the northern shield and the Caldera de Taburiente. The Bejenado volcano forms the left-hand wall of the Caldera.

The Seamount Series of La Palma only outcrops inside the Caldera de Taburiente (Fig. 11), exposed by the deep incision originated by a large gravitational collapse and subsequent erosion. However, it forms the deep core of the northern shield, where its extension and disposition have been determined by Coello (1987) through observation in *galerías* (Fig. 12). It consists of two main units, an extrusive sequence of layered lavas and an intrusive (plutonic) sequence. However, according to Staudigel (1981), both series grade progressively from shallow water lavas (see Fig. 13 A, B) to a plutonic core (Fig. 13 C).

## The extrusive Seamount Series

Staudigel (1981, 1997) and Staudigel and Schmincke (1984) have described this Series in detail. The outcrop of the Barranco de Las Angustias consists of a layered sequence of pillow lavas and volcaniclastics grading to a sheeted dyke swarm (Figs. 13 and 14). Two sections have been separated by these authors (Fig. 14): a shallow-water and a deep-water facies, the deepest outcropping inside the Caldera at El Carbón (365 m asl), and the shallowest at La Viña (145 m asl). These represent a 1.8-km section at the flank of the seamount. The layered sequence of the NW-SE-trending submarine lavas and volcaniclastics are tilted 50° to the SW, parallel to the axis of the barranco, caused by endogenous growth and intrusion. The shallow-water facies include a large fraction of volcaniclastics, whereas the deep-water facies are predominantly made of thick pillow lavas, similar to deep abyssal hills on the ocean floor (Staudigel, 1981, 1997).

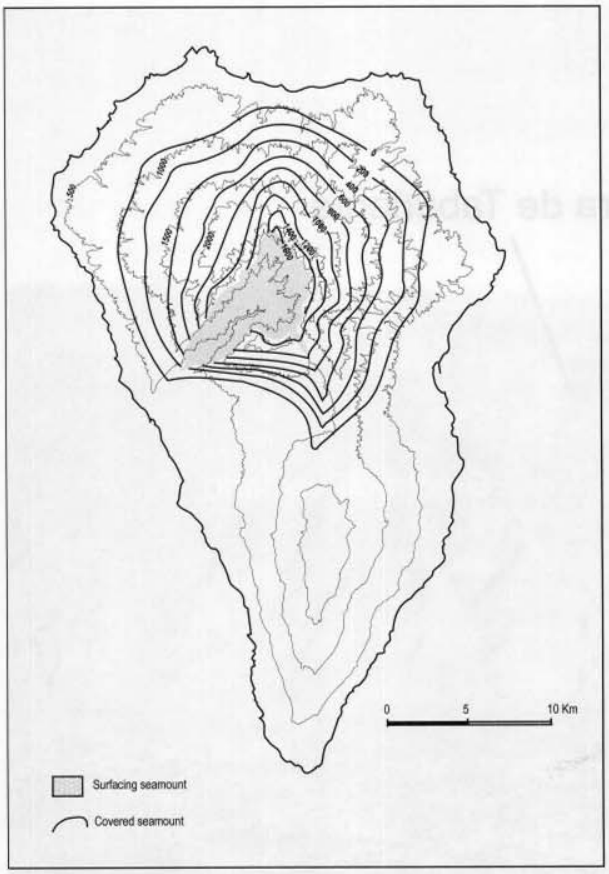


Fig. 12.—Disposition and approximate extension (from Coello, 1987) of the seamount. Contours of the subaerial volcanoes and the underlying seamount are indicated for comparison.

An interesting feature of the extrusive Seamount Series is the continuous prograde hydrothermal metamorphism. First described by Hernández Pacheco and Santín (1974) and later by Staudigel (1981), metamorphism grades from low (<10 °C) alteration at the top of the formation to medium-grade metamorphism (greenschist facies metamorphism) near the base (Hernández Pacheco and Fernández Santín, 1974; Staudigel and Schmincke, 1984; Schiffman and Staudigel, 1994, 1995). For these last authors, the paragenesis and mineralogical zonation observed imply a metamorphic gradient of 200-300 °C/km and the circulation of a high rate of fluids over a long period, that has almost completely altered the original igneous minerals of these rocks. Hydrothermal alteration has likewise contributed to erase the original magnetization of the rocks (Gee et al., 1993) and has led to significant variations in the concentration of certain elements such as Re and Os (Marcantonio et al., 1995).

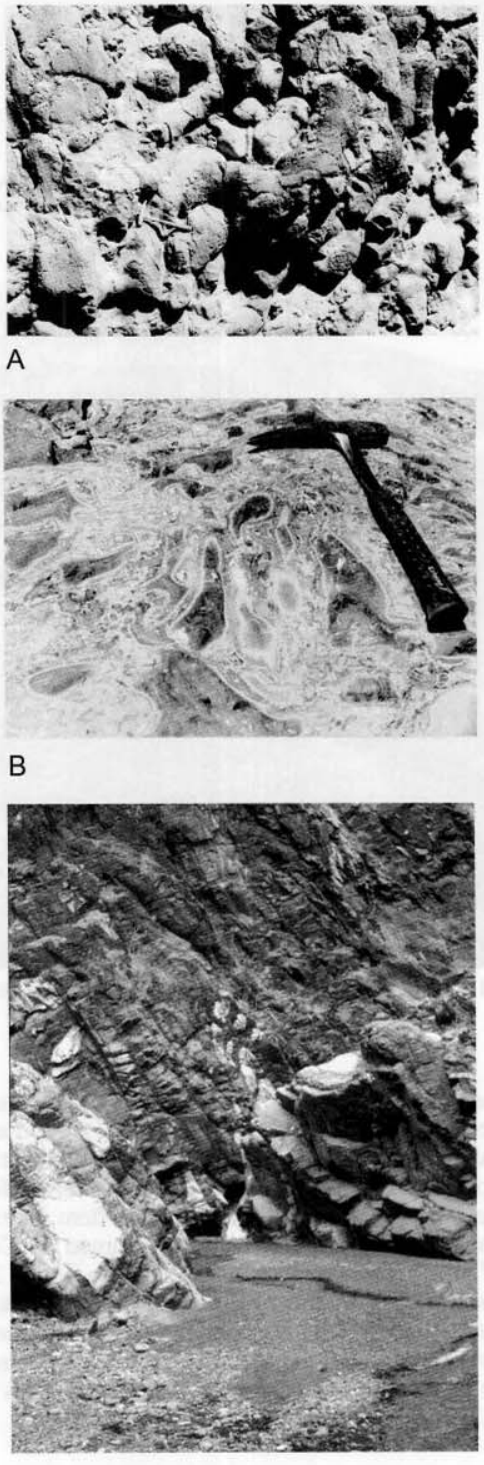


Fig. 13.—View of increasingly deeper facies of the seamount in the bed of Bco. de Las Angustias. A) Shallow pillow lavas. B) Hyaloclastite breccias. C) Dyke swarm intruding the submarine formations.

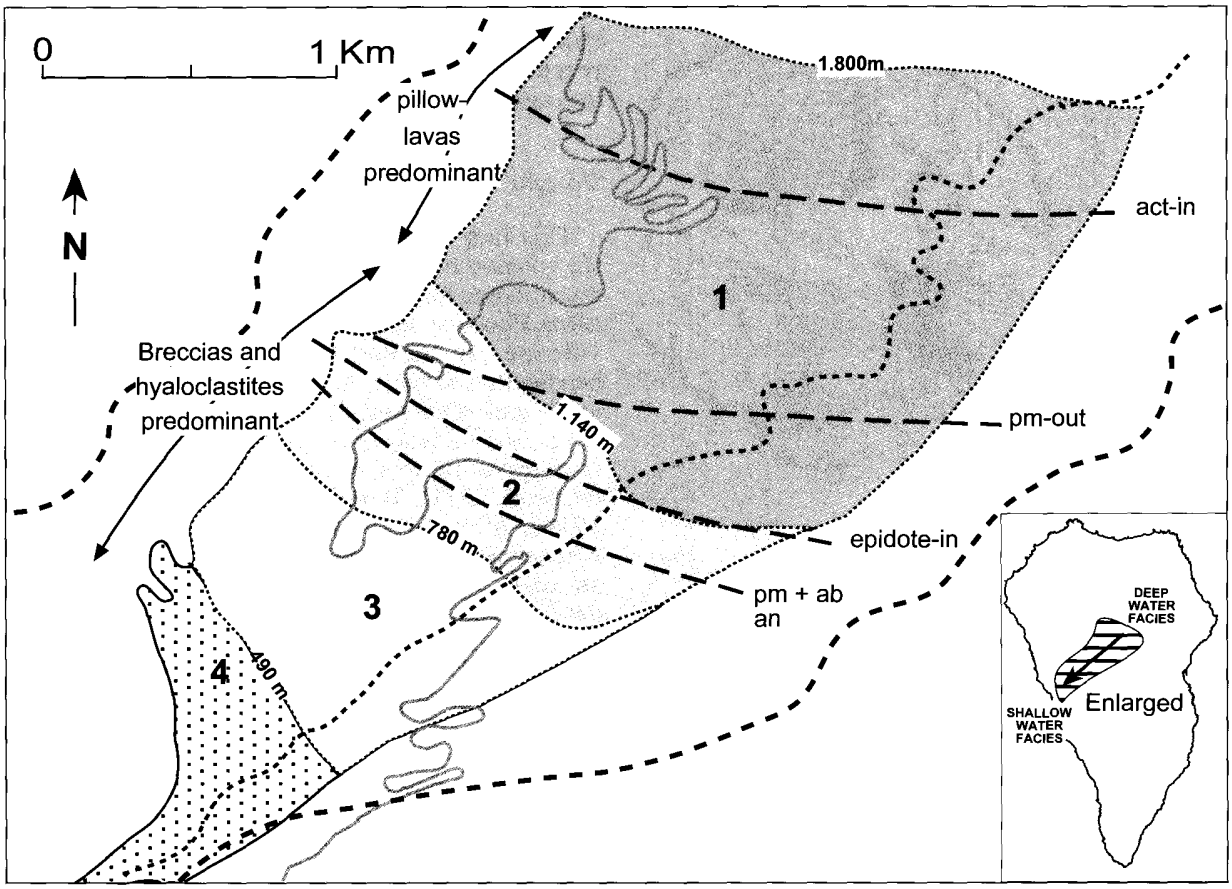


Fig. 14.—Submarine extrusive sequence in the Caldera de Taburiente (modified from Staudigel and Schmincke, 1984). 1 to 4 indicate different facies of increasing water depth.

The intrusive Seamount Series

Intrusions inside the Caldera correspond to the seamount and the subsequent subaerial volcanism, and can be separated into three main groups:

1. *Trachytic-phonolitic domes of Dos Aguas.* This unit outcrops in an arc between the Barranco de Taburiente, Dos Aguas, El Carbón and Los Brecitos and extends approximately over some 2 km$^2$. These materials have previously been interpreted as salic rocks (Hernández Pacheco and Fernández Santín, 1974), and keratophyres or metatrachytes (Staudigel and Schmincke, 1984). In any case, they remain considerably indeterminate, due, on the one part, to the fact that they appear as metric-sized fragments between the dense dyke swarm and, on the other, to their high degree of compositional and textural alteration.

De la Nuez recognized two main types of facies (1984), a coarse-to-medium-grain breccia and a massive facies. The breccias are preferentially localized close to the contact with the submarine volcanic formation, while the massive facies are located towards the centre of the formation. Clasts of pillow lavas of a trachytic composition are observed in the breccias, indicating that they were probably formed in a marine environment. Relict flow structures and some fragments that seem to correspond to pyroclastic products have been detected in the massive facies. This trachytic and phonolitic formation, probably corresponding to one or several domes intruding the basaltic submarine formation in the deepest sequences, appear crossed by a dense dyke swarm and by several plutonic bodies several tens to hundreds of metres thick.

2. *Intrusive plutonic rocks.* Numerous plutonic bodies, tens to hundreds of metres thick, outcrop at the bottom of the Caldera de Taburiente over an area of several km$^2$. They correspond to multiple intrusions associated to submarine and subaerial eruptions,

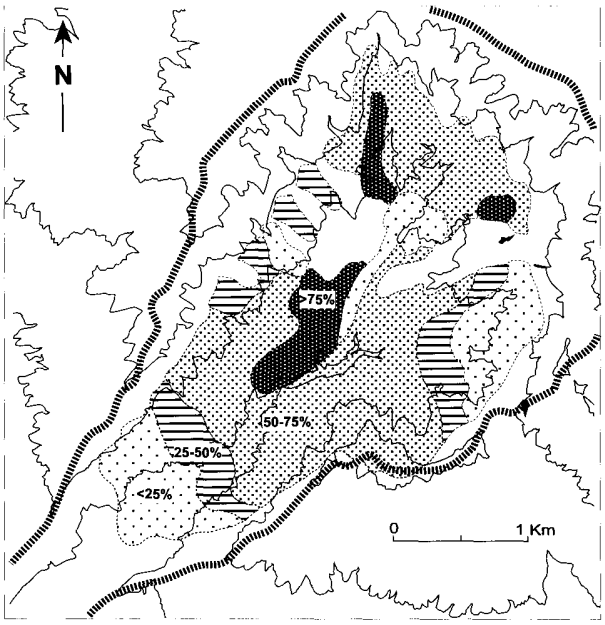


Fig. 15.—Percentage of dykes and sills in the Caldera de Taburiente.

reaching, in places 75% of the rock (Fig. 15). However, it is very difficult to individualize plutonic bodies or separate those belonging to the seamount from those corresponding to the subaerial Garafía, Taburiente and Bejenado volcanoes.

Three main groups of gabbros have been separated (see geological map), the first two corresponding to the submarine edifice, and the third to intrusions related to the subaerial volcanism (Carracedo et al., 2001 a, b). The oldest gabbros outcrop in the northern half of the Caldera, the most probable location of the submarine emission centres. The most recent gabbro intrusives are located to the south, probably related to the emission centres of the Taburiente and Bejenado volcanoes.

3. *Dyke swarms.* The dyke network is highly developed throughout the submarine edifice, with a maximum density at the centre of the Caldera de Taburiente and along the Barranco de Las Angustias, decreasing gradually towards the edges and downwards. The maximum intrusion can make up as much as 100% of the rock (always more than 75%) in the barrancos of Taburiente, Verduras de Alfonso and Los Cantos, while down at La Viña dykes constitute less than 10% of the rock (Fig. 15).

Staudigel and coworkers (1986) separated three groups of dykes with different ages and general orientation. The two older groups are rotated due to the tectonic uplift of the seamount prior to the emergence of the island and, therefore, feed the submarine formation. The third group, more recent and unrotated, is related to the subaerial volcanoes.

*Garafía Volcano*

This first subaerial volcanism formed the Garafía volcano overlying in clear angular and erosive discordance and entirely mantling the uplifted and tilted Pliocene seamount. Outcrops of the Garafía volcano are limited to erosive windows at the headwalls and beds of the deepest barrancos of the north and southwest flanks of the northern shield (Fig. 16). These outcrops were interpreted as corresponding to the Basal Complex (Hernández Pacheco, 1974), Taburiente I (Navarro and Coello, 1994), or as Lower Old Series (Coello, 1987; Ancochea and coworkers, 1994). However, there are reasons for separating this volcano as an independent unit. The radiometric and palaeomagnetic data indicate that this volcano formed between 1.722 and 1.208 ma, the period corresponding to the Matuyama post-Olduvai and the Cobb Mt event (see Figs. 7, 8 and 16 and Table 1). The lower limit of this volcano can be set at 1.77 ma, since the normal polarity lavas of the Olduvai event (see Fig. 8) have not been found at the basal sequences of the volcano, even at the discordant contact with the underlying seamount formations, as occurs in the *galerías* Los Hombres and Cuevitas (Fig. 10).

The volcanic activity in the northern shield continued without significant interruptions until about 0.4 ma (see Fig. 8). The separation of the Garafía and the subsequent Taburiente volcanoes has been feasible because in many areas their contact is an angular and/or erosive discordance, originated by the afore-mentioned gravitational collapse of the south flank of the former volcano approximately 1.2 ma ago. The large collapsed portion of the volcano, and the superposition of about 1.000 m of lavas of the subsequent Taburiente volcano made the approximate reconstruction of the extension and configuration of the Garafía volcano difficult. However, its distribution in the subsoil has been approximately defined by means of the numerous *galerías* excavated for groundwater mining in the northern shield (Coello, 1987; Carracedo et al., 2001 a, b). These observations indicate that the Garafía volcano developed as a steep cone, with lava flows consistently exceeding 20°, frequently 30-35°, and closely centred over the seamount (see Fig. 16). The mean thickness of the formation (some 400 m)

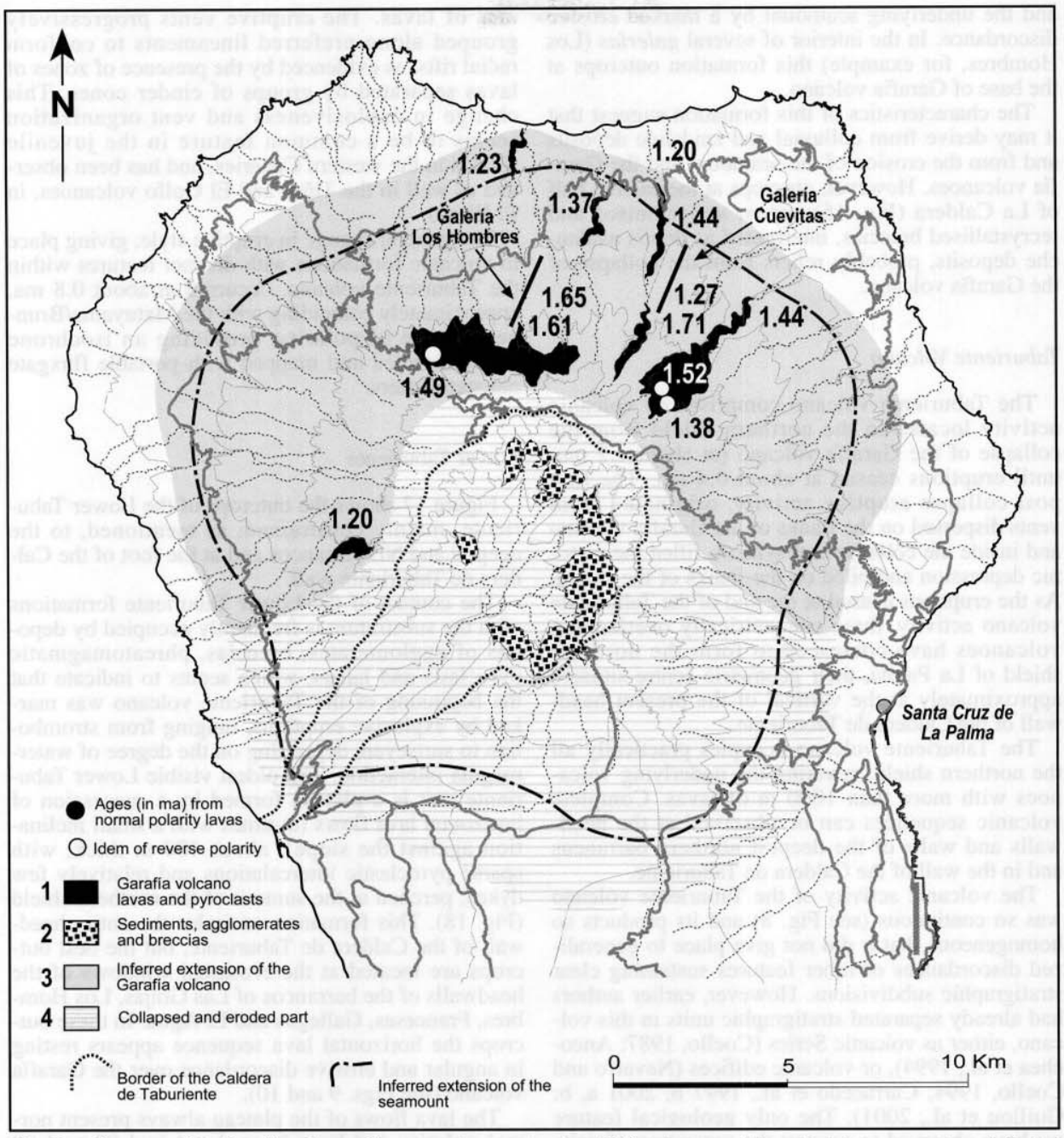


Fig. 16.—Outcrops of the Garafía volcano. The approximate extension of this volcano and the underlying seamount are indicated for comparison.

points to a volcanic edifice at least 2.000 m high and around 25 kms in diameter, with a volume of about 160 km$^3$ (after subtracting the volume of the seamount, of about 166 km$^3$). The corresponding eruptive and growth rates near 0.3 km$^3$/ka and 0.8 mm/y, respectively.

*Sediments, agglomerates and breccias in the interior of the Caldera de Taburiente.* A several hundred metres-thick sequence of sediments, agglomerates and breccias outcrops in the Caldera de Taburiente (Fig. 16 and geological map), at the base of the Taburiente volcano and is separated from this

and the underlying seamount by a marked erosive discordance. In the interior of several *galerías* (Los Hombres, for example) this formation outcrops at the base of Garafía volcano.

The characteristics of this formation suggest that it may derive from colluvial and landslide deposits and from the erosion of the seamount and the Garafía volcanoes. However, outcrops at the eastern half of La Caldera (Fig. 16) appear as tectonised and recrystallised breccias, interpreted as debris avalanche deposits, probably relicts from the collapse of the Garafía volcano.

### *Taburiente Volcano*

The Taburiente volcano comprises de volcanic activity located in the northern shield from the collapse of the Garafía volcano (at about 1.2 ma) until eruptions ceased at about 0.4 ma. The first post-collapse eruptive activity, originated from vents dispersed on the flanks of the Garafía volcano and inside the collapse embayment, filled the tectonic depression and piled on the flanks of the shield. As the eruptions ceased at the end of the Taburiente volcano activity, three concentrically overlapping volcanoes have coalesced to form the northern shield of La Palma, their geometric centre situated approximately at the vertical of the present headwall of the Caldera de Taburiente.

The Taburiente volcano occupies practically all the northern shield, covering the underlying volcanoes with more than 1000 m of lavas. Complete volcanic sequences can be observed at the headwalls and walls of the deepest northern barrancos and in the wall of the Caldera de Taburiente.

The volcanic activity of the Taburiente volcano was so continuous (see Fig. 8) and its products so homogeneous that it did not give place to generalized discordances or other features sustaining clear stratigraphic subdivisions. However, earlier authors had already separated stratigraphic units in this volcano, either as volcanic Series (Coello, 1987; Ancochea et al., 1994), or volcanic edifices (Navarro and Coello, 1994; Carracedo et al., 1997 b, 2001 a, b; Guillou et al., 2001). The only geological feature we have observed to support the separation of units in this volcano is based on a change in eruptive style. The lower volcanic sequences outcropping at the headwalls and beds of the deepest barrancos are characterized by the predominance of pyroclastic deposits densely crossed by dykes. These features suggest a wide dispersion of the initial, predominantly explosive eruptive centres. In the advanced stages of the Taburiente volcano the eruptions changed to more effusive, with emission of large volumes of lavas. The eruptive vents progressively grouped along preferred lineaments to conform radial rifts, as evidenced by the presence of zones of lavas separated by groups of cinder cones. This change in explosiveness and vent organization seems to be a common feature in the juvenile shields in the western Canaries, and has been observed as well in the Tiñor and El Golfo volcanoes, in El Hierro.

The general change in eruptive style, giving place to volcanic formations with distinct features within the Taburiente volcano, occurred at about 0.8 ma, approximately coinciding with the Matuyama/Brunhes change of polarity, providing an isochrone easily detected and mapped with portable fluxgate magnetometers.

#### Lower Taburiente

Figure 17 shows the outcrops of the Lower Taburiente, mainly constrained, as mentioned, to the deep N and NE barrancos and at the foot of the Caldera de Taburiente wall.

The contact of the Lower Taburiente formations with the substratum is frequently occupied by deposits of agglomerates, breccias, phreatomagmatic pyroclasts and lahars, which seems to indicate that the beginning of the Taburiente volcano was marked by explosive eruptions, ranging from strombolian to surtseyan, depending on the degree of water-magma interaction. The oldest visible Lower Taburiente unit is a plateau formed by a succession of horizontal lava flows (at times with a small inclination against the slope), about 400 m thick, with sparse pyroclastic intercalations and relatively few dykes, perched at the summit of the northern shield (Fig. 18). This formation encircles the entire headwall of the Caldera de Taburiente, but the best outcrops are located at the erosional windows of the headwalls of the barrancos of Las Grajas, Los Hombres, Franceses, Gallegos and El Agua. In these outcrops the horizontal lava sequence appears resting in angular and erosive discordance over the Garafía volcano (see Figs. 9 and 10).

The lava flows of the plateau always present normal polarity and have been dated in 1.02 to 1.08 ma. They therefore seem to correspond to the Jaramillo normal polarity event (0.996-1.053 ma) and have been apparently emitted at extremely fast rates (>6 mm/y), apparently a common characteristic of post-collapse volcanism, such as the Bejenado, El Golfo, Post-Cañadas, etc. This plateau was first explained by Coello (1987) and Navarro and Coello (1994) as the filling-up with lavas of two large ravines excavated at the contact between Garafía volca-

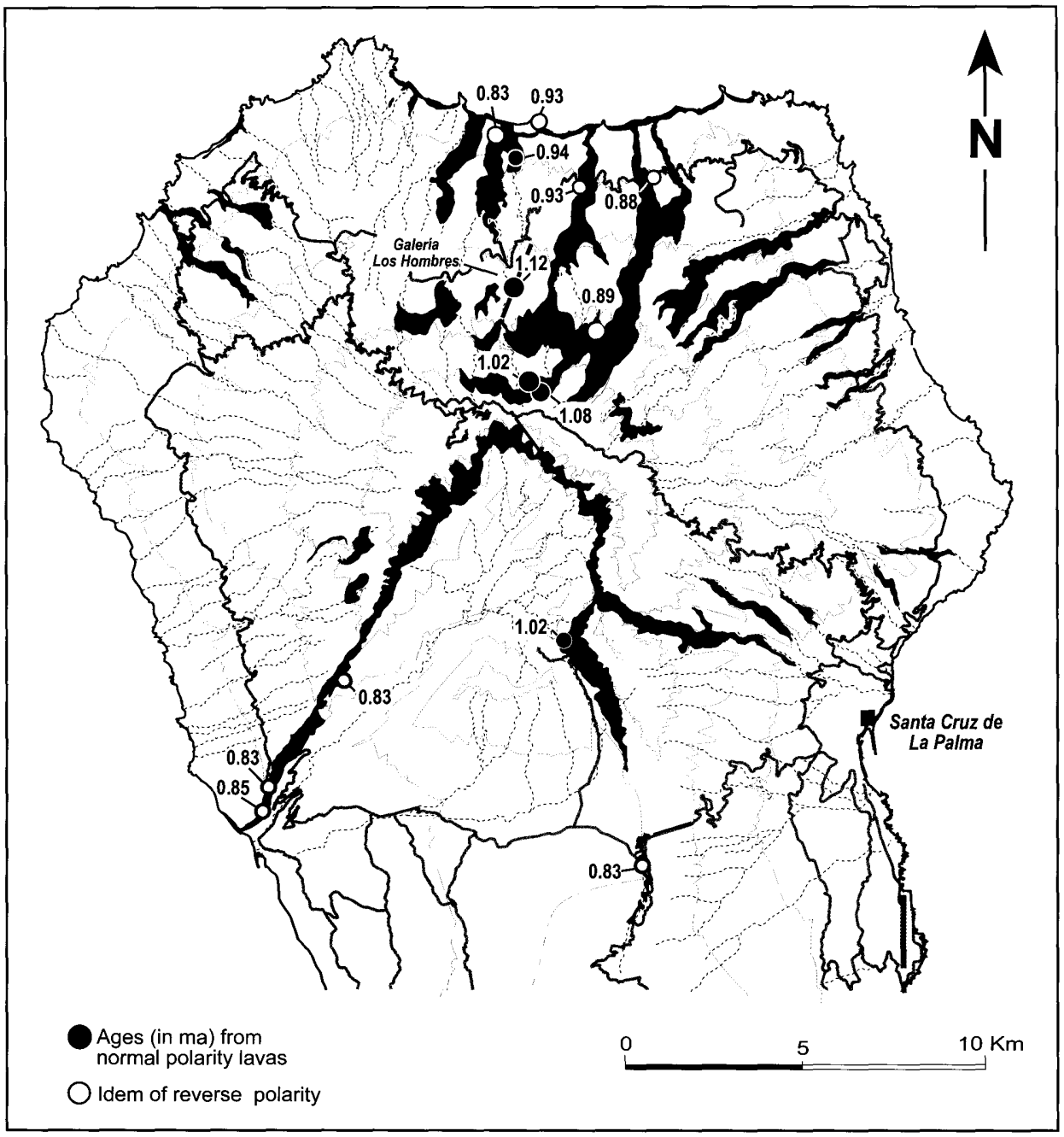


Fig. 17.—Outcrops of the Lower Taburiente volcano.

no (Taburiente I for these authors) and the submarine basement. However, the lack of significant interruptions in the eruptive activity shown by the radiometric ages seems incompatible with the successive incision of several hundreds of metres deep, steep barrancos, their subsequent filling with lavas, and the erosion required to generate the lava plateau by relief inversion. A more plausible explanation, consistent with the geochronological and stratigraphical data, is the filling with lavas of the depression formed in the lateral collapse of the south flank of Garafía volcano already described.

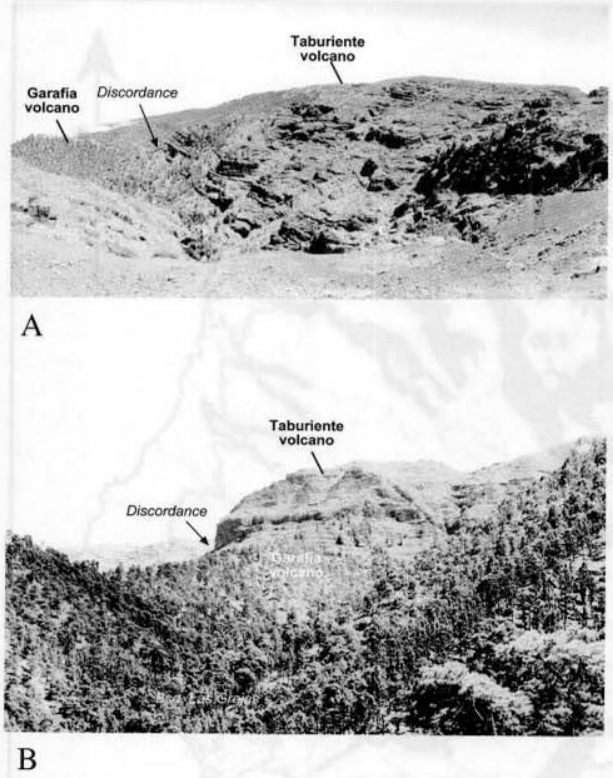


Fig. 18.—Views of the Lower Taburiente horizontal lavas overlying unconformably the Garafía volcano. A) The Tamagantera section. B) View from the NW (from Bco. de Las Grajas).

## Upper Taburiente

The Upper Taburiente unit completely mantles the northern shield (Fig. 19), except in the erosional windows at the headwalls of the deep northern barrancos and at the Caldera de Taburiente. Instead of enlarging significantly the extension of the northern shield, this volcanic phase built a progressively higher and steeper volcano. The Upper Taburiente formation corresponds to the culmination of the construction of the northern shield, involving the emission of a sequence of lavas about 1000-m thick, erupted from about 0.8 ma to some 0.4 ma (see Fig. 8).

The Upper Taburiente lavas present great structural and morphological uniformity, appearing in thick sections of basaltic lava flows with sparse pyroclastic beds and dykes, except in the rift zones, where cinder cones are predominant and dykes are abundant (see Figs. 19 and 35). Coastal hydromagmatic cones are relatively abundant, such as the spectacular tuff cone of La Galga, north of Puntallana, with phreatomagmatic eruptions of slightly differentiated magmas that emitted very thick ignimbrites, and the tuff cone of La Caldereta, near Santa Cruz de La Palma.

The final stages of activity of the Upper Taburiente may have formed a central volcano, possibly reaching 2.500-3.000 m asl, with late stages of terminal differentiated lavas and explosive eruptions. Although salic materials have not previously been described from Taburiente volcano, flows of mafic phonolites and trachytes outcrop at the rim of the Caldera de Taburiente, as well as several metres-thick block and ash flow deposits, possibly associated with eruptions that emitted juvenile phonolites (see geological map).

Eruptive activity seems to have started a constant southward migration at the final stages of the Upper Taburiente, finally leaving the northern shield inactive. Eruptions concentrated in the southern part, developing the Cumbre Nueva rift that became progressively steeper and unstable. The collapse of the western flank of the rift formed the southern depression that initiated the Caldera de Taburiente (see Fig. 19). Post-collapse activity in the northern shield mainly concentrated inside the collapse embayment to form the nested Bejenado volcano, although disperse eruptions on the flanks of the shield postdated the Bejenado volcano until 0.4 ma.

### *The Bejenado volcano*

The Bejenado volcano is the continuation of the Upper Taburiente volcanism immediately after the above-mentioned Cumbre Nueva gravitational collapse (see Fig. 8). The separation of this volcano from the remainder of Taburiente is based, similarly to the Garafía volcano, on the occurrence of a gravitational collapse generating a general discordance, over which the Bejenado volcano developed. This volcano illustrates spectacularly the structural and magmatic evolution of post-collapse volcanism, with parallelisms in the cases of Las Cañadas in Tenerife and El Golfo in El Hierro (Ancochea et al., 1990; Guillou et al., 1996).

The construction of this stratovolcano was extremely fast, as shown by the radiometric ages (Figs. 6-8 and Table 1), possibly only a few tens of thousands of years. In this short time the lavas built a very steep volcano, partially dismantled at present by the progression of erosion in the Caldera de Taburiente. The summit of Bejenado reaches 1.864 m asl, but only the top 600 m belong to this volcano, which appears forming the SE wall of the Bco. de Las Angustias, at the exit of the Caldera de Taburiente (see Fig. 11). There is a clear lack of correspondence in the western and eastern walls of the Caldera de Taburiente, as pointed out by Sapper in

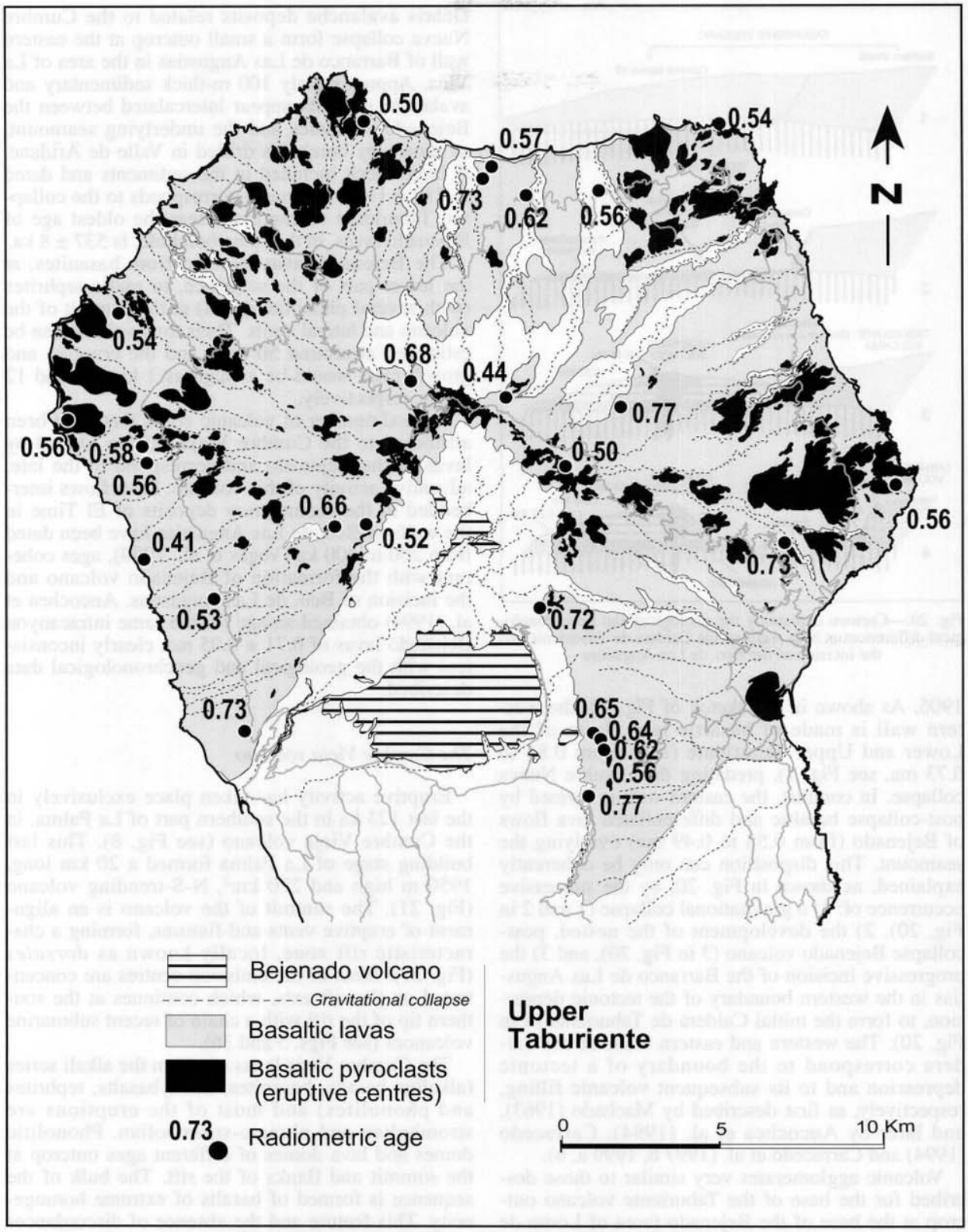


Fig. 19.—Outcrops of the Upper Taburiente and Bejenado volcanoes.

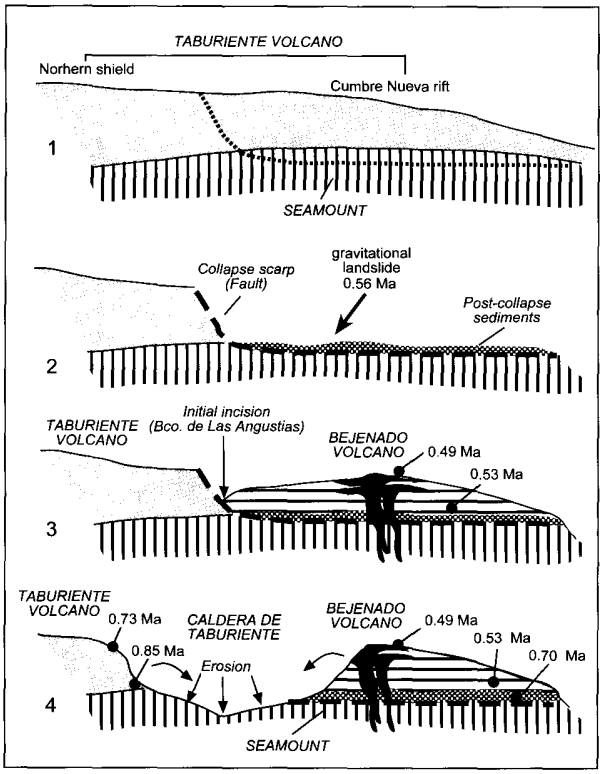


Fig. 20.—Cartoon explaining the geological and geochronological differences at both walls of the Caldera de Taburiente and the incision of the Bco. de Las Angustias

1906. As shown in the sketch of Fig. 20, the western wall is made of basaltic lava flows of the Lower and Upper Taburiente (ages from 0.85 to 0.73 ma, see Fig. 7), predating the Cumbre Nueva collapse. In contrast, the eastern wall is formed by post-collapse basaltic and differentiated lava flows of Bejenado (from 0.58 to 0.49 ma) overlying the seamount. This disposition can only be coherently explained, as shown in Fig. 20, by the successive occurrence of: 1) a gravitational collapse (1 and 2 in Fig. 20), 2) the development of the nested, post-collapse Bejenado volcano (3 in Fig. 20), and 3) the progressive incision of the Barranco de Las Angustias in the western boundary of the tectonic depression, to form the initial Caldera de Taburiente (4 in Fig. 20). The western and eastern walls of the Caldera correspond to the boundary of a tectonic depression and to its subsequent volcanic filling, respectively, as first described by Machado (1963), and later by Ancochea et al. (1994), Carracedo (1994) and Carracedo et al. (1997 b, 1999 a, b).

Volcanic agglomerates very similar to those described for the base of the Taburiente volcano outcrop at the base of the Bejenado (area of Lomo de Los Caballos and along the road to La Cumbrecita). Debris avalanche deposits related to the Cumbre Nueva collapse form a small outcrop at the eastern wall of Barranco de Las Angustias in the area of La Viña. Approximately 100 m-thick sedimentary and avalanche deposits appear intercalated between the Bejenado volcanics and the underlying seamount, as shown by boreholes drilled in Valle de Aridane. A large block included in the sediments and dated in 710 ± 11 ka obviously corresponds to the collapsed Taburiente volcano, whereas the oldest age of Bejenado lavas, in the same borehole, is 537 ± 8 ka.

The Bejenado lavas evolved from basanites, at the lower part of the sequence, to mafic tephrites (with several phonolite dykes) at the summit of the volcano and lateral vents. Their total volume can be estimated at around 50 $km^3$, and the eruptive and growth rates would be as high as 1 $km^3$/ka and 12 mm/y, respectively.

A good number of volcanic cones that have been attributed to the Cumbre Vieja rift are topped by lavas of the Bejenado and correspond to the late, adventive activity of this volcano. Lava flows interbedded in the sedimentary deposits of El Time in the walls of Bco. de Las Angustias have been dated from 200 to 400 ka (Vegas et al., 1999), ages coherent with the formation of Bejenado volcano and the incision of Bco. de Las Angustias. Ancochea et al. (1994) obtained an age for the same intracanyon Bejenado lavas of 0.71 ± 0.05 ma, clearly inconsistent with the geological and geochronological data described.

### *The Cumbre Vieja volcano*

Eruptive activity has taken place exclusively in the last 123 ka in the southern part of La Palma, in the Cumbre Vieja volcano (see Fig. 8). This last building stage of La Palma formed a 20 km long, 1950 m high and 220 $km^2$, N-S-trending volcano (Fig. 21). The summit of the volcano is an alignment of eruptive vents and fissures, forming a characteristic rift zone, locally known as *dorsales* (Fig. 21). Most of the emission centres are concentrated on the rift axis, which continues at the southern tip of the rift with a chain of recent submarine volcanoes (see Figs. 5 and 36).

The Cumbre Vieja lavas are from the alkali series (alkaline basalts, basanites, trachybasalts, tephrites and phonolites) and most of the eruptions are strombolian and phreato-strombolian. Phonolitic domes and lava domes of different ages outcrop at the summit and flanks of the rift. The bulk of the sequence is formed of basalts of extreme homogeneity. This feature and the absence of discordances or other stratigraphic markers make it very difficult

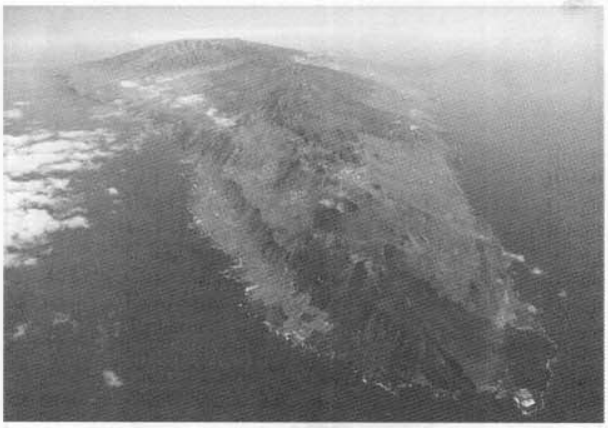

Fig. 21.—Oblique aerial view of the Cumbre Vieja rift volcano (photograph S. Socorro).

to separate volcanostratigraphic units in this volcano. The stratigraphy defined has, therefore, been based significantly on radiometric dating (K/Ar and $C^{14}$) with a highly restrictive sampling system and a dating technique that has proven useful in lavas only a few thousand years old (Guillou et al., 1996, 1998, 2001). A total of 25 new radiometric ages have been obtained, as indicated in Fig. 7 and Table 1. As discussed above, earlier ages reported for this relatively recent volcano lack the necessary accuracy (see Fig. 6) and only the ages determined by Guillou and co-workers (1998) and Carracedo and co-workers (2001 b) were used to define the volcanostratigraphic units of this volcano. The flanks of Cumbre Vieja, especially the western one, have undergone important marine erosion, giving place to considerably high coastal cliffs. Lava flows from recent eruptions streamed over these cliffs to form coastal platforms (Fig. 22 A). The correlation of the radiometric ages obtained from lavas forming cliffs and those forming coastal platforms indicates that they form distinct chronostratigraphic sequences, the former systematically presenting ages greater than about 20 ka, while the latter yield consistently more recent ages. This feature can be used as an isochrone to define the volcanostratigraphy of the volcano, that coincides with the peak of the last glaciation (Fig. 22 A). The lavas emitted before and during the glacial maximum were eroded to form coastal cliffs, while those emitted subsequently fossilized the cliffs to form coastal lava platforms (Fig. 22 B).

These data and geochronological criteria have allowed the definition in Cumbre Vieja (and in the island of El Hierro, as discussed later) of the volcanostratigraphic units described below, used in the elaboration of the geological map of the island.

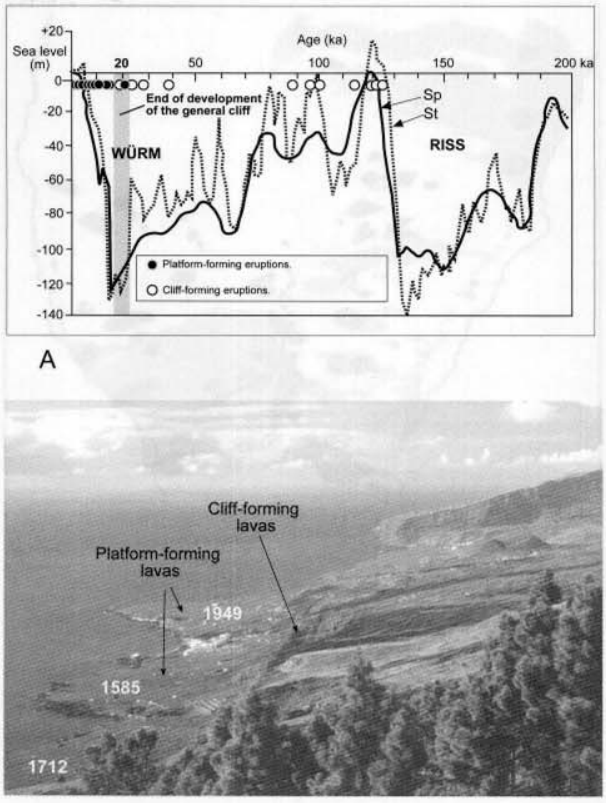


Fig. 22.—A) Correlation of ages of Cumbre Vieja lavas with the low sea level stand in the last glacial maximum and separation of cliff- and platform-forming eruptions. B) View of the western cliff of Cumbre Vieja and the coastal platforms formed by historical (1585, 1712 and 1949) eruptions.

## Cliff-forming eruptions

Although these eruptions form the bulk of the Cumbre Vieja volcano, they outcrop mainly in the northwest and eastern flanks, the remainder of the volcano being resurfaced by more recent eruptions. They form a cliff over 100 m high at the NW, decreasing towards the south end of the island and at the eastern flank, correlatively with the progressive decrease in age of the lavas (see Figs. 7 and 21).

The eruptive centres corresponding to this unit are distributed over the entire volcano, forming a scarcely defined multiple rift, with a slight predominance of NW and NE directions from the centre of the rift (Fig. 23). The great part of the emission centres form strombolian cones, but there are relatively abundant phreato-strombolian vents interbedded in the lava sequences at the coastal cliffs, such as the tuff cone of Puerto Naos, on the west coast, and those of Mña. Vento

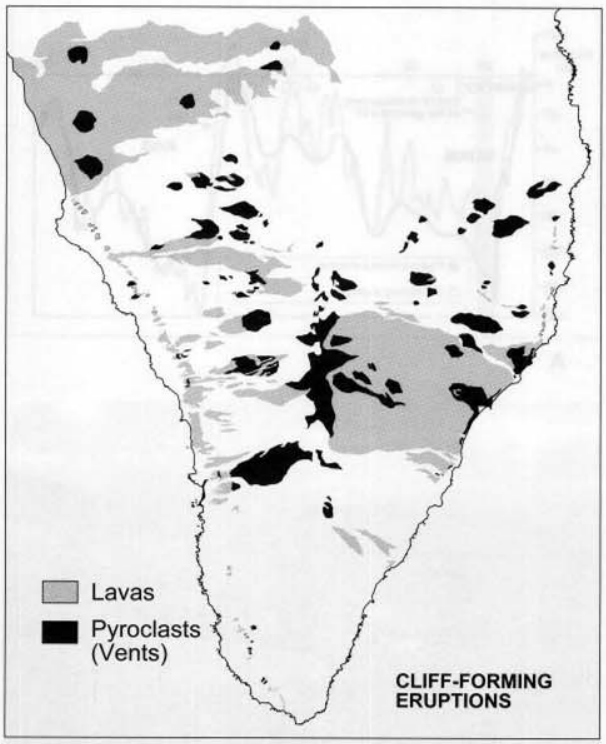


Fig. 23.—Distribution of cliff-forming eruptive vents and lava flows in the Cumbre Vieja volcano.

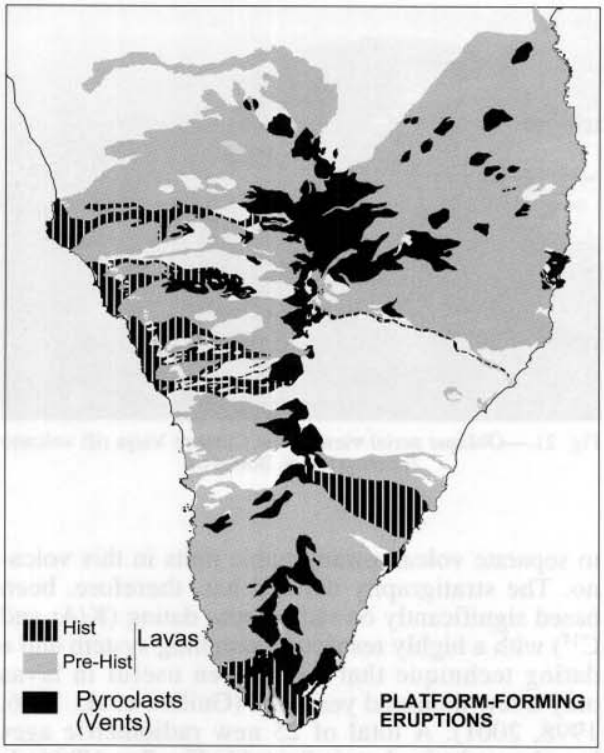


Fig. 24.—Distribution of platform-forming eruptive vents and lava flows in the Cumbre Vieja volcano. Note the reorganization of vents from about 7 ka clustering along the N-S main rift.

and Roque de Guerra to the east. The lavas are basaltic, frequently with high contents of large mafic xenoliths.

Phonolitic domes and lava domes are relatively abundant in Cumbre Vieja, their age ranging from the 56 ka of Roque Teneguía to the 26 ka of Mendo, although others must be considerably older, such as Mña. Enrique, which could not be dated due to the extreme weathering of the rock. The tephri-phonolitic and phonolitic composition of these domes was determined by Hausen (1969) and by Hernández Pacheco and de La Nuez (1983). These last authors interpreted these intrusions to be a single salic Mid-Pleistocene unit forming the basement of the Cumbre Vieja rift. However, the different ages yielded by the intrusions show that they correspond to younger intrusive episodes spread along the whole volcanic history of the Cumbre Vieja rift (see Table 1). Their abundance may reflect, as in Bejenado, the rapid evolution of the magmas of Cumbre Vieja, parallel to their equally fast construction. These salic domes are frequently associated to recent basaltic eruptions, probably because they are highly fractured and provide a pathway for magma to reach the surface.

### Platform-forming eruptions

This unit comprises eruptions younger than about 20 ka and was emitted by eruptive centres forming an increasingly concentrated alignment along the N-S axis of Cumbre Vieja (Fig. 24). This reorganization of volcanism in Cumbre Vieja, with a progressive concentration of emission centres in a progressively better-defined rift, is a characteristic feature of the volcanism of La Palma and oceanic volcanic islands in general (Carracedo, 1979, 1984, 1994, 1996, 1999; Walker, 1992), and will be discussed in greater detail in section II.6.

The lava flows of this unit have resurfaced most of the Cumbre Vieja volcano (Fig. 24), frequently forming wide coastal platforms (see Figs. 4 and 22 B). They are predominantly basaltic in composition, although tephrites and phonolitic tephrites abound.

Some groups of volcanoes are noteworthy, such as the tephritic and basaltic-tephritic Mña. Cabrera and Mña. Faro volcanoes built on the summit of the rift 15 and 18 ka ago, respectively. Other interesting volcanoes are the tephritic and phonolitic-tephritic Birigoyo-La Barquita volcanic group, dated in 6±2 ka and forming a pair of volcanoes situated on the

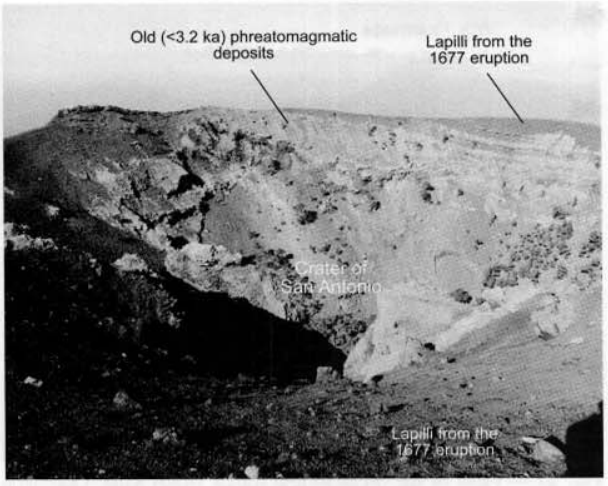


A

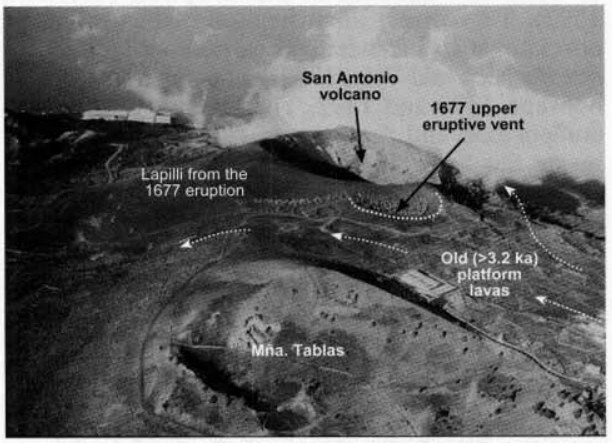


B

Fig. 25.—Views of the prehistorical eruption of San Antonio. A) Crater of the prehistorical San Antonio volcano mantled with pyroclasts of the 1677 Fuencaliente eruption. B) Oblique aerial view of prehistorical lavas older than 3.2 ka encircling the San Antonio volcano.

northern edge of the rift. An especially interesting group is that of the San Antonio-La Caldereta volcanoes, both phreatostrombolian vents located close to the town of Fuencaliente. The San Antonio volcano has been related to the 1677 eruption, although evidence that this eruptive centre, with clear indications of relatively high-energy phreato-strombolian stages, is much earlier than the 1677 eruption, has already been published (Carracedo et al., 1996; Day et al., 2000). This can be synthesized as follows: 1) The cone is surrounded by clearly prehistorical lavas (Fig. 25) dated in 3±2, 4±2 and 3.3±0.1 ka (Guillou et al., 1998); 2) The phreatic stages, with the generation of lateral explosions, must have extended explosive deposits over a wide area around the cone, as can be observed in the La Caldereta vent. However, in the access roadcut to the San Antonio volcano, scarcely 100 m from the cone, the pyroclasts of the 1677 eruption overlie the afore-mentioned prehistorical lavas with no intercalated explosive deposits; 3) Despite the explosivity of the volcano, no important damage to the town, only a few hundred metres distant, is reported in the eye-witness accounts; 4) Remains of an aboriginal settlement have been located on the flanks of the San Antonio volcano (Pais Pais, personal communication); 5) The San Antonio cone appears on a map drawn by Torriani in 1586.

As described later, the true 1677 eruption consists of a small vent resting upon the northern flank of the San Antonio volcano, and several eruptive fissures at the southern base of this volcano, from which abundant lavas were emitted (Carracedo et al., 1996). Pyroclasts from the 1677 and 1971 eruptions covered the San Antonio cone and give it the appearance of a recent volcano. On the other hand, confusion in the identification of eruptions is relatively frequent, even where eye-witness accounts are available (Day et al., 2000). A similar misidentification occurred in La Palma with the 1585 and 1646 eruptions (Hernández Pacheco and Vals, 1982), and part of the 1646 eruption (Carracedo et al., 2001 b).

## Dated prehistorical eruptions

Include dated eruptions older than the colonization of the island in 1492 and, therefore, without eye-witness reports, as well as those initially considered to be historical and later found to be earlier (see Table 1).

*Malforada-Nambroque.* This group of cones and emission centres is situated at the summit of the rift, overlying a large and fractured salic lava dome (Fig. 26 A). Both the Malforada and Nambroque groups are apparently similar in age and composition, although only the Nambroque lavas have been dated, with $C^{14}$, giving an age of 1045±95 years (Carracedo et al., 1999 a). The lavas of both eruptive centres vary from phonolitic tephrites to phonolites, with very thick, short-reaching lava flows (Fig. 26 B).

An interesting aspect of this eruption is the discovery of a burial site containing human and archaeological remains consisting of pottery and partially carbonized human bone fragments, dated by $C^{14}$ in 1090±50 years, embedded in spatters. An analysis

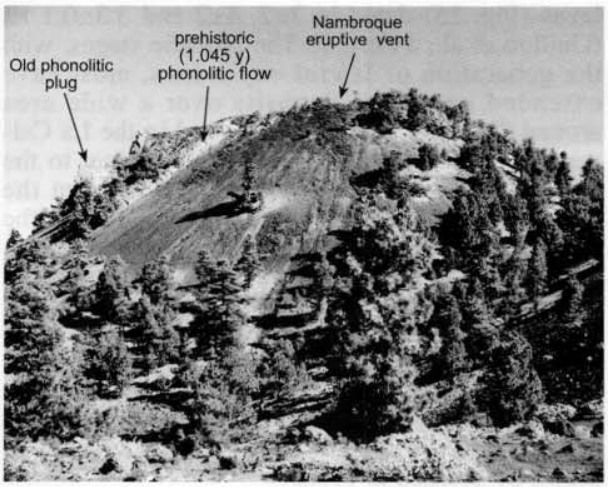


Fig. 26.—Views of the prehistorical Nambroque-Malforada volcanic group. A) Main eruptive centre of the Nambroque eruption (916 AD) showing the pre-existing phonolitic plug and the prehistorical vent and lavas. B) Oblique aerial view of the 1949 basaltic lavas cascading over the Malforada and Nambroque phonolite lavas.

of the recent eruptions of Cumbre Vieja pointed to the Nambroque eruption*.

*Mña. Quemada-Martín Volcano.* The eruption that gave place to the volcanic cone of Mña. Quemada (Fig. 27), very recent in appearance and located at the northern end of the Cumbre Vieja rift, has been mistaken for that of 1585 on the basis of interpretation by Santiago (1960) and Machado (1963) of Torriani's account of this eruption (Torriani, 1592). The correct identification of this eruption, also known as Tacande, was carried out by Hernández Pacheco and Vals (1982), who dated it by $C^{14}$ at between 1470 and 1492. The lavas are basaltic in composition and flow towards the north and west inside the Valle de Aridane, stopping about 2 km from the western coast.

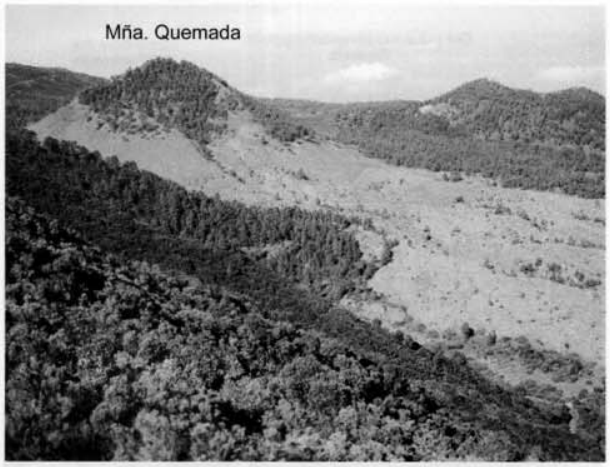


Fig. 27.—View of the prehistorical (circa 1480) Mña. Quemada volcano.

A similar confusion seems to have arisen with the 1646 eruption, in which the interpretation of eye-witness accounts led to the inclusion in this eruption of a group of cones and lava flows, the Martín volcano group, that seem to correspond to a prehistorical event. This group of volcanic cones, tightly clustered on the axis of the rift, is topped with phreatostrombolian ash, providing evidence of explosive eruptive episodes. Attached to the south flank of the Martín volcanic group is a lineament of vents and hornitos issuing abundant lavas towards the coast, unambiguously assigned to the 1646 eruption. The reasons for separating the Martín group, as prehistorical, from the 1646 eruption, are based on the fact that only those that are believed to be prehistorical are covered with phreatomagmatic ash related to the final explosive stages of the Martín vents. The lavas are colonised by a relatively well-developed plant association, absent from any of the historical eruptions of La Palma, and prehistorical archaeological remains were found inside lava tubes of this volcanic group (Pais Pais, personal communication).

## Historical eruptions

This unit comprises the eruptions that occurred in the last 500 years, the historical period of the

* Studies in progress indicate the phreato-strombolian eruption of Montaña Goteras, close to the burial site and an important prehistorical dwelling, to be of similar composition to the spatter englobing the human bones dated at 866 AD, and therefore the most probable age for this prehistorical eruption.

Canary Islands, and all are documented by eye-witness accounts. They frequently present a number of common features, such as the above-mentioned association with fractured phonolitic domes, that act as favoured paths for the magma, and the presence of multiple eruptive vents in a single eruption, frequently along several kilometres long fissures, several of them oblique to the axis of the rift. These vents are predominantly explosive at the summit area (White and Schmincke, 1999) and effusive at the flanks (Klügel et al., 1999).

The duration and other characteristics of the historical eruptions of La Palma have been summarized in Hernández Pacheco and Vals (1982).

*XVIth Century Eruptions.* Only one eruption, the Tahuya, Tajuya or Jedey eruption, took place in La Palma during this century. It is described in an account by Torriani (1592), who witnessed it. A detailed study of this eruption appeared in the work of Hernández Pacheco (1990) and Hernández Pacheco and Vals (1982).

The 1585 eruption includes several cones and emission centres situated over an old phonolitic dome (Fig. 28), located above the village of Jedey, on the western flank of Cumbre Vieja rift. The lava flows cascade down the coastal cliffs towards the sea, forming wide coastal platforms at the shoreline (see Fig. 22 B). An interesting feature of this eruption is that juvenile phonolite lavas were emitted along with basaltic flows, the former intruded as domes and cryptodomes because of their extreme viscosity. These phonolites differ from those corresponding to the older dome over which the eruption took place. The pressure of the lava seems to have lifted the old phonolites to form spines, in a process reported by Torriani (1592) as accompanied with strong seismicity. Falling phonolite blocks appear englobed in the 1585 basaltic flows and show magmatic assimilation and dissolution features.

*XVIIth Century Eruptions.* Two eruptions took place in La Palma in this century, in 1646 and 1677.

The 1646, Tigalate or Martín eruption has eye-witness accounts (Santiago, 1960) reporting two eruptive centres: the upper one at the flank of the prehistorical Martín volcano and the lower vent at the coast (see geological map). Both formed conelets and hornitos and emitted very fluid basaltic lavas.

The 1677 eruption, erroneously associated to the older San Antonio volcano, as already discussed, has been described by Carracedo and co-workers (1996) as having two eruptive vents: the upper, strombolian vent, located at the northern flank of the San Antonio volcanic cone (Fig. 29 A), and the lower vent, which comprises several spatter hornitos along a NW-SE eruptive fissure at the southern

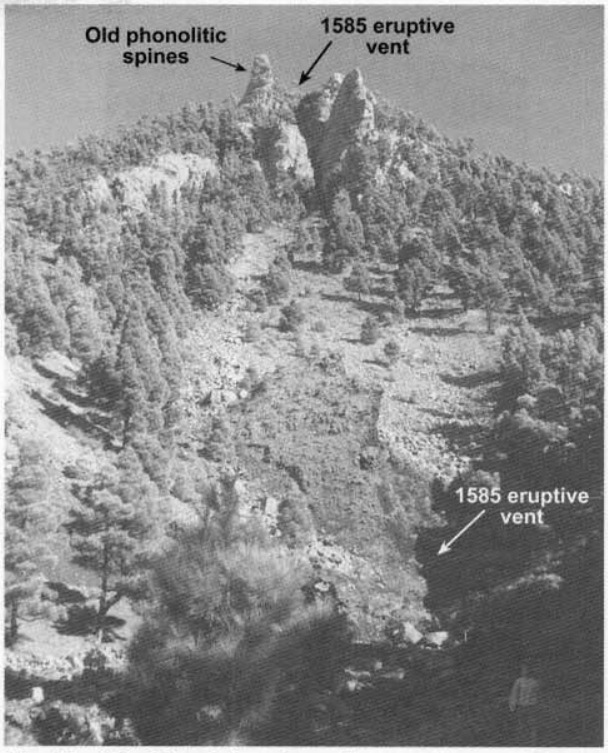


Fig. 28.—The Mña. Jedey, formed by an old phonolitic plug mantled by the vents and lavas of the 1585 eruption.

flank of the San Antonio cone (Fig. 29 B). The latter vent emitted several lava flows that formed an extensive coastal platform. A contemporary picture depicts a recumbent human figure and some livestock lying on the ground (circle in Fig. 29 C), possibly asphyxiated by volcanic gases during the eruption, a rare document illustrating human casualties in relation to volcanic events.

*XVIIIth Century Eruptions.* Only the 1712 or El Charco eruption occurred in this century. This eruption, poorly documented with eye-witness accounts (Santiago, 1960), comprises a large cinder cone (Mña. Lajiones, Fig. 30 A) and several eruptive vents aligned in a NW-SE, 2.5-km-long eruptive fissure from which several lava flows cascaded down the western cliff to form a wide platform (Fig. 30 B).

*XXIth Century Eruptions.* The last two eruptive episodes of La Palma, in 1949 and 1971, are the best studied and documented. The 1949 event, which occurred after a very long quiescence period (237 years), has been described by Bonelli Rubio (1950), Romero Ortiz (1950), Benitez Padilla (1951), San Miguel et al. (1952), and Martel San Gil (1960). Recent detailed studies include those of

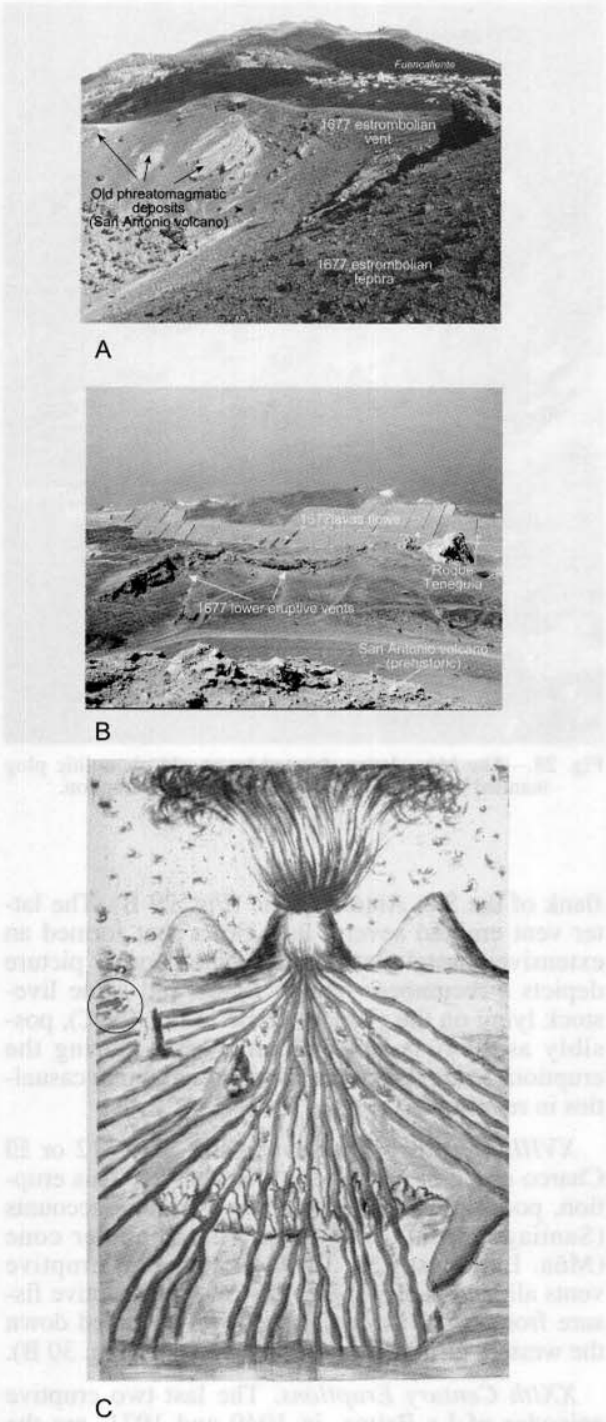


Fig. 29.—View of the southern end of the Cumbre Vieja rift with the upper strombolian vent of the 1677 Fuencaliente volcano mantling the prehistorical San Antonio volcano, the latter showing phreatic surge deposits. B) Lower fissure vents and lava platform of the 1677 eruption. C) Contemporary painting of the 1677 Fuencaliente eruption. Note the recumbent human figure and livestock, indicating casualties (apparently asphyxiated by volcanic gases) in this eruptive event.

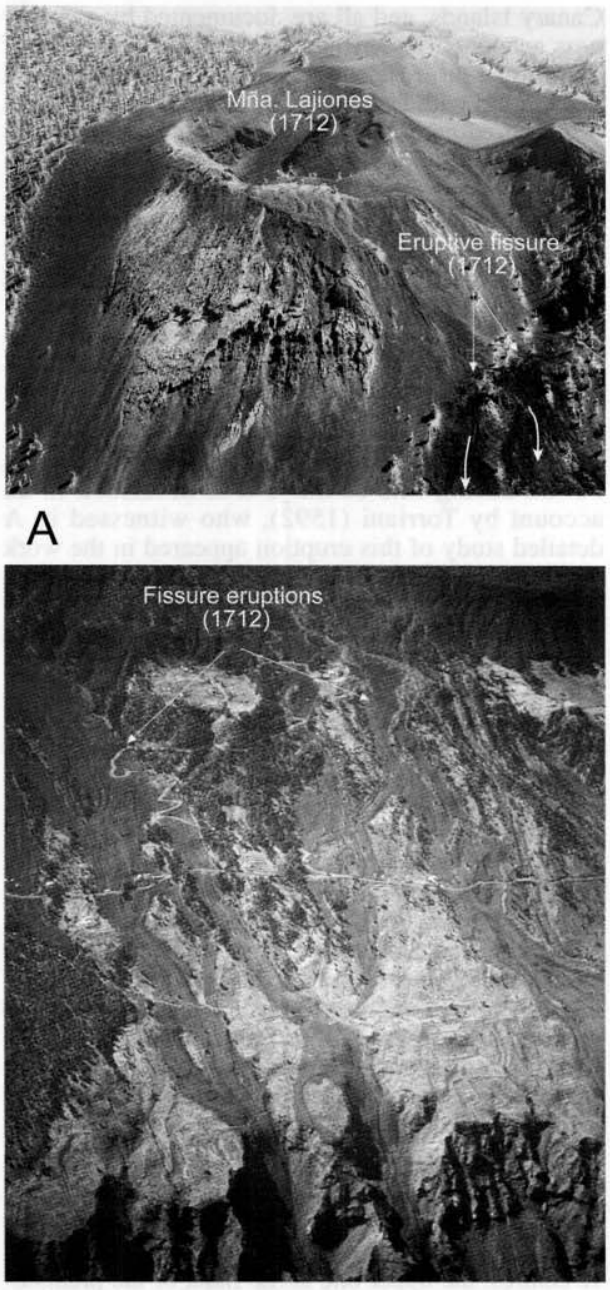


Fig. 30.—Aerial views of the 1712 eruption. A) The main strombolian and phreatostrombolian vent of Mña. Lajiones and the eruptive fissures of 1712. B) Flows from the western eruptive fissures cascading over the cliff at El Remo-Puerto Naos.

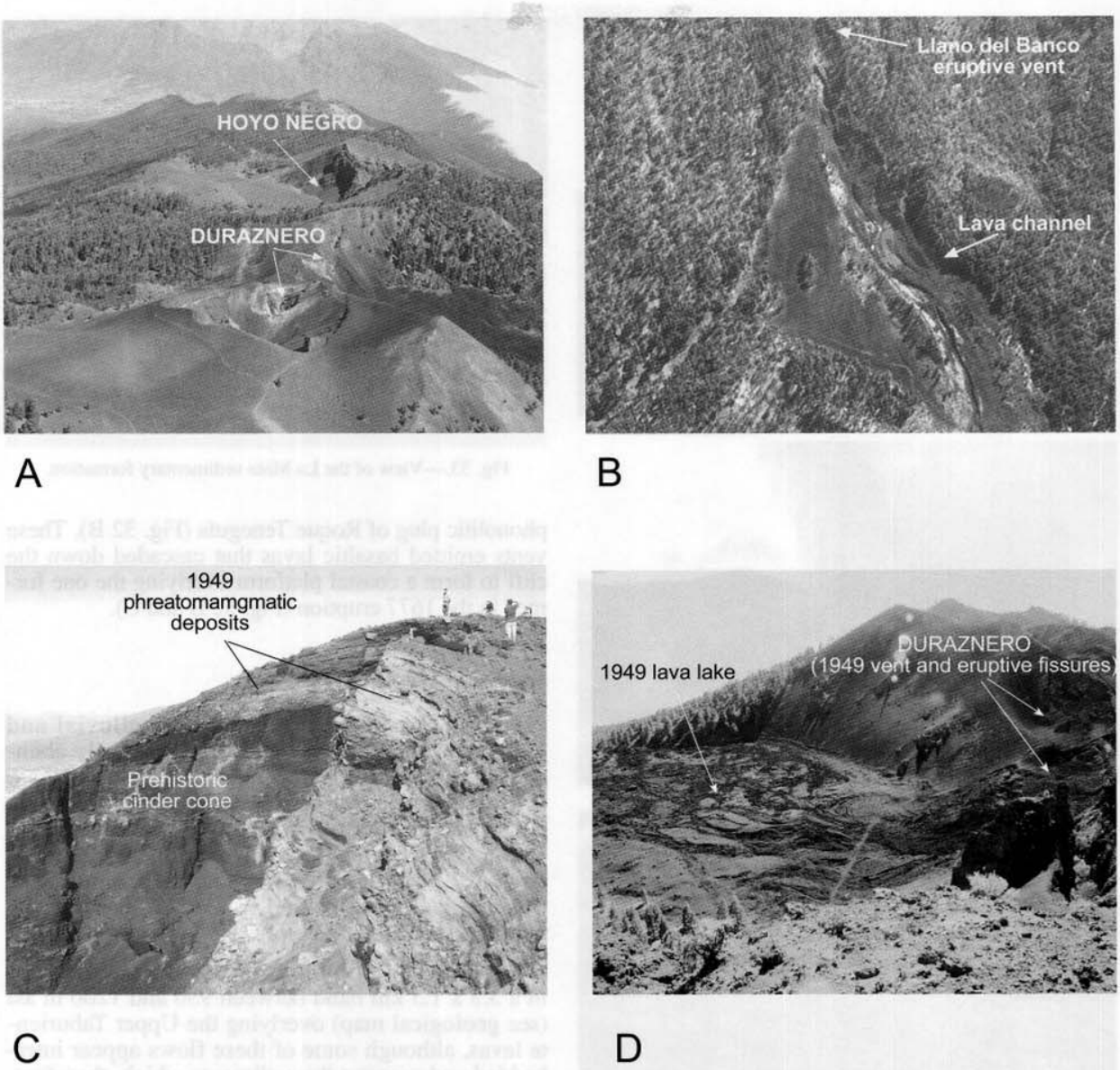


Fig. 31.—Views of the different vents of the 1949 eruption. A) Oblique (from the south) aerial view of the Duraznero and Hoyo Negro 1949 vents. B) Aerial view (from the west) of the Llano del Banco vent and lava flows. C) Phreatomagmatic deposits of the 1949 Hoyo Negro vent mantling a prehistorical strombolian cone. D) Eruptive fissure and lava lake of the 1949 Duraznero emission centre.

Klügel (1998), Klügel et al. (1997, 1999), White and Schmincke (1999), and Day et al. (1999).

Three eruptive vents opened in different phases of this eruption along a 2-km lineation (Klügel et al., 1999). The upper ones, Hoyo Negro and El Duraznero, are located at the summit of the rift in a N-S trend (Fig. 31 A), while the lower one, the Llano del Banco vent opened at 1300 m asl at the western flank (Fig. 31 B). The Hoyo Negro vent was essentially explosive (Fig. 31 C), with several phreatomagmatic phases (White and Schmincke, 1999). Contrarily, the El Duraznero and Llano del Banco vents were predominantly effusive, the former emitting basaltic lavas that formed a lava lake (Fig. 31 D) and descended the eastern flank to a few metres from the coast. The lower vent discharged large volumes of very fluid basaltic lavas that formed a 6 x 3.5-km coastal platform (Fig. 22 B).

The 1971 eruption, the last to occur in La Palma and in the Canaries, has been described in detail in a special volume of Estudios Geológicos (Teneguía volcano, Estudios Geológicos Spec. vol., 1974)




Fig. 32.—Views of the 1971 Teneguía volcano eruption. A) Initial eruptive fissure activity. B) Strombolian vents. C) Oblique aerial view (from the SE) of the group of strombolian cinder cones and lava flows of the 1971 Teneguía volcano eruption. The 1949 coastal platform formed over the previous 1677 coastal lava platform.

Praegel (1986). The eruption started as an eruptive fissure (Fig. 32 A), which progressed to form a group of cinder cones located close to the lower eruptive vents of the 1677 eruption, and both, to the fractured phonolitic plug of Roque Teneguía (Fig. 32 B). These vents emitted basaltic lavas that cascaded down the cliff to form a coastal platform overlying the one formed in the 1677 eruption (Fig. 32 B and C).

Fig. 33.—View of the La Mata sedimentary formation.

*Sedimentary formations*

Sedimentary formations, such as alluvial and beach deposits, aeolian sands, etc., relatively abundant in the older, posterosional eastern islands, are of little significance in the juvenile islands of La Palma and El Hierro. Interesting exceptions, however, are the thick and extensive sedimentary formations of El Time and La Mata, at the mouth of the Caldera de Taburiente and in the NW flank of the northern shield, respectively.

*Sediments of La Mata.* This formation outcrops in a 3.5 x 1.5 km band between 950 and 1200 m asl (see geological map) overlying the Upper Taburiente lavas, although some of these flows appear interbedded and capping the sediments which, therefore, can be located in the Pleistocene.

This deposit, which can be observed in cuts of the northern road above La Mata, shows different facies with gradual lateral changes. The most common is a several metres thick matrix supported conglomerate of rounded to subangular clasts, sometimes exceeding 1 m in diameter and predominantly basaltic (Fig. 33). The structure is predominantly massive with poor reverse grading in places and interbedded alluvial layers. The matrix is clay without traces of volcanic ash. These features suggest a complex mix of massive debris-flows and alluvial deposits.

*Sediments of El Time.* This sedimentary formation is located at the mouth of the Barranco de Las Angus-

tias and extends upriver to the area of La Viña (see geological map). This thick (up to 300 m) succession of poorly sorted conglomerates (Fig. 34 A and B) appears attached discordantly to the Upper and Lower Taburiente lava sequences, and interbedded with the Bejenado volcanics. It was first reported by Lyell (1855) and many other authors thereafter, but the first detailed analysis was carried out by Vegas and co-workers in 1999 and Carracedo and co-workers in 2001. The former authors defined two main units: a volcanic Pyroclastic Unit and a sedimentary Epiclastic Unit. This interpretation has been questioned by the latter authors, who constrain the volcanic pyroclasts to a parasitic vent of the Bejenado volcano, the El Time formation being exclusively made of sediments, as previously generally interpreted.

The genesis of the epiclastic unit is related to *fan delta* deposition (Vegas et al., 1999), prograding in only a few kilometres from the coast to depths of about 4000 m. Subsequent coastal regression favoured the progressive incision of the Bco. de Las Angustias. This process explains why the clasts of the lower part of the sediments are predominantly volcanics of the Taburiente and Bejenado volcanoes, and why clasts corresponding to the submarine lavas and associated intrusives only appear in the upper part of the sequence.

*Beachrocks.* Beachrocks have been located along the SW coast of La Palma, from Punta Naos to Fuencaliente (Calvet et al., in press). They are formed by sand to gravel size sediments in different stages of carbonate cementation, on the beaches of Punta Naos, Charco Verde, Las Zamoras, Chica and Echentive, developed on platform-forming lavas of the Cumbre Vieja volcano (see geological map).

## Petrology and geochemistry

### *Submarine volcano*

The petrographic characteristics of the pillow lavas, pillow breccias and hyaloclastites that form the submarine volcano have been analysed by Hernandez-Pacheco and Fernandez Santín (1974), Staudigel (1981), Staudigel y Schmincke (1984), and in the MAGNA of Northern La Palma (Carracedo et al., 2001a). These lavas comprise different types of basalts, grading from plagioclase basalts to doleritic basalts (oceanites-ankaramites), in relation to the relative content of plagioclase and olivine-pyroxene and textural characteristics (Hernandez-Pacheco and Fernandez Santín, 1974; Staudigel and Schmincke, 1984).

These basalts are strongly altered by metasomatism, giving place to new paragenetic sequences (albite, clorite, epidote, actinolite, andradite, zeolites and calcite), as well as by propylitization, possibly as a result of the different intrusions (Hernandez-Pacheco and Fernandez Santín, 1974; Staudigel, 1981; Staudigel and Schmincke, 1984; De La Iglesia et al., 1996).

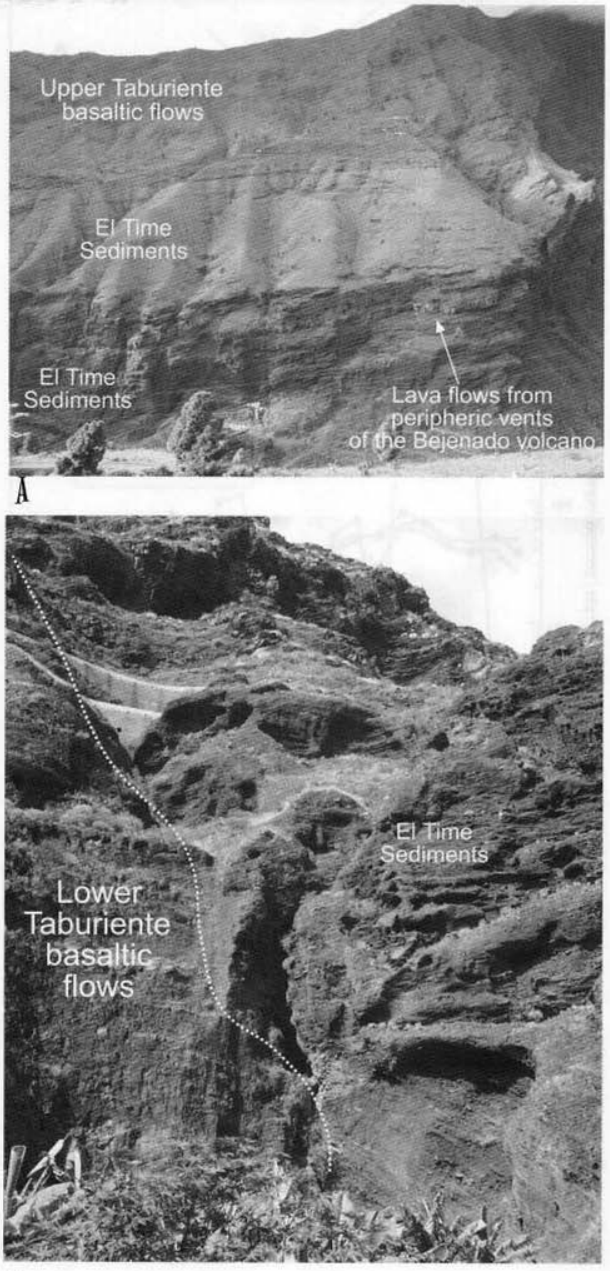


Fig. 34.—Sediments of El Time. A) Epiclastic formations of El Time with interbedded lava flows of the Bejenado volcano outcropping in the western wall of the Caldera de Taburiente. B) Close-up of the sediments of El Time, attached unconformably to the Lower Taburiente volcanic sequence at the western wall of the Caldera de Taburiente.

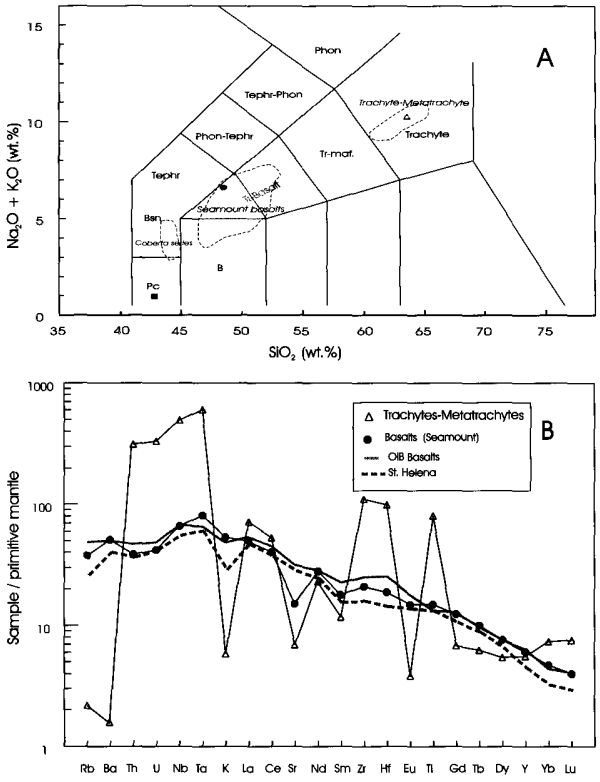


Fig. 35.—A) Total Alkali vs. Silica (TAS) diagram for submarine lavas and trachytic domes. The limits are from Hernández Pacheco and Fernandez Santín (1974), Staudigel and Schmincke (1984). The boundaries are from Le Bas et al. (1986). B) Primitive mantle normalized diagram (Sun and McDonough, 1989), for incompatible trace elements of seamount basalts and trachytes. The OIB data and primitive basalt from St. Helena, are taken from Sun and McDonough (1989).

The pyroxene-plagioclase basalts forming the pillow lavas in the Barranco de Las Angustias (Table 2-1, Sample-95) plot in the TAS diagram of Fig. 35A in the basalt-trachybasalt field, clearly separated from the oceanitic-picritic terms (Hernandez-Pacheco and Fernandez Santín, 1974). Their primitive mantle normalized values are close to the mean values of many other oceanic volcanoes (OIB) and St. Helena HIMU basalt, as proposed by Sun and McDonough, 1989 (Fig. 35B).

## *Intrusive formations*

*Trachytic domes and lava domes.* Mainly made of breccia fragments with flowage textures (Hernandez-Pacheco and Fernandez Santín, 1974), they were termed as metatrachytes by Staudigel and Schmincke (1984) because they frequently appear altered to albite, biotite, clorite and epidote.

These intrusives (Table 2-1, Sample 105) are grouped in the trachyte field in the TAS diagram of Fig. 35A. However, they show important elemental variations, as shown in Fig. 35B, probably due to metasomatism. Staudigel and Schmincke (1984) emphasized the significant enrichment in incompatible elements, as shown by the low content in Rb and Ba. Another interesting feature is the high positive anomalies (Th, U, Nb, Ta, Zr and Hf), negative anomalies (K, Sr, Eu), and enrichment in heavy rare earth elements (HREE).

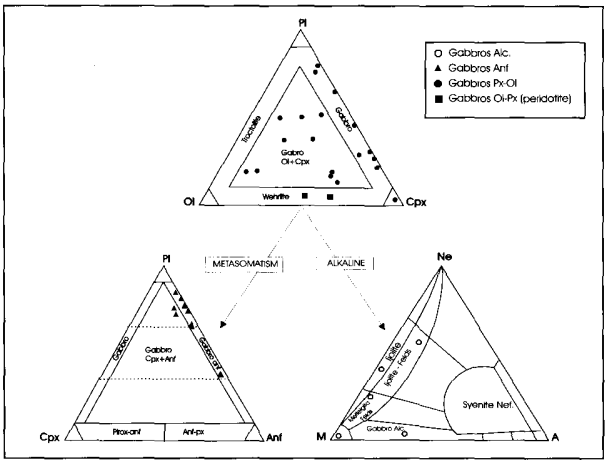


Fig. 36.—Modal composition of intrusive gabbros inside the Caldera de Taburiente. Data from De La Nuez (1984).

*Gabbros.* De La Nuez (1984) and Carracedo et al. (2001) confirmed the petrological and geochemical variability of the plutonic intrusions inside the Caldera de Taburiente. The former author separated two different groups: «Gabbros» and «Olivine gabbros» (De La Nuez, 1984, Table 7 and Fig. 85). The composition and alteration processes of representative plutonic samples obtained inside the Caldera in the MAGNA of Northern La Palma by Carracedo and co-workers (2001) are shown simplified in Fig. 36.

Gabbro plutonics outcropping inside the Caldera, clearly independent of the seamount and most probably related to the feeding of the subaerial volcanoes (Table 2-1, Samples 103-104-108), have been separated in the MAGNA (Carracedo et al., 2001) and in the geological map from those intruding the seamount (Table 2-1, Samples 96,59,98,109). As shown in the plots of Fig. 37A and 37B, the petrological characteristics are less discriminating than field observations, mainly because of the wide range of compositional variation of the rocks. However, these younger gabbros clearly differ in the lack of significant hydrothermal alteration.

*Dyke swarms.* The significant petrological and geochemical diversity of the different dyke swarms has been quoted by many authors (Hernández Pacheco, 1975; Staudigel, 1981; Staudigel and Schmincke, 1984, Staudigel et al., 1986; De La Nuez, 1984, 1991; Carra-

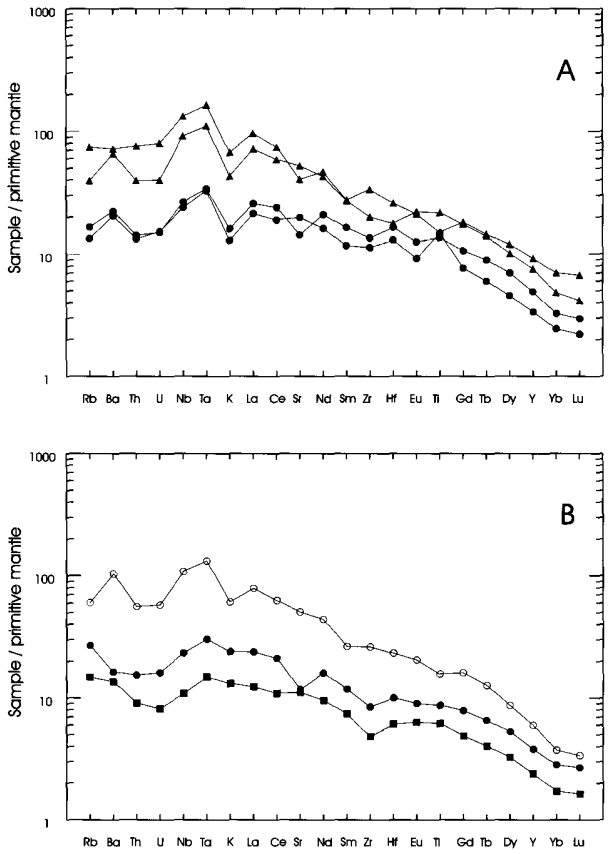


Fig. 37.—A) Primitive mantle normalized diagram (Sun and McDonough, 1989) of incompatible trace elements of intrusive gabbros intruding the seamount. B) Idem from gabbros postdating the seamount and feeding the subaerial volcanoes. The primitive mantle element concentrations are from Sun and McDonough (1989). Symbols as in Fig. 36A.

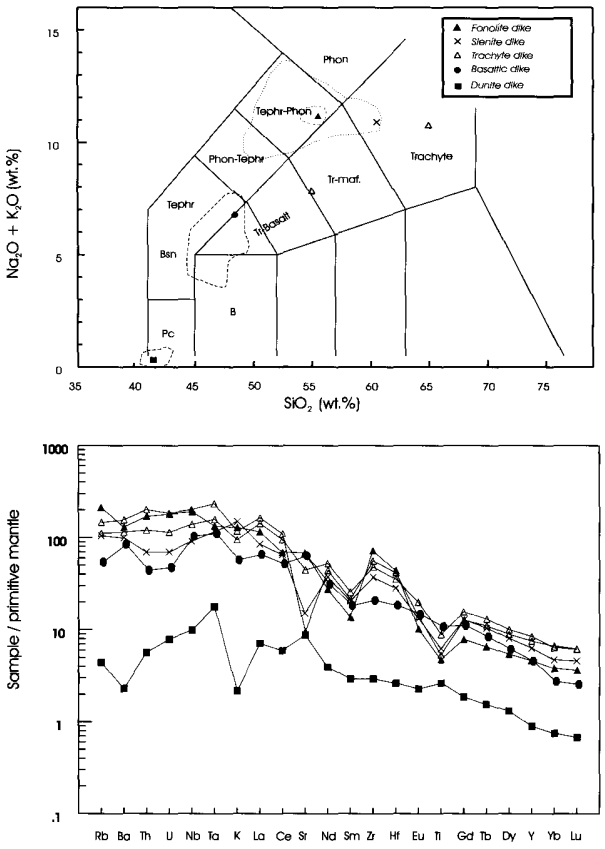


Fig. 38.—A) TAS diagram for intrusive dykes inside the Caldera de Taburiente. The limits are from Hernández Pacheco and Fernández Santín (1974), and Staudigel and Schmincke (1984). The boundaries are from Le Bas et al. (1986). B) Primitive mantle normalized diagram (Sun and McDonough, 1989) for incompatible trace elements from dykes inside the Caldera de Taburiente.

cedo et al., 2001). As shown in the TAS diagram of. 38A, basaltic dykes are predominant with respect to trachytic and phonolitic, with fewer syenite and dunite intrusives (Hernández Pacheco, 1974, 1975).

The geochemical characteristics of representative samples of the different types of dykes are shown in Table 2-1 (samples 102 a 181) and Fig. 38B, where the dunite dykes separate because of the lower elemental content from the other groups of more differentiated intrusives. The latter show significant enrichment in REE and incompatible elements, with Zr and Hf positive anomalies and negative Ti, Sm and Sr, the latter absent in the phonolitic dykes.

### *The Northern Shield*

*The Garafia Volcano.* Lavas from this volcano are mainly olivine-pyroxene and olivine-pyroxene-plagioclase alkali basalts, the former presenting frequently porphyritic to aphyric (trachytoid) textures and subophitic the later. The olivine-pyroxene-plagioclase basalts form the bulk of the earlier stages of the volcano and outcrop in the headwall of the deep northern barrancos and inside the galería Los Hombres.

Many of the samples (Table 2-2, samples 77, 80, 157, 172) with primary characteristics (Mg#> 60 and Ni > 200-300 ppm) plot in the basaltic field, whereas the more evolved samples plot in the trachybasaltic field (Fig. 39A). The elemental variation diagram of Fig. 39B evidences a progressive increase in elemental content, from the less enriched olivine-pyroxene-plagioclase basalts to the trachybasalts, but with clear subparalle trends. Some significant differences can be observed when the normalized values (Sun and McDonough, 1989) of the primitive basal from St. Helena (Mg# ~ 65) are shown for comparison. The highly incompatible elements presenting uniform subparallel trends, with progressive increments and marked positive (Rb, Ba, Th and U) anomalies

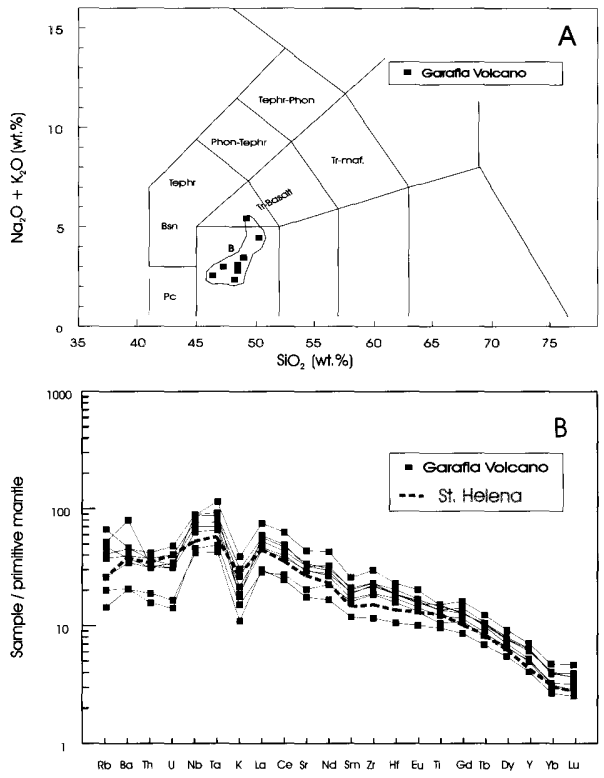


Fig. 39.—A) TAS diagram from basaltic lavas of the Garafía volcano. Boundaries from Le Bas et al. (1986). B) Primitive mantle normalized diagram (Sun and McDonough, 1989), for incompatible trace elements from basaltic lavas of the Garafía volcano. The data of a primitive basalt from St. Helena, are taken from Sun and McDonough (1989).

towards the more differentiated terms. Similarly, light rare earth element (LREE) and Zr enrichment is progressive from the ol-px basalts to trachybasalts, with K and Sm showing negative anomalies. The lesser importance of feldspars is evidenced by the normal values of Eu. Analogous HREE progressive enrichment can be observed, trends with similar subparallel coinciding with St. Helena values.

Elemental variations are shown in the plots of Fig. 40. Variations of major elements in the Garafía volcano lavas are constrained by MgO content, with minor increment of $SiO_2$, $Fe_2O_3t$, $TiO_2$ y $P_2O_5$, and a better definition of decrements in $CaO/Al_2O_3$ towards the more differentiated terms (MgO < 8%). Decrement patterns in compatible elements Ni, Cr, Co and Sc may be in relation to the fractionation of ferromagnesian components.

*The Taburiente volcano.* The entire Taburiente volcano presents similar compositional trends, with prevalent alkali basalt to trachybasalt lavas. However, a clear diversification towards basanites-tephrites can be observed as the volcano developed, culminating in the terminal stages of the Upper Taburiente with the emission of more differentiated tephri-phonolitic lavas.

The Lower Taburiente sequences outcropping in the lower part of the Caldera de Taburiente show a remarkable petrographic uniformity, predominantly olivine-pyroxene basalts. Outcrops in the slopes and deep barrancos of the northern shield are frequently aphasic trachytoid basalts.

The Upper Taburiente volcano lava sequences are more complex, with abundant ol-cpx, ol-cpx-plg and amphibole basalts. Phonolitic tephrites and phonotephrites are the typical terms in the differentiated lavas of the terminal stages of the Upper Taburiente volcano. A representative lithologic section is the northern wall of the Bco. Jurado, where the volcanic sequence is made from bottom to top of ol-px basalts—ol-px-plg basalts—amphibolic basalts—mafic haüyne tephrites. The latter outcrop as well along the Caldera de Taburiente rim (see geological map), with diverse mineralogical and textural characteristics giving place to different typologies (mafic tephrites, phono-tephrites and trachyphonolites).

An interesting type of rock is related to the hydromagmatic eruptive vent of La Galga, north of Puntallana, a welded-tuff type of ignimbrite, with abundant subrounded clasts of basalts; fragments of inclusions of pyroxene and clinopyroxene crystals, oxidized olivine and opaque minerals; and juvenile crystals of biotite and amphibole. The ensemble is cemented by a hypo-microcrystalline groundmass with abundant vesicles filled with zeolite and carbonates.

*Geochemical features of the Taburiente volcano.* The analytical data from representative lavas of the Taburiente volcano, shown in Tables 2-3 to 2-5, indicate the nearly primary character (Mg# > 60, Ni (>200 ppm) of the Lower Taburiente lavas, in contrast with the consistently more evolved and differentiated characteristics of the Upper Taburiente ones. These features are consistent with the uniform trends observable for the entire sequence in the elemental variation vs. MgO% plots of Fig. 40, with the only exception of an interruption in the range of ~ 8% MgO, very similar to that described for the Garafía volcano. The evident drop in Cr and Ni content in the range of MgO < 6% may reflect the important role of olivine and clinopyroxene fractionation. The major elements show a general decrease in these diagrams in $SiO_2$ vs. MgO%, in contrast with the general positive trends in the remaining major elements ($CaO/Al_2O_3$), $Fe_2O_3t$, $TiO_2$ and $P_2O$, even for MgO < 6%. These features suggest fractionation of clinopyroxene and Fe-Ti oxides in the entire sequence for MgO < 6%, possibly associated to apatite segregation in the more differentiated tephri-phonolite lavas.

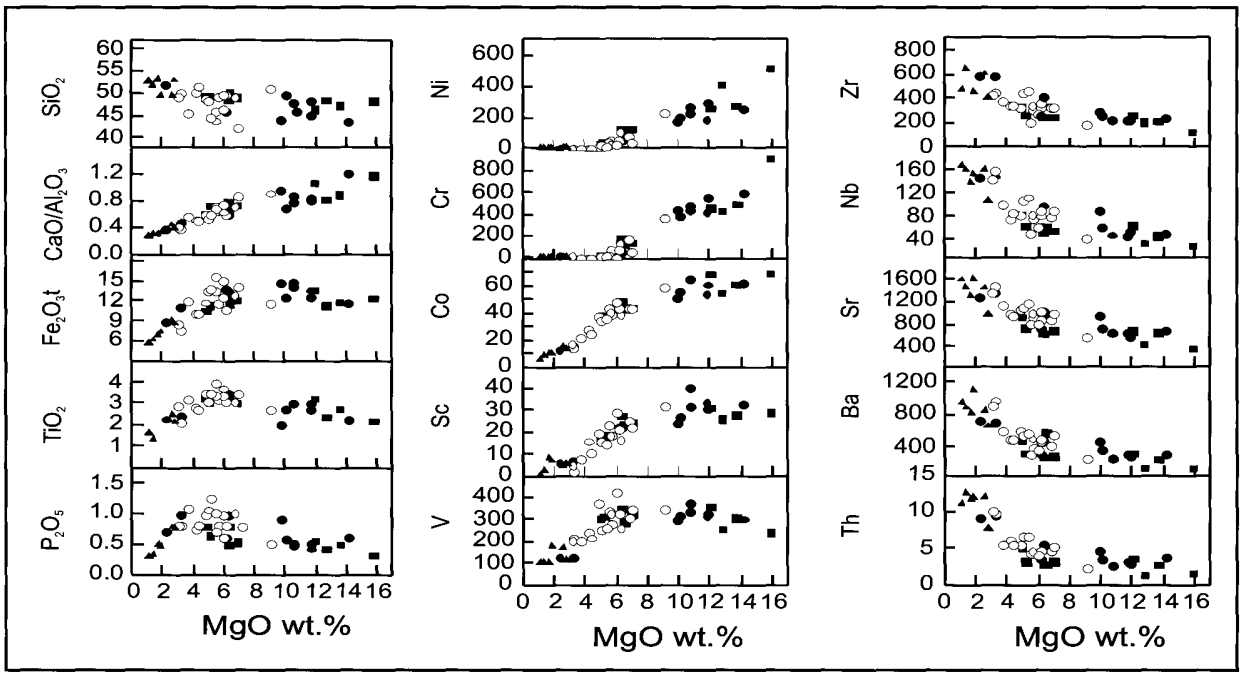


Fig. 40.—Variation diagrams for major, trace and REE elements for the Garafía and Taburiente volcano. Symbols as in Figs. 39 A and 41.

The TAS diagrams of Fig. 41A evidence these compositional variations in the entire Taburiente volcano. The Lower Taburiente volcano lavas plot mainly in the basalt field, with deviations towards the subsaturated basanitic terms in the sequences of the lower part of the Caldera de Taburiente wall and lesser representation of more differentiated trachybasalt and phono-tephrite lavas. The Upper Taburiente lavas overlap this succession, with a distinct tendency towards the basanite-tephrite fields. The more differentiated samples group in the phono-tephrite and tephri-phonolite fields, corresponding, as mentioned, with the terminal differentiated eruptions of the northern shield. Similar tendencies towards progressive differentiation in the Taburiente volcano can be concluded from the sequential overlapping of the normalized diagrams in Fig. 41B. The Lower Taburiente lavas show normalized values, Sun and McDonough (1989), with similar subparallel trends to the St. Helena and significantly higher than those corresponding to the Garafía volcano (see Fig. 39B).

The terminal eruptions of the late stages of development of the Taburiente volcano seem to be, therefore, the culmination of the differentiation process of a period of continued magmatism along the entire construction of the northern shield. This conclusion is consistent with the homogeneity of the geochemical features and the geological observations. Initial ol ± cpx ± mt-ti crystal fractionation and apatite segregation, in the more differentiated lavas, seem the main processes involved, resulting in a progressive increment in the more incompatible elements.

*The Bejenado volcano.* As described before, this stratovolcano developed extremely rapidly, nested in the embayment originated in the collapse of the Taburiente volcano. The patterns of differentiation observed during the entire construction of the northern shield are presented here in a very short time, probably less than about 50 ka. In this period the sequence evolved from initial basanitic rocks to differentiated lavas in the latest stages.

The bulk of the stratovolcano is made of olivine-pyroxene and pyroxene-amphibole basalts, with typical porphyritic textures. In contrast, the terminal differentiated vents erupted mainly tephrites and mafic haüyne phonolites, with subordinate haüyne-nepheline foidites. Textures are typically porphyritic, with dominant mafic minerals and less abundant feldspar —feldspathoids in a hypo— to microcrystalline groundmass with flowage patterns. The tephrites with foiditic trends are scant, and show an association of large nepheline phenocrystals, microcrystals of haüyne and abundant inclusions, in a hypocrystalline groundmass of clinopyroxene, opaque minerals and subidiomorfic feldspathoids.

The dykes and sills outcropping in the summit of the Bejenado volcano show the most evolved rocks of the entire volcano, typically mafic phonolites with predominant feldspar phenocrysts and subordi-

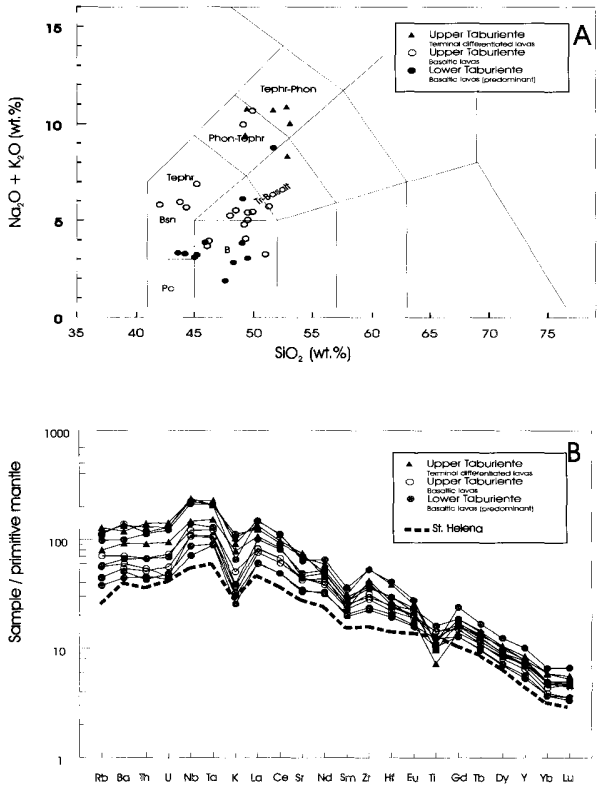


Fig. 41.—A) Total alkali vs. silica (TAS) diagram for the Taburiente volcano. Boundaries from Le Bas et al. (1986). B) Primitive mantle normalized diagram (Sun and McDonough, 1989), for incompatible trace elements for the Taburiente volcano. The data of a primitive basalt from St. Helena are taken from Sun and McDonough (1989).

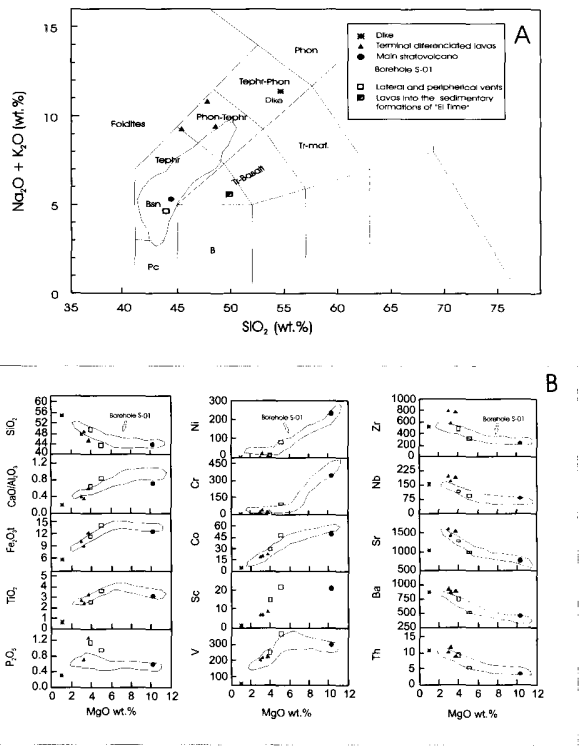


Fig. 42.—A) TAS diagram from lavas and dykes of the Bejenado volcano and adventive vents. Boundaries from Le Bas et al. (1986). B) Variation diagrams for major, trace and REE elements from lavas and dykes of the Bejenado volcano and adventive vents. The borehole S-01 limit for major, trace and REE elements is from Drury et al. (in progress). Symbols as in Fig. 42 A.

nate mafic minerals, including accessory apatite microcrystals. The hypocrystalline groundmass is made of needlelike microlites of feldspar with flow patterns embedded in a hyalopilitic glass.

Adventive vents of the Bejenado volcano emitted the lava flows that outcrop at both sides in the walls of the Bco. de Las Angustias interbedded in the El Time sediments. These lavas are primarily olivine-pyroxene and pyroxene-amphibole basalts.

The most significant geochemical feature of the Bejenado volcano is the absence of alkali basalts in comparison with the pre- and post-collapse Taburiente volcanics. Most Bejenado lavas are basanites and tephri-phonolites, as reported by Drury et al. (in progress). The plotting of the analytical data (Table 2-6) in the diagram of Fig. 42A shows a distinct separation of the basanites of the main stratovolcano from the more differentiated lavas of the terminal vents and sills. Representative samples of borehole S-01, located in the flank of the Bejenado and crossing the entire volcano to the seamount basement (Carracedo et al., 1999 a; Drury et al., in progress) show a greater petrological dispersion, from tephri-phonolites at the upper part, to tephrites and basanites at the bottom. Similar evidence is indicated by the variation diagram of Fig. 42B), where the content in $SiO_2$ vs. MgO% show inverse relations, a tendency clearly illustrated in the sequence of borehole S-01 by Drury et al. (in progress). The $CaO/Al_2O_3$, $Fe_2O3t$ and $TiO_2$ vs. MgO% provide evidence of the role of mineral fractionation in the evolution of the Bejenado volcano. The positive correlation of $CaO/Al_2O_3$ vs. MgO% in the range of MgO < 6 % indicates significant clinopyroxene and ferromagnesian fractionation. Subparallel variation trends shown by $Fe_2O3t$ and $TiO_2$ and positive correlations of Ni, Cr, Co, Sc and V vs. MgO% confirm the increasing fractionation of Fe-Ti oxides in the more differentiated lavas. In contrast, incompatible elements such as Zr, Nb, Sr, Ba and Th present increasingly negative correlations towards the more evolved tephri-phonolitic terms, with an end-point in the sills at the top of the volcano.

The normalized plots of Fig. 43A show a positive anomaly for the Ba, Nb and Ta in the basanites of the

main stratovolcano (Sun and McDonough, 1989). The differentiated lavas appear clearly enriched in all the elements except Ti, with positive anomalies Nb, Ta, Zr and LREE. Lavas from the adventive vents show similar trends, as shown in the diagrams of Fig. 43B.

In general, the main geochemical features of the Bejenado volcano suggest a distinct crystal fractionation of olivine, clinopyroxene and spinel, and the crystallization of amphibole in the more differentiated terminal phases. Contrarily, significant fractionation of plagioclase seems absent, as evidenced by the lack of Eu anomaly, with the probable exception of the sills crossing the top of the volcano.

Modelling and characterization of the isotopic heterogeneity of the original mantle source is detailed in Drury et al. (in progress).

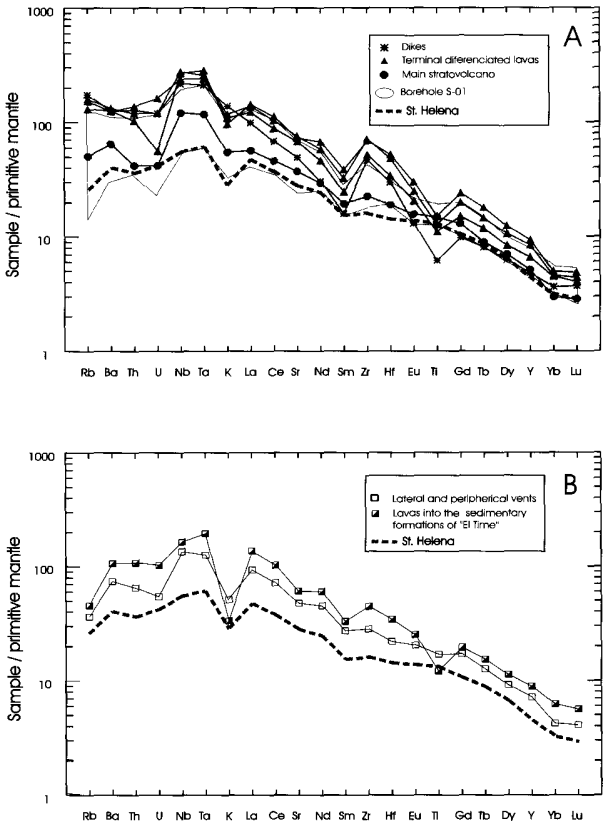


Fig. 43.—A) Primitive mantle normalized diagram for incompatible trace elements from lavas and dykes of the Bejenado Edifice. The borehole S-01 limit is from Drury et al. (in progress). B) Primitive mantle normalized diagram (Sun and McDonough, 1989), for incompatible trace elements of adventive vents of the Bejenado volcano. The data of a primitive basalt from St. Helena are taken from Sun and McDonough (1989).

*The Cumbre Vieja volcano*

*Cliff- and Platform-forming eruptions.* The last activity in La Palma, located exclusively in the Cumbre Vieja rift volcano (Carracedo, 1994; Carracedo et al., 1997, 1998, 1999a,b, 2001b; Guillou et al., 1998, 2001), shows an ample petrologic diversity (Klügel et al., 1999), with predominance of basanitic, tephritic and phono-tephritic lavas and phonolitic and tephri-phonolitic intrusives (domes and lava domes). The most significant feature is the existence of repetitive cycles in which basaltic (principally basanitic) lavas are largely predominant, with minor derivations to tephritic and phono-tephritic eruptions (Carracedo et al., 1977a,b). In general, the petrological characteristics of the Cumbre Vieja volcano are distinctly different from those of the preceding subaerial volcanoes (the Garafía, Taburiente and Bejenado volcanoes).

As described in Section II.3, two main stratigraphic units –cliff-forming and platform-forming eruptions– have been defined in the Cumbre Vieja volcano, separated by the isochrone of about 20 ka, the approximate time of occurrence of the last maximum glacial (Carracedo et al., 1997a,b, 1998).

The cliff-forming eruptions include a sequence of lava flows and intrusive rocks in the form of phonolitic domes and lava domes. Hausen (1969) and Hernández Pacheco and De La Nuez (1983) have defined the petrologic characteristics of the phonolitic intrusions. As already mentioned, these authors believed all the phonolitic intrusions in the Cumbre Vieja volcano being of the same age (Mid-Pleistocene) and forming the basement of the Cumbre Vieja rift. However, radiometric dating of these rocks shows them to form independent intrusive events along the entire volcanic history of the Cumbre Vieja volcano (Carracedo et al., 1997a,b; Guillou et al., 1998, 2001). The conclusion of the latter authors is consistent with the diverse composition of the different domes. The phonolitic tephrites of the Los Campanarios, El Cabrito and Mendo domes are the more basic and frequent terms, but mafic phonolites also abound, as in the Roque de la Fuente, Pino de La Virgen, Dña. María and Roque Niquiamo. Finally, the Roque Teneguía and other domes, cryptodomes and lava domes in the cliff near the Teneguía volcano are formed by phonolites, more alkaline and differentiated than the former. Trachytic phonolites are rare, the only outcrop being the dome of Mña Enrique, a rock made of subidiomorphic sanidine phenocrystals, euhedral microcrystals of haüyne and scant mafic minerals in a feldspatic groundmass. The rock is deeply weathered and dating has been unfeasible.

The petrological characteristics of the lava sequences of the cliff-forming unit correspond predominantly to olivine-clinopyroxene and clinopyroxene-amphibole basalts. Plagioclase basalt lavas are

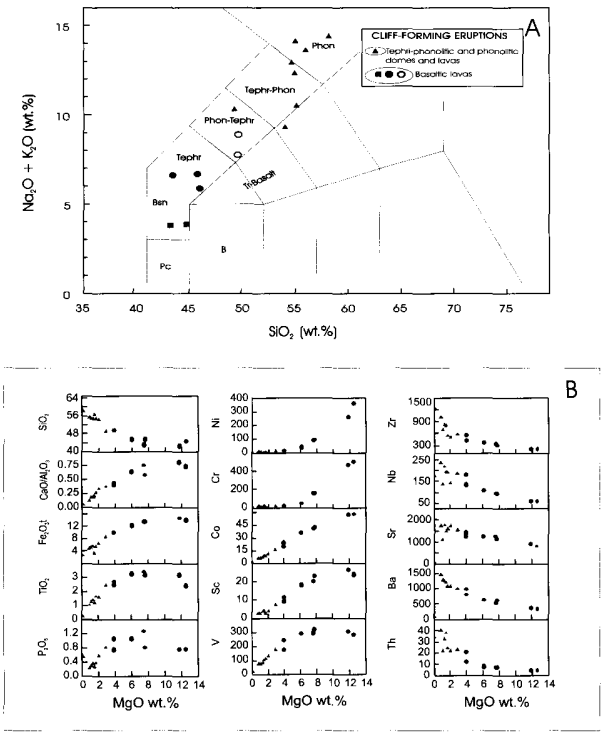


Fig. 44.—A) TAS diagram for basaltic lavas and phonolitic domes of the Cumbre Vieja volcano (cliff-forming eruptions). Boundaries from Le Bas et al. (1986). B) Variation diagrams for major, trace and REE elements from basaltic lavas and phonolitic domes of the Cumbre Vieja volcano (cliff-forming eruptions). Symbols as in Fig. 44 A.

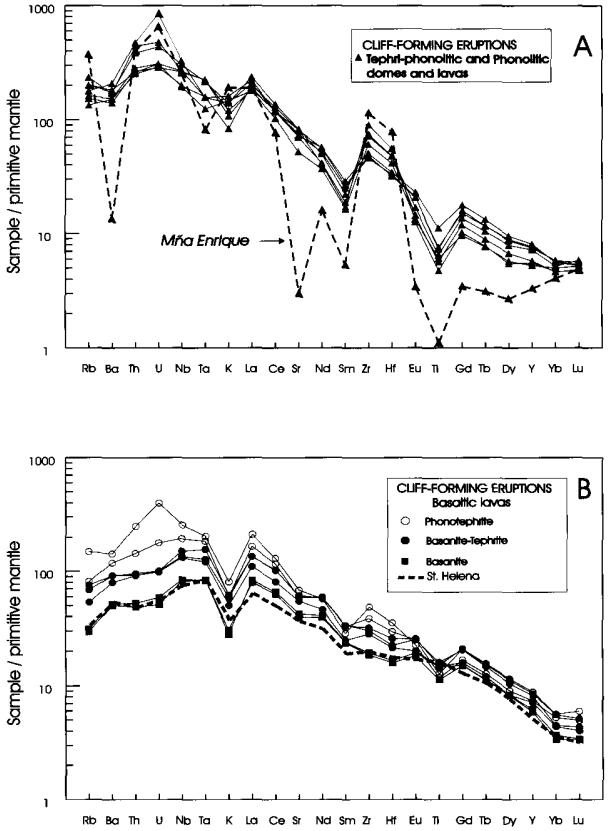


Fig. 45.—A) Primitive mantle normalized diagram (Sun and McDonough, 1989), for incompatible trace elements of tephri-phonolitic and phonolitic domes and lavas of the Cumbre Vieja volcano (cliff-forming eruptions). B) Idem of basaltic lavas of the Cumbre Vieja volcano (cliff-forming eruptions). The data of a primitive basalt from St. Helena are taken from Sun and McDonough (1989).

constrained to the pahoe-hoe lava field near Tigalate, in the SE flank of the rift.

The geochemical data and main characteristics of this unit are shown in Tables 2-7 and 2-8, and Fig. 44A. As shown in the TAS plot of Fig. 44A, most cliff-forming basaltic lavas are basanites and tephrites, with a secondary trend towards picritic basalts, probably in relation to accumulative processes, while the more differentiated lavas are phono-tephrites. The phonolitic domes show a wider dispersion, ranging from phono-tephrites similar to the more differentiated lavas, to phonolites s.s. The major element vs. MgO% diagram of Fig. 44B confirms the overlap of the more evolved basaltic lavas and the less evolved intrusions evidenced in the TAS plot. These trends are suggested in the negative correlation of $SiO_2$ and the positive correlation of $CaO/Al_2O_2$ vs. MgO%, possibly in response to clinopyroxene fractionation. The $Fe_2O_3t$ and $TiO_2$ vs. MgO% correlations suggest a significant fractionation in the range of MgO < 6% in the more differentiated lavas. A similar tendency is observed in the $P_2O_5$ possibly in relation to apatite fractionation in the phono-tephrite lavas. The minor element variations of Fig. 44B confirm the features described, as well as in the normalized plots of Fig. 45A, where the enrichment in highly incompatible elements (Rb, Ba, Th and U) and LREE reaches a peak in the tephri-phonolitic and phonolitic domes and lava domes, with the clear exception of the trachytic phonolite dome of Mña Enrique. The basaltic cliff-forming lavas elemental trends (Fig. 45B) show basanite normalized values similar to those of St. Helena (Sun and McDonough, 1989), clearly separated from the values of the differentiated tephri-phonolitic lavas. The most noticeable feature is the marked Th-U positive anomaly, not observed in the lavas of the Taburiente and Bejenado volcanoes (see Figs. 41B and 43A). In contrast, the Nb-Ta anomalies are present in these northern shield volcanoes and in the basanite cliff lavas of the Cumbre Vieja volcano.

In summary, the distinct compositional divergences of the cliff-forming lavas of Cumbre Vieja and the associated intrusives evidence a significant geochemical break. A possible explanation, as suggested by

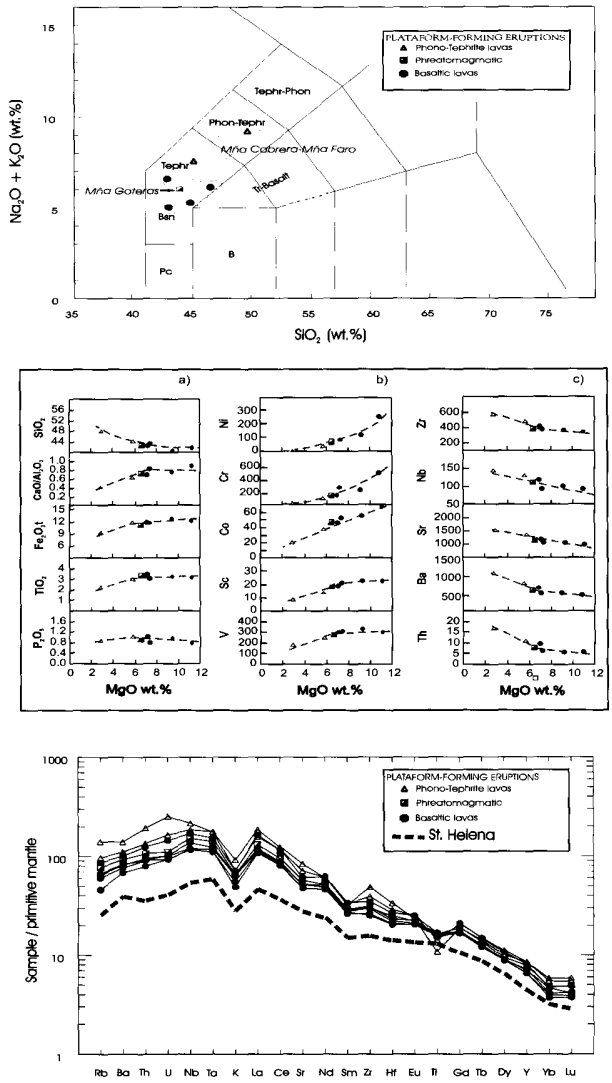


Fig. 46.—A) TAS diagram for lavas of the Cumbre Vieja volcano (platform-forming eruptions). Boundaries from Le Bas et al. (1986). B) Variation diagram for major, trace and REE elements for lavas of the Cumbre Vieja volcano (platform-forming eruptions). Symbols as in Fig. 46A. C) Primitive mantle normalized diagram (Sun and McDonough, 1989), of incompatible trace elements for lavas of the Cumbre Vieja volcano (platform-forming eruptions). Symbols as in Fig. 46A. The data of a primitive basalt from St. Helena are taken from Sun and McDonough (1989).

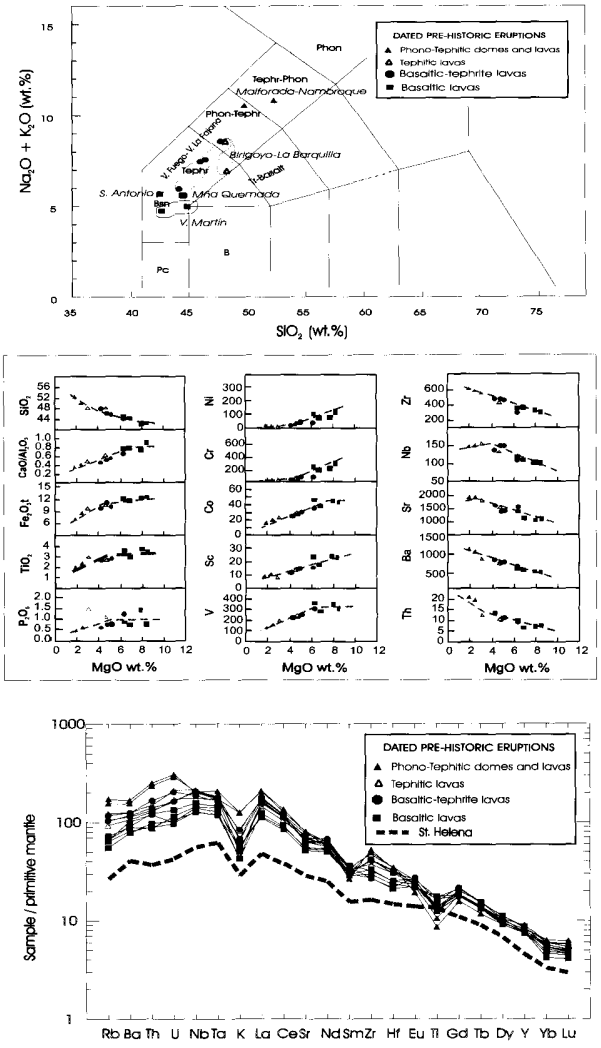


Fig. 47.—A) TAS diagram of lavas of the Cumbre Vieja volcano (dated prehistorical eruptions). The limits are from Yllescas (1977), Hernández Pacheco and Vals (1982), and De Vicente Mingarro (1986). The boundaries from Le Bas et al. (1986). B) Variation diagram for major, trace and REE elements of lavas of the Cumbre Vieja volcano (dated prehistorical eruptions). Symbols as in Fig. 47A. C) Primitive mantle normalized diagram (Sun and McDonough, 1989), of incompatible trace elements for lavas of the Cumbre Vieja volcano (dated prehistorical eruptions). Symbols as in Fig. 47A. The data of a primitive basalt from St. Helena are taken from Sun and McDonough (1989).

Klügel et al. (1999), is the role of fractionation/crystallization of mafic minerals (ol ± cpx ± amphib), feldspar, oxides and apatite in the magmatic evolution of this stage of growth of the Cumbre Vieja volcano.

The separation of the platform-forming eruptions has been useful in the definition of the volcanostratigray and in the geological maps of the Cumbre Vieja volcano, as already mentioned and described in detail in Section II-4. However, this stratigraphic division does not have a correlation in the petrological or geochemical characteristics (Table 2-9 and Fig. 46), that appear to be very similar to those of the cliff-forming eruptions. Similar trends are observed in the prehistorical lavas and intrusives dated (Table 2-10 and Fig. 47), analysed separately for comparison.

The petrological characteristics of the platform-forming lava sequences correspond predominantly to olivine-clinopyroxene and clinopyroxene-amphibole

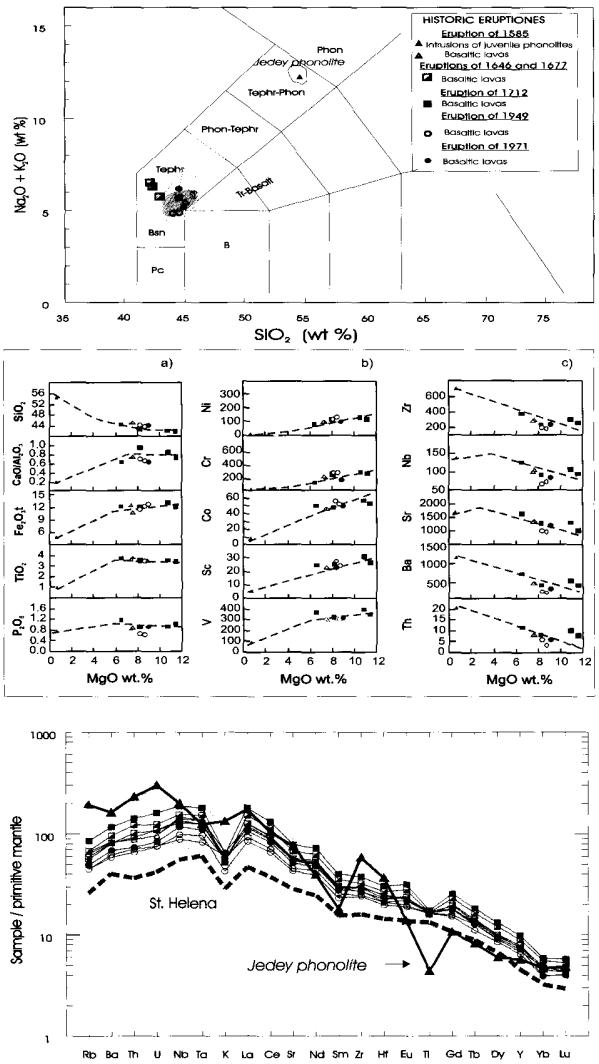


Fig. 48.—A) TAS diagram of lavas of the Cumbre Vieja volcano (historical eruptions). The limits are from Hernández Pacheco and Vals (1982), De Vicente Mingarro (1986) and Klügel et al. (1999). The boundaries from Le Bas et al. (1986). B) Variation diagrams for major, trace and REE elements of lavas of the Cumbre Vieja volcano (historical eruptions). Symbols as in Fig. 48A. C) Primitive mantle normalized diagram (Sun and McDonough, 1989), of incompatible trace elements of lavas of the Cumbre Vieja volcano (historical eruptions). The shadowed area corresponds to the 1949 eruption (Klügel et al., 1999). Symbols as in Fig. 48A. The data of a primitive basalt from St. Helena are taken from Sun and McDonough (1989).

basalts, with phono-tephrites in the more differentiated lavas (Mña Cabrera-Faro and Fuego volcano). The domes and lava domes are characteristically tephri-phonolitic (Malforada-Nambroque), their geochemical characteristics showing similar trends to the cliff-forming eruptions. The normalized plots (Figs. 46, 47), show significantly higher values than those corresponding to St. Helena (Sun and McDonough, 1989).

*Historical eruptions.* Although the separation of the eruptive activity of the island in the last 500 years has no stratigraphical, petrological or geochemical meaning, these historical eruptions have been traditionally analysed separately from the remaining eruptions of Cumbre Vieja volcano, because they have detailed eye-witness accounts and are easily separated in the geological maps. Petrological and geochemical data of the different historical eruptions of La Palma have been described and analysed by Hernández Pacheco and Valls (1982), De Vicente Mingarro (1986), Praegel (1986), Elliot (1919), Klügel, et al. (1999) and Carracedo et al. (2001b).

The historical lavas are consistently basaltic, with the only mentioned exception of the juvenile haüyne tephri-phonolite lavas and intrusives of the 1585 (Jedey) eruption. The predominant lithologies are ol-cpx basalts and ol-cpx basalts with amphibole. Klügel et al. (1999) quotes three typologies (basanites, tephrites and phono-tephrites) in the 1949 eruption. The last eruption (Teneguía volcano, 1971) emitted clinopyroxene-amphibole basalts, with subordinate olivine in the initial stages, while at the end of the eruption the composition changed to ol-cpx basalts with subordinate amphibole.

The geochemical characteristics of the historical eruptions shown in Table 2-11 and Fig. 48 confirm the general features described for the Cumbre Vieja volcano and evidence the homogeneity of volcanism along the entire volcanic history of the volcano, with the afore-mentioned preponderant role of fractionation/crystallization of mafic minerals (ol ± cpx ± amphib), feldspars, oxides and apatite, similar to the process proposed by Klügel et al. (1999) for the 1949 eruption.

## Structural geology

The island of La Palma is an excellent scenario to analyse the main structural features developed in the shield stage of oceanic islands: dyke swarms, rift zones and gravitational landslides.

### *Dyke swarms*

The majority of dykes in La Palma outcrop inside the Caldera de Taburiente, the Cumbre Nueva collapse scarp and the erosional windows at the headwalls of the deepest northern barrancos. In the remainder of the northern shield and the Cumbre Vieja volcano dykes are scarce (black lines in Fig. 49). However, the abundant *galerías* excavated in the northern shield (SPA-15, 1975; Coello, 1987) allowed the observation in the subsoil of the number and direction of dykes (grey in Fig. 49).

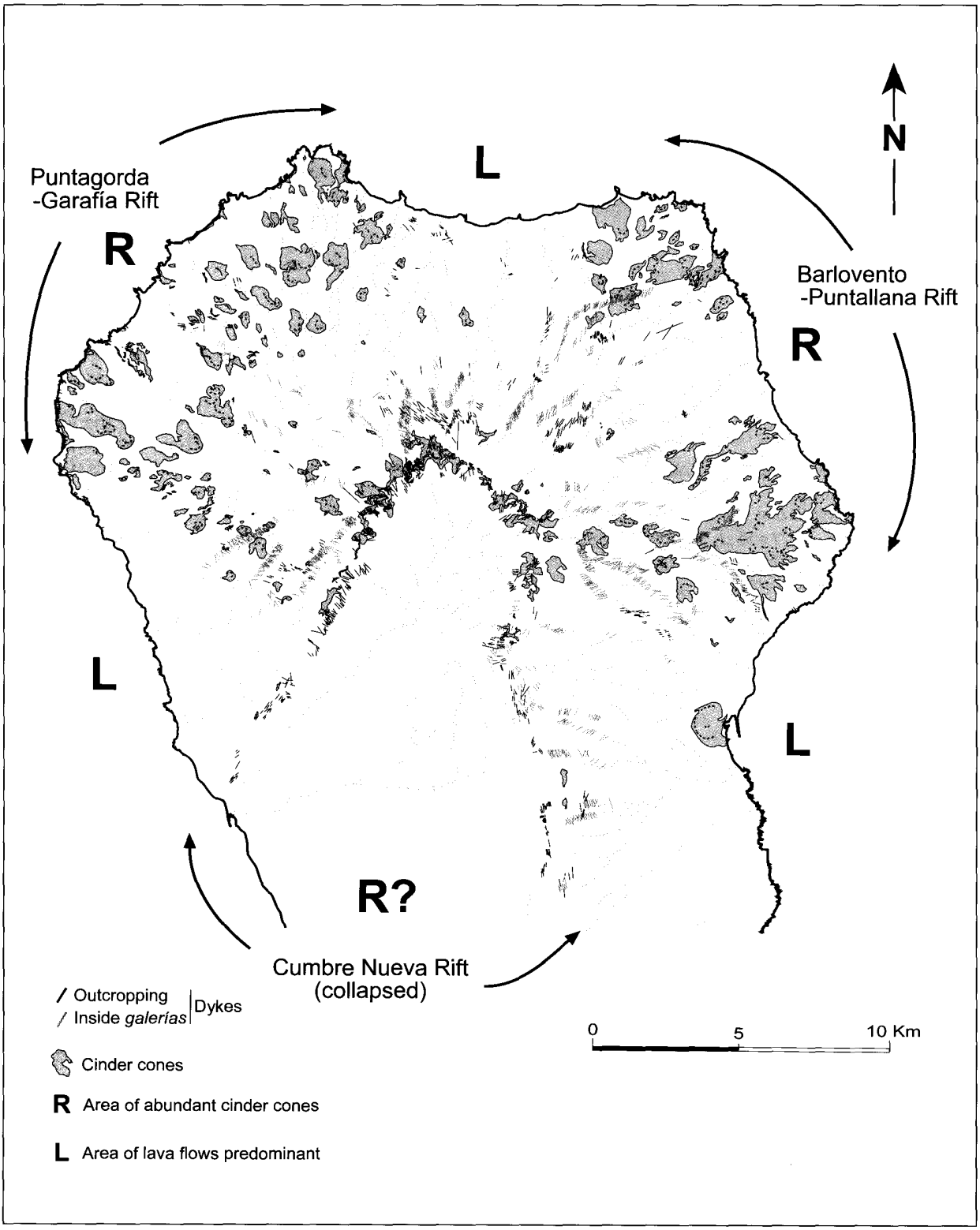


Fig. 49.—Distribution of zones where eruptive vents predominate (incipient, incompletely defined rift zones) and zones with predominance of lava flows (R and L, respectively). Dykes crossed in galerías are shown in grey, outcropping dykes in black.